8-2017

Acetate Metabolism: The physiological role of ADP-forming acetyl-CoA synthetase and acetate kinase in Entamoeba histolytica

Thanh Dang
Clemson University, Thanhd@g.clemson.edu

Acetate Metabolism: The Physiological Role of ADP-forming Acetyl-CoA Synthetase and Acetate Kinase in *Entamoeba histolytica*

A Dissertation
Presented to
the Graduate School of
Clemson University

In Partial Fulfillment
of the Requirements for the Degree
Doctor of Philosophy
Biochemistry and Molecular Biology

---

by
Thanh Dang
August 2017

Accepted by:
Cheryl Ingram-Smith, Committee Chair
James C. Morris
Kerry S. Smith
Lesly Temesvari

ABSTRACT

Entamoeba histolytica is a protozoan parasite that causes amoebic colitis and liver abscess in approximately 90 million people each year, resulting in 50,000-100,000 fatalities. Even though *Entamoeba* poses a significant public health problem worldwide, research dedicated to understanding the biology of this unique protozoan has been limited. This amitochondriate parasite lacks many essential biosynthesis pathways including the tricarboxylic acid (TCA) cycle and oxidative phosphorylation. As a result, substrate level phosphorylation plays a necessary role in ATP production. Unlike the standard glycolytic pathway, *E. histolytica* glycolysis requires pyrophosphate (PP_i) by replacing ATP–dependent phosphofructokinase and pyruvate kinase with PP_i–dependent phosphofructokinase and phosphate pyruvate dikinase.

E. histolytica infects and colonizes the human colon where glucose is limited and short chain fatty acids (acetate, propionate, and butyrate) are plentiful. Acetate is also a major end product that is excreted when *E. histolytica* is grown axenically on glucose. Acetate has been demonstrated to act as carbon and energy source for cellular growth in other organisms, acetogenesis can regenerate NAD^+, recycle coenzyme A, and produce ATP when the TCA cycle or oxidative phosphorylation does not operate or when the carbon flux into the cell exceed its capacity.

In *E. histolytica*, acetate can be generated by acetate kinase (ACK) and ADP–forming acetyl–CoA synthetase (ACD). ACK converts acetyl phosphate + orthophosphate (P_i) to acetate + PP_i. Previous biochemical and kinetic characterization of

recombinant ACK showed that it strongly prefers the acetate/PP_i-forming direction. We hypothesized that ACK may function to supply PP_i for the PP_i oriented glycolytic pathway in *E. histolytica.* Recombinant ACD displayed high activity in both directions of the reaction to convert acetyl-CoA + orthophosphate + ADP to acetate + ATP + CoA. ACD may function to extend the glycolytic pathway to increase ATP production by 40% per molecule of glucose, or in the alternative direction to convert acetate to acetyl-CoA to meet the cell's metabolic needs.

Using reverse genetics, an *Ehacd* silenced strain displayed a growth defect in normal high glucose media, while *Ehack* silenced cells showed enhance growth in medium without added tryptone and glucose. The presence of acetate and butyrate showed no effect on *E. histolytica* growth in the absence of glucose regardless of ACK or ACD activity. The presence of propionate, however, improved *E. histolytica* growth and impaired growth of the *Ehacd* silenced strain implicated ACD as the cause of this improvement. Our data suggest ACD plays a role in increasing ATP production during growth on glucose and utilization of propionate as a growth substrate. Our data do not support the previously hypothesized role for ACK but instead suggest it possesses a novel function.

The basis for *E. histolytica* ACK's divergence from all other ACKs in phosphoryl substrate utilization was also explored. Currently, *E. histolytica* ACK is the only known ACK that uses pyrophosphate (PP_i) or inorganic phosphate (P_i) as the phosphoryl donor or acceptor. All other known ACKs utilize ATP or ADP. *In silico* structural comparison and modeling of *E. histolytica* ACK against other ACKs identified structural differences

that could affect substrate binding and selection. ACK variants were generated to test these predictions. Inhibition and structural activity relationship studies revealed an occlusion in the ADENOSINE motif of *E. histolytica* ACK reduced ATP and ADP binding affinity. However, alterations to alleviate the constriction did not confer activity with ATP or ADP. Our results suggest controlling access of the adenosine pocket influences phosphoryl substrate binding but is not the sole determinant of enzyme activity.

DEDICATION

I would like to dedicate this to my Mom, Dad, and Joanne. Without your support and encouragement, this would not have been possible. I am blessed and thankful for having such a loving family.

ACKNOWLEDGEMENT

I would like to thank my advisor, Dr. Cheryl Ingram-Smith. You are kind, patient, and understanding. I am truly grateful for the opportunity to work and learn from you. The lessons I gained here will stay with me for the rest of my career.

Additionally, I would like to thank my committee members. Dr. Kerry Smith: thank you for the valuable discussions and insightful inputs during our numerous joint lab meetings. Dr. Lesly Temesvari: thank you for your advice and expertise toward my *Entamoeba* research. Dr. James Morris: thank you for your constant wisdom and wild ideas that have kept my perspective in check.

I would also like to acknowledge the students from both the Ingram-Smith and Smith labs. Without everyone's advice and helpful technical assistance, I would have made more mistakes, repeated more experiments, and not learned as much as I have. Thank you Cheryl Jones, Jordan Wesel, and Diana Nguyen, my fellow Ingram-Smith lab mates, for being a platform to screen new ideas and experimental designs. From the Smith lab, thank you Tonya Taylor, Katie Glenn, and Satyanarayana Lagishetty for being so welcoming and of great assistance during my graduate career.

Lastly, I would like to extend a special thanks to Brenda Welter and Hollie Hendrick from Dr. Temesvari's lab. Your assistance was critical to my work with *Entamoeba histolytica.* I would like to also express great thanks to the faculty, staff, and graduate students from Clemson University Genetics and Biochemistry department and the Eukaryotic Pathogens Innovation Center. In particular, I would like to thank Logan

Crowe, Sophie Altamirano, Michael Harris, Jimmy Suryadi, and Steven Cogill for their support and advice in matters of science and life. Most of all, without everyone's technical assistance, valuable input, and words of encouragement, graduate school would not have been as enjoyable and achievable. So, thank you!

TABLE OF CONTENTS

Page

Table of Contents (Continued)

Page

LIST OF TABLES

LIST OF FIGURES

List of Figures (Continued)

CHAPTER I

LITERATURE REVIEW

INTRODUCTION:

Entamoeba histolytica, an amitochondriate parasite, infects and resides within the human colon. Due to its reductive metabolism and lack of oxidative phosphorylation, glycolysis is widely accepted as the main pathway of energy and carbon metabolism. During *E. histolytica* growth, acetate and ethanol are the two major end-products that are always produced. Moreover, acetate represents one of the most abundant short chain fatty acid found in the human large intestine from fermentative metabolism by the colon flora. Thus, acetate production and utilization by *E. histolytica* is of great interest. Two enzymes identified in *E. histolytica* that produce acetate are acetate kinase (EhACK) and ADP-forming acetyl CoA synthetase (EhACD) and are the subject of this dissertation research.

Acetate kinase (ACK) is widespread in bacteria, but is found in just one genus of archaea and a few eukaryotic microbes. ACK interconverts acetate and acetyl phosphate using ATP and ADP. Even though EhACK can interconvert acetate and acetyl phosphate *in vitro*, kinetic analysis indicates its physiological direction is likely limited to the acetate-forming direction due to its considerable preference for this direction. Additionally, EhACK uses pyrophosphate (PP_i) and inorganic phosphate (P_i) instead of ATP and ADP for catalysis. Currently, EhACK is the only known ACK to show this phosphoryl substrate selectivity.

Acetate metabolism is a common process in many organisms. Acetate production and utilization have been shown to have a significant role in growth. Moreover, acetate has also been reported to be involved in regulating pathogenesis, histone acetylation, gene expression and motility [7, 11-13, 58-59, 80].

In bacteria ACK partners with phosphotransacetylase in a reversible pathway to convert acetyl-CoA to acetate to produce ATP and recycle coenzyme A. Conversely, AMP-forming acetyl-CoA synthetase (ACS) functions unidirectionally to activate acetate into acetyl-CoA. *E. histolytica* lacks ACS and instead has the bidirectional ACD. Although acetate is a primary metabolic product during *E. histolytica* growth on glucose, the majority of *E. histolytica* infection resides within the glucose-limited environment of the large intestine. This presents a need to further explore alternative metabolic pathways within this parasite. EhACK and EhACD may present two such pathways for energy conservation and acetate activation that allow adaptability for survival and growth by *E. histolytica* in the acetate rich environment of the large intestine.

The purpose of this review is to provide an overview of the significant impact of acetate and introduce acetate metabolism pathways. *E. histolytica* metabolism is discussed with a focus on its central carbon metabolism. Lastly, a history of acetate kinase is also provided.

ACETATE METABOLISM:

Acetate is a common short chain fatty acid (SCFA) metabolite in many organisms. In the human colon, SCFAs compose >60% of the anion concentration (110-120 mM) [(1)], mainly as acetate, propionate and butyrate with a relative molar mass ratio of 57:22:21 [(2)], respectively. These SCFAs are rapidly absorbed by the colonic mucosa [(1)] with less than 5% SCFA produced by bacteria found in feces [(3)]. Butyrate acts as the main energy source for colonocytes [(3)], propionate is readily absorb by the liver, and acetate enters the peripheral circulation to be taken up by peripheral tissues [(4)].

Acetate can originate from a multitude of sources. This SCFA can be obtained from the diet, generated by the liver, or produced locally and intracellularly through enzymatic reactions. The main source of acetate within the human body arises from fermentation by commensal gut microbiota [(9, 10)]. Acetate assimilation as an alternative carbon source has been demonstrated in bacteria cells in limited nutrient environments [(1)]. Acetate excretion, on the other hand, is often observed to fulfill a need to generate additional ATP and regenerate NAD^+ and Coenzyme A when oxidative phosphorylation is nonfunctional or in circumstances where the carbon flux exceeds the capacity of the central carbon metabolic pathways [(1)]. As a result, acetate production is often considered to be an “overflow” metabolic pathway.

Acetate from fermentation within the colon can also traverse the blood brain barrier and enter the brain [(5)]. This results in an increase in hypothalamic acetate concentration and can regulate appetite. Perry *et al.* [(6)] further showed increased

production of acetate in the gut can lead to metabolic syndrome such as obesity and diabetes. Acetate has also been linked to tumor growth [7, 8]. Using [1,2-^{13}C] acetate, Mashimoto *et al.* [8] have shown that as much as 50% of TCA cycle intermediates are acetate-derived in brain tumor cells even when glucose is abundant. More strikingly, they observed a 40% increase in acetate-derived carbon incorporated into TCA cycle intermediates in tumor cells compared to non-tumor cells, illustrating the significant role of acetate in meeting the high biosynthetic and bioenergetics demands of tumor cells. Additionally, acetate has been reported to also influence growth; motility in *Escharichia coli* and *Salmonella enterica*; histone acetylation in yeast, mice, and human; pathogenesis *E. coli*; and pathogenic gene regulation *S. enterica* [7, 11-13, 58-59, 80]. This illustrates acetate metabolism not only may affect the host but also the surrounding microbiome.

Acetate metabolism in bacteria

Acetate metabolism is well studied in bacteria, most notably in *Escherichia coli.* Acetogenesis in *E. coli* takes place through either an acetate kinase (ACK; EC 2.3.1.8)[14] – phosphotransacetylase (PTA; EC 2.7.2.1)[15] pathway or by pyruvate dehydrogenase (ubiquinone) (POXB; EC 1.2.5.1) [1, 11]. PTA catalyzes the reversible conversion of acetyl-CoA to acetyl phosphate and releases coenzyme A [16] (Eq. 1). Subsequently, ACK transfers the phosphate from acetyl phosphate to ADP to produce acetate and ATP in a reversible reaction (Eq. 2). Acetate can also be generated by a pyruvate decarboxylating enzyme, POXB, which decarboxylates pyruvate to acetate, releasing carbon dioxide and reducing ubiquinone (Eq. 3) [1, 17]. Dittrich *et al.* [11] found ACK-PTA was the main

acetate producing pathway during exponential growth and POXB dominated during stationary phase.

In certain lactobacilli, *Pediococcus*, and *Streptococcus*, a second type of pyruvate oxidase (POX-AP; EC 1.2.3.3) is present to convert pyruvate to acetyl phosphate instead of acetate (Eq. 4) [(1)]. Other enzymes that produce acetyl phosphate are xylulose-5-phosphate/fructose-6-phosphate phosphoketolase (Eq. 5), sulfoacetaldehyde acetyltransferase (Eq. 6), and glycine reductase (Eq. 7). Xylulose-5-phosphate (X5P)/fructose-6-phosphate (F6P) phosphoketolase (XFP; EC 4.1.2.9, EC 4.1.2.22) cleaves X5P/F6P into acetyl phosphate and glyceraldehyde-3-phosphate (G3P)/erythose-4-phosphate (E4P). This phosphoketolase is found in heterofermentative lactobacilli and organisms such as *Acetobacter xylinum, Butyrivibrio fibrisolvens, Fibrobacter succinogenes* and *Fibrobacter intestinalis* [(1, 18)].

Sulfoacetaldehyde acetyltransferase (XSC; EC 2.3.3.15) desulfonates sulfoacetaldehyde into acetyl phosphate and sulfite. This enzyme has been identified within several gram-positive bacteria and Proteobacteria [(1, 19-21)]. Lastly, certain strictly anaerobic gram-positive bacteria use glycine reductase (GR; EC 1.21.4.2) to convert glycine (Gly), phosphate (P_i), and thioredoxin (Trx) to acetyl phosphate (AcP), ammonia, thioredoxin sulfite (TrxS), and water [(1)]. Several studies have shown these enzymes can partner with ACK and/or PTA for anabolic metabolism or ATP production [(22)].

Eq. 1: PTA Acetyl-CoA + P_i ←→ acetyl phosphate + CoA

Eq. 2: ACK Acetyl phosphate + ADP ←→ acetate + ATP

Eq. 3: POXB Pyruvate + ubiquinone + H_2O → acetate + CO_2 + ubiquinol

Eq. 4: POX-AP Pyruvate + O_2 + P_i → acetyl phosphate + CO_2 + H_2O_2

Eq. 5: XFP X5P/F6P + P_i → acetyl phosphate + H_2O + G3P/E4P

Eq. 6: XSC Sulfoacetaldehyde + P_i → acetyl phosphate + sulfite

Eq. 7: GR Gly + P_i + Trx → AcP + NH_3 + TrxS + H_2O

During conditions of nutrient depletion, cells can undergo a process termed the "acetate switch" (Figure 1.1) [(1)]. This is defined as when the cell shifts to utilizing acetate as the alternative carbon source when glucose is absent and acetate is abundant. Acetate activation can happen through either the ACK-PTA pathway or an AMP-forming acetyl-CoA synthetase (ACS; EC 6.2.1.1), which converts acetate and ATP directly to acetyl-CoA (Eq. 8) [(12)]. Acetate assimilation occurs largely by ACS while dissimilation mainly occurs through the ACK-PTA pathway. However, ACK-PTA reversibility can contribute to acetate utilization [(1, 12)]. Kumari *et al.* [(12)] demonstrated an *acs* deletion mutant grew poorly at low acetate concentration, whereas *ack* and *pta* deletion mutants grew poorly at high acetate concentrations and mutants with all three genes deleted did not grow at all on acetate. This proves both pathways are used for acetate utilization but at different environmental acetate concentrations.

Eq. 8: ACS Acetate + ATP + CoA → acetyl-CoA+ PP_i + AMP

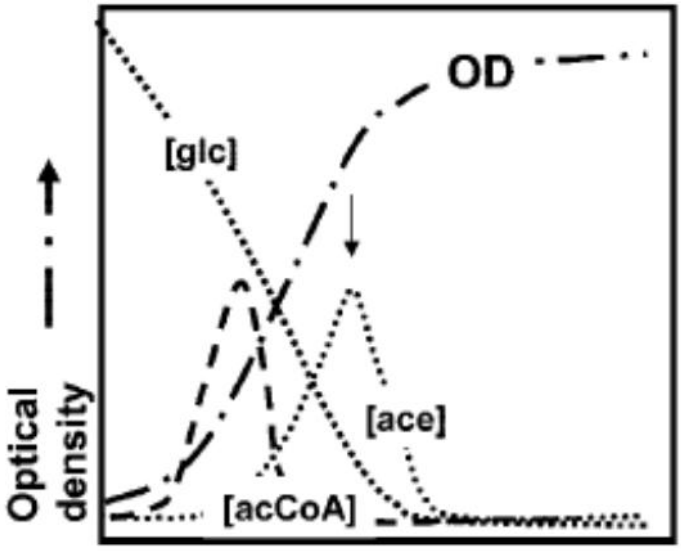

Figure 1.1: Schematic displaying the "acetate switch" during aerobic growth with glucose as the sole carbon source. The arrow denotes the point of the "acetate switch" where glucose becomes depleted and acetate production is switched to acetate utilization. OD: optical density, ace: acetate; acCoA: acetyl-CoA; glc: glucose. Figure obtained and modified from [1] with permission.

ADP-forming acetyl-CoA synthetase (ACD; EC 6.2.1.13), converts acetyl-CoA and ADP to acetate and ATP (Eq. 9). ACD activity was first described in the thermophilic archaeon *Pyrococcus furiosus* [23], where it plays a crucial role in energy conservation during sugar metabolism [24]. Though not widespread, ACD has also been identified in several archaea, such as *Pyrococcus woesei, Desulfurococcus amylolyticus, Hyperthermus butylicus, Thermococcus celer, Archaeoglobus fulgidus, Halobacterium saccharovorum, Haloarcula marismortui, Methanococcus jannaschii, Pyrobaculum aerophilum* and *Thermococcus kodakarensis* [23, 25-29], and has also been identified in the bacterium *Chloroflexus aurantiancus* [30]. In prokaryotes, ACD belongs to the superfamily of NDP-forming acyl-CoA synthetases.

Eq. 9: ACD $\quad$ Acetyl-CoA + ADP + P_i ←→ acetate + ATP + CoA

Besides carbon and energy metabolism, acetate production and utilization have been linked to pathogenesis and motility in bacteria. Fukuda *et al.* [31] reported a prolonged survival in mice infected with *E. coli* O157:H7 if the mice were colonized by *Bifidobacterium longum* prior to infection. Data showed acetate production increased in the presence of *B. longum*. *In vitro* experiments demonstrated acetate inhibited the permeability of epithelial monolayer caused by *E. coli* O157 infection, preventing Shiga toxin from *E. coli* O157:H7 translocation into the blood from the gut [31, 32].

In 2002, Lawhon *et al.* [13] found acetate activates BarA, a kinase that interacts with SirA to initiate expression of the SPI-1 virulence genes in *Salmonella enterica*. This suggests acetate may act as a signal for invasive gene expression in the intestine.

Recently, Nakamura *et al.* [33] also reported acetate can inhibit *Salmonella* flagellar motility. However, the mechanism of inhibition is still poorly understood but was suggested to relate to regulation of the acetyl phosphate pool.

Acetyl-phosphate in signal transduction: Acetyl phosphate is a high energy compound, possessing a greater ΔG^{O} of hydrolysis (-43kJ/mol) than ATP (-30kJ/mol) [1]. This is the foundation of acetyl phosphate's suggested role as a global signaling molecule [34, 35] by phosphorylating members of the two components transduction system (2CTS) [1, 36-38]. 2CTS consists of a histidine kinase (HK) being phosphorylated by ATP. HK-P in turn phosphorylates the second component of the signaling system, the response regulator (RR), to elicit a response.

An abundance of *in vitro* evidence demonstrated acetyl phosphate's interaction and autophosphorylation of the RR component of 2CTS pathway (Table 1.1). *In vivo*, mounting evidence showed controlling the acetyl phosphate pool affects biofilm formation, nitrogen assimilation, phosphate assimilation, flagella biogenesis, and pathogenesis [1, 38, 39]. Support for acetyl phosphate's effect on flagellar motion was also established. Wolfe *et al.* [40] reported exogenous acetate increased clockwise rotation of *E. coli* flagella. Dailey and Berg [41] later presented evidence relating acetyl phosphate synthesis to flagellar rotational direction. In 2007, Klein *et al.* [42] showed acetyl phosphate can directly phosphorylate RR of the 2CTS based on the abundance of intracellular acetyl phosphate in *E. coli*, further supporting acetyl phosphate proposed role as a global signal.

Organism	HK	RR
Pseudomonas aeruginosa	AlgZ	AlgR
Bordetella pertussis	BvgS	BvgA
Klebsiella pneumonia	CitA	CitB
Escherichia coli	CheA	CheY
Sinorhizobium meliloti	CheA	CheY1, Y2
Rhodobacter sphaeroides	CheA	CheY1, Y3-6
Helicobacter pylori		CheV2
Bacillus subtilis	ComP	ComA
Shigella sonnei, E. coli	CpxA	CpxR
Streptococcus pyogenes	CsrS	CsrR
Spirulina platensis	CyaC	CyaC
E. coli	DcuS	DcuR
Sinorhizobium melilori	FixL	FixJ
Clostridium acetobutylicum	KdpD	KdpE
E. coli	KdpD	KdpE
Mycobacterium tuberculosis	MprB	MprA
E. coli	NarX	NarL
Bradyrhizobium japonicum	NodV	NodW
E. coli	NR_{II} (NtrB)	NR_{I} (NtrC)
E. coli	EnvZ	OmpR
E. coli	PhoR	PhoB
Salmonella enterica	PhoQ	PhoP
R. sphaeroides	PrrB	PrrA
Calothrix sp. strain *PCC7601*	CphA	RcpA
Calothrix sp. strain *PCC7601*	CphB	RcpB
Dictyostelium discoideum	RdeA	RegA
E. coli, S. enterica	None	RssB
S. enterica	BarA	SirA
Saccharomyces cerevisiae	SLN1-YPD1	SSK1
Enterococcus faecium	VanS	VanR

Table 1.1: List of two-component response regulators from various microbes previously shown to be influenced by acetyl phosphate. Figure obtained and modified from [1] with permission.

Acetate metabolism in eukaryotes

ACK, PTA and XFP were originally thought to function only in prokaryotes. However, Blast searches have identified open reading frames for ACK, PTA and XFP in a number of eukaryotic microbes [(43)]. In *Chlamydamonas*, acetate was observed to be one of the major metabolites excreted during anoxic growth [(44)]. The same study also detected an increase in *ack1*, *ack2*, *pta1*, and *pta2* transcripts during anaerobic growth. Consistent with this finding, Yang *et al*.[(45)] showed disruption of *ack1* and *pta2* expression in *Chlamydamonas* substantially reduced acetate production during anoxic growth. PTA from the oomycete *Phytophtora ramorum* has also been identified and characterized [(46)]. *Cryptococcus neoformans* does not possess a PTA but does contains two XFPs and an ACK [(47, 48)] . However, to date only one *C. neoformans* XFP has been biochemically and kinetically characterized [(48)]. In *Entamoeba histolytica*, ACK activity has been detected both from recombinant enzyme and cell lysate [(49, 50)]. However, distinct from other ACKs, *E. histolytica* ACK (EhACK) is pyrophosphate dependent (Eq. 10).

Eq. 10: EhACK $\quad$ Acetate + PP_i $\leftarrow\rightarrow$ acetyl phosphate + P_i

ACS is also present in both prokaryotes and eukaryotes. As in prokaryotes, eukaryotic ACS activates acetate into acetyl-CoA for energy conversion and anabolic metabolism. Mammals express three isoforms of ACS. ACSS2 is localized in the nucleus and cytosol while ACSS1 and ACSS3 are compartmentalized within the mitochondria [(51, 52)]. Only ACSS1 and ACSS2 have been shown to be able to use acetate as a substrate.

Currently, the classification of ACSS3 as an acetyl-CoA synthetase remains speculative with no report of detectable enzymatic activity. Cytosolic ACS is usually found in the liver and plays a role in generating acetyl-CoA for fatty acid and cholesterol biogenesis [53]. Mitochondrial ACS is found in heart and skeletal muscle [54]. Acetyl-CoA generated by mitochondrial ACS is used for energy metabolism via oxidative phosphorylation. As such, ACS activity has been connected to tumor growth and metabolic syndrome such as obesity and diabetes [6-8].

In other eukaryotes, two isoforms of ACS generally exist (ACS1 and ACS2) [55]. In *Candida albicans*, ACS2 is crucial for survival and growth on most carbon sources, including glucose [56]. ACS has also been identified in *Trypanosoma* and has a vital role in fatty acid biosynthesis in procyclic *Trypanosoma brucei* [57]. Additionally, ACS involvement in histone acetylation has been reported. Eisenberg *et al.* [58] detected activation of ACS2 during cytosolic accumulation of acetate, triggering histone acetylation and reducing autophagy in yeast. A similar relationship between ACS and acetylation has been observed in both mice and human [7, 59, 60].

Other acetate producing pathways in eukaryotes include acetylaldehyde dehydrogenase (ALDH; EC 1.2.1.5), acetate:succinate CoA transferase (ASCT; EC 2.8.3.18), ADP-forming acetyl-CoA synthetase, and acetyl–CoA hydrolase (ACH; EC 3.1.2.1). ALDH converts acetylaldehyde to acetate with the reduction of $NADP^+$ (Eq. 11). In *Saccharomyces cereviseae*, ALDH partners with pyruvate decarboxylase (PDC; EC 4.1.1.1) and ACS to form a pyruvate dehydrogenase bypass for the conversion of

pyruvate into acetyl-CoA[61, 62]. Saint-Prix *et al.* [61] demonstrated that deletion of the *ALDH* gene decreased acetate production and reduced growth in *Saccharomyces*.

ACH is responsible for the interconversion of acetyl-CoA and acetate (Eq. 12). In *Candida* and *Saccharomyces,* ACH contributes to the utilization of acetate as an alternative carbon source [56, 63]. ACH can also function in the acetate-forming direction to shuttle acetyl-CoA out of the mitochondria in *Saccharomyce*s by converting acetyl-CoA to acetate for transport [64]. In the cytosol, acetate can be converted back into acetyl-CoA by ACS.

Of the acetate producing enzymes in eukaryotes, only two have been identified in parasites: ASCT and ACD. ASCT is a CoA transferase which produces acetate in a succinate dependent manner. ASCT transfers the CoA moiety from acetyl-CoA to succinate, generating succinyl-CoA and acetate (Eq. 13). ASCT can work with succinyl-CoA synthetase (SCS) to recycle CoA, regenerate succinate and produce ATP from ADP [65]. This ASCT-SCS cycle has been identified in *Tritrichomonas foetus, Trichomonas vaginalis, Faschiola hepatica, Trypanosoma brucei, Leishmania mexicana, Leishmania infantum, Phytomonas* and *Neocallimastix* [66-72].

Eq. 11: ALDH Acetylaldehyde + H_2O + $NADP^+$ → acetate + NADPH

Eq. 12: ACH Acetyl-CoA + H_2O ←→ acetate + CoA

Eq. 13: ASCT Acetyl-CoA + succinate → succinyl-CoA + acetate

ACD exists in all three domains of life but is not widespread. ACD was first observed in *Entamoeba histolytica* [73] and later observed in *Giardia lamblia* [74]. Recombinant ACD has been purified from *E. histolytica* and *G. lamblia* and biochemically characterized [75, 76]. Sequence analyses have also identified ACD in *Blastocystis hominis* and several *Plasmodium* spp [77, 78].

Overall, an array of acetate producing pathways are available (Figure 1.2), reflecting how acetate metabolism adds adaptability for survival of an organism. These pathways also demonstrate acetate's impact beyond carbon and energy metabolism.

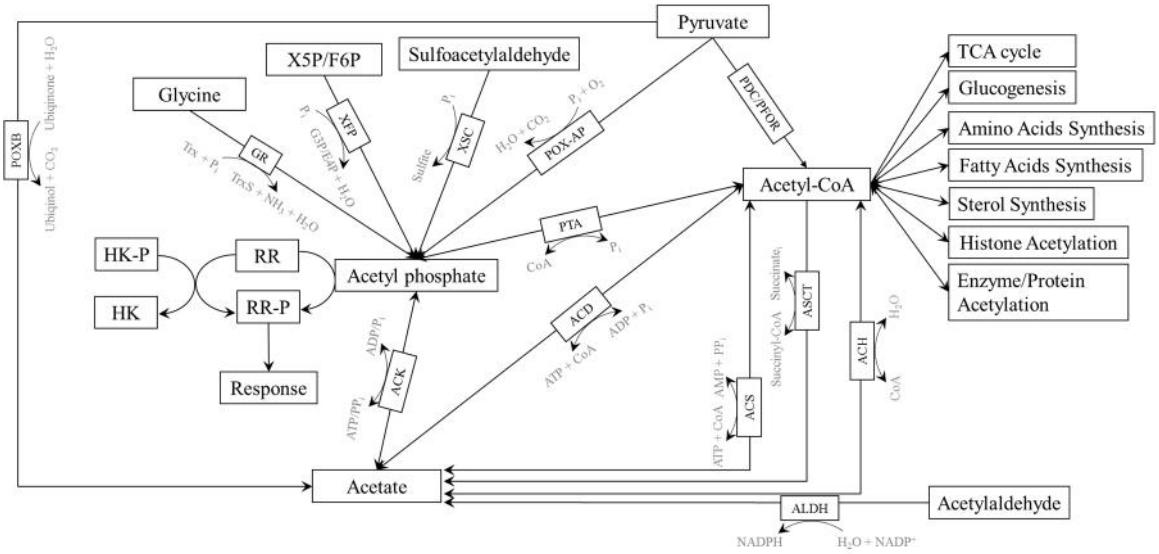

Figure 1.2: Common acetate metabolic pathways. HK: histidine kinase; HK-P: phosphorylated histidine kinase; RR: response regulator; RR-P: phosphorylated response regulator; ACK: acetate kinase; GR: glycine reductase; XFP: xylulose-5-phosphate/fructose-6-phosphate phosphoketolase; XSC: sulfoacetaldehyde acetyltransferase; POX-AP; pyruvate oxidase (acetyl phosphate forming); POXB: pyruvate oxidase; ACD: ADP-forming acetyl-CoA synthetase; PDC; pyruvate dehydrogenase; PFOR: pyruvate ferredoxin oxidoreductase; ACS: AMP-forming acetyl-CoA synthetase; ASCT: acetate: succinate CoA transferase; ACH: acetyl-CoA hydrolase; ALDH: acetylaldehyde dehydrogenase; PTA: phosphotransacetylase.

Entamoeba Histolytica:

Entamoeba Histolytica is a microaerophilic protozoan responsible for amebiasis, a disease that causes amebic colitis and liver abscess in humans. Even though Fedor Losch first described intestinal amebiasis in 1875, *E. histolytica* was not identified as the causative agent until 30 years later by Fritz Schaudinn [(79)]. Amebiasis is prevalent in developing areas of the world due to poor sanitation. High risk areas include India, Africa, Bangladesh, Thailand, Mexico, and parts of South and Central America. Annually, 90 million people develop symptomatic amebiasis, leading to 50,000-100,000 deaths [(80)].

E. histolytica is a nonflagellated, pseudopod forming parasite that infects humans and possibly other primates as natural hosts [(81)]. As the name suggests, this parasite causes proteolysis, tissues lysis, and host cell apoptosis [(82)]. Symptoms of amebic colitis include abdominal pain, watery or bloody diarrhea, fever and weight loss that can persist for several weeks. Extraintestinal infection can also develop, often leading to liver infection which includes tissue destruction and abscess. In rare cases, *E. histolytica* can end up in the lung, heart, brain, or other organs. If untreated, extraintestinal infection will lead to death.

E. histolytica exists in two life stages: cyst and trophozoite. The cyst represents the infectious form and ranges from 10-16 µm in size, whereas the trophozoite is the motile form and is 20-40 µm in size [(83)]. *E. histolytica* infection is passed through an oral-fecal route. Amebiasis is initiated when cysts are ingested. After ingestion, the cysts will

travel through the host's digestive tract and begin excystation after reaching the small intestine. During excystation, cysts differentiate into trophozoites and migrate toward the large intestine for colonization (Figure 1.3).

In most cases, the infection remains asymptomatic and new cysts are released within the host's stool to continue the cycle. Cyst formation provides a survival mechanism for *Entamoeba* in adverse environmental conditions. The *Entamoeba* cyst wall is characterized by a mix of chitin and protein [84] and provides environmental resistance. The stimuli and molecular mechanism of encystation in *E. histolytica* remain largely undefined due to lack of an *in vitro* system to stimulate *E. histolytica's* stage differentiation. However, *Entamoeba invadens*, a relative of *E. histolytica* which causes similar invasive infection in reptiles, is used as a model system to study encystation. In *E. invadens*, stimuli involved in cyst formation include glucose starvation [85], osmotic shock [86, 87], autocrine catecholamine[88, 89], and cholesteryl sulfate [90]. Heat shock protein [91], chitin metabolism [92, 93], and enolase [94, 95] have also been shown to play a role in the process of encystation.

In some infected individuals, *E. histolytica* trophozoites will invade the intestinal mucosa, causing amoebic colitis. The parasites can then enter the bloodstream and migrate beyond the intestine to infect other organs, most commonly the liver [80]. The host employs a number of defense mechanism to fight against *Entamoeba* infection. Unfortunately though, the parasite has developed several methods to evade host

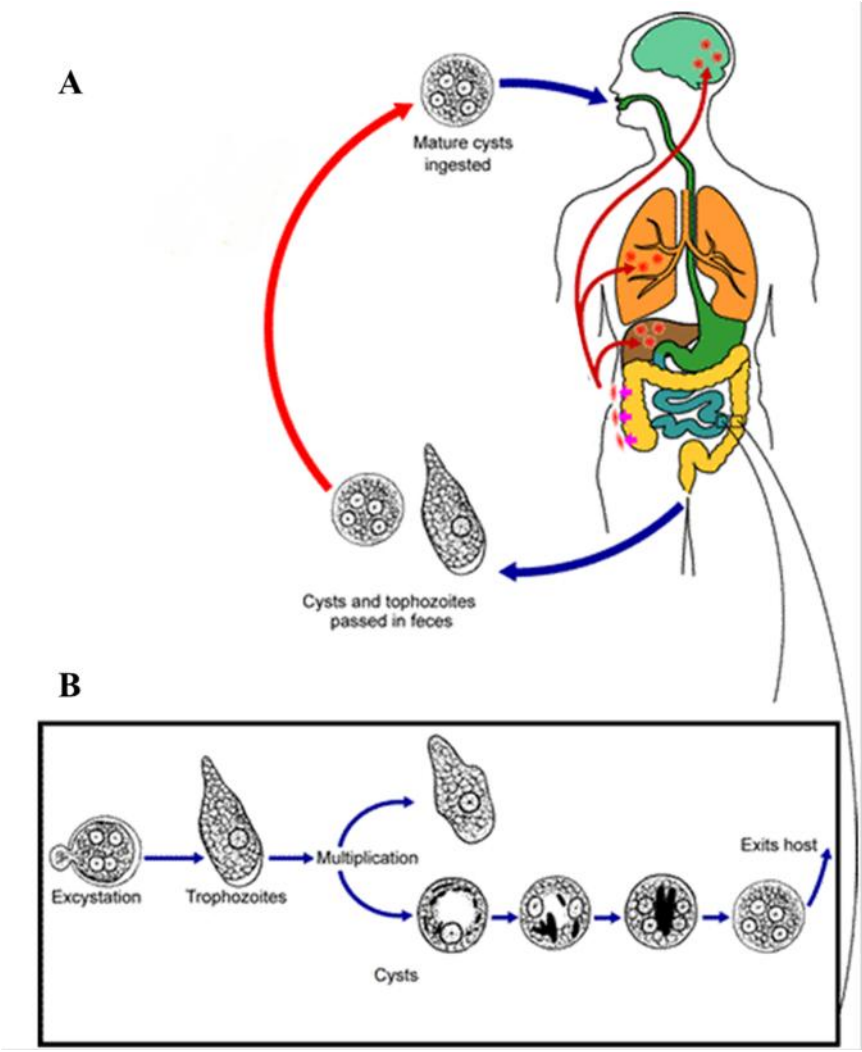

Figure 1.3: *Entamoeba histolytica* life cycle. A: *E. histolytica* infection route in humans. Infection proceeds through an oral-fecal route. Cysts differentiate into trophozoites in the small intestine to colonize within the colon. Cysts and trophozoites can be expunged from the host to continue its life cycle or infect extraintestinal organs (red arrows). **B**: *E. histolytica* differentiation cycle and life stages. Figure obtained and modified from the CDC website[(80)].

immunity. Stomach acid acts as the first line of defense against *E. histolytica.* Strong acid protects against enteropathogens by lysing acid-sensitive organisms. However, the *E. histolytica* cyst cell wall allows the parasite to survive within this extreme environment.

Other immune evasion mechanisms and virulence factors deployed by the trophozoite include Gal/GalNac lectins, cysteine protease, amoebapore, and peroxidoxin. Both Gal/GalNac lectin and cysteine protease have been demonstrated as crucial in *E. histolytica* pathogenesis and invasion [96-98]. Gal/GalNac lectin enables *E. histolytica* to adhere to the intestinal mucus layer [96, 99, 100]. The mucus layer acts as the second layer of innate immunity. *E. histolytica* overcomes this by secreting cysteine protease, causing destruction of the intestinal mucus layer. Cysteine proteases have also been reported to degrade complement immune factors [101].

Gal/GalNac lectin also shares similarity and cross-reactivity with CD59, allowing the parasite to circumvent some of the host complement immunity [102]. Nitric oxide and reactive oxygen species released by host neutrophils and macrophages are also utilized to defend against infection. However, *E. histolytica* kills neutrophils far more effectively [103] and express peroxidoxin, a surface protein, to provide antioxidant properties against oxidative defense [104]. Lastly, *E. histolytica* secretes amoebapore, a pore forming peptide that causes cytolysis of host and bacteria cells [105-108]. Zhang *et al.* [109] have shown amoebapore expression is required for full virulence of *E. histolytica.*

Treatment for amebiasis consist of a combination of drugs or surgical procedure. Luminal infections can be treated with oral drugs such as diloxanide furnoate,

paromomycin, and iodoquinol [82]. The drug of choice to treat invasive infection is metronidazole. Treatment is often followed by luminal drugs to prevent relapse. Tinidazol treats symptomatic infection as an alternative to metronidazol and has been shown to have a higher cure rate [110]. Percutaneous drainage can also be employ as a therapy for liver infection [111].

Metabolism

E. histolytica contains a unique metabolic system. It lacks many major components commonly present in other eukaryotes. *E. histolytica* is unable to synthesize nucleotide, fatty acids, or amino acids except for serine and cysteine [112]. Thus, scavenging plays a critical role in this organism's ability to overcome and accommodate its metabolic needs [113].

E. histolytica is capable of engulfing extracellular components through multiple means. Phagocytosis allows trophozoites to consume bacteria and solid debris during colonization of the host intestinal mucosa. Along with nutrient acquisition, phagocytosis has been associated with virulence [114, 115]. Alternatively, macropinocytosis allows *E. hisotlytica* to uptake fluid and nutrients from the environment [116]. In a recent report, *E. histolytica* was also shown to ingest host cells in fragments in a process termed trogocytosis instead of engulfing them whole. This ceases when the host cell dies [117].

E. histolytica also lacks mitochondria, a tricarboxylic acid cycle and a functional pentose phosphate pathway [118]. Instead, a closely related mitochondrial organelle called the mitosome is present. A mitosome is a metabolically specialized organelle that is

found in many pathogens occupying low oxygen environments. The central role of the mitosome in *E. histolytica* still remains undefined. However, several studies have indicated *E. histolytica's* mitosome may be involved in iron-sulfur cluster formation and sulfate activation pathways [119-121].

Due to the absence of a mitochondrion and oxidative phosphorylation, *E. histolytica* ATP synthesis is primarily restricted to substrate level phosphorylation with glycolysis as the main ATP-generating pathway [118]. Instead of having an ATP-driven phosphofructokinase, *E. histolytica* uses a PP_i–dependent phosphofructokinase (PP_i–PFK) to convert fructose-6-phosphate to fructose-1, 6-bisphosphate [122]. Similarly, a PP_i-dependent pyruvate phosphate dikinase (PPDK) replaces pyruvate kinase in the final step of glycolysis (Figure 1.4) [123].

Another deviation in this parasite's glycolytic pathway is the absence of pyruvate dehydrogenase. In its place, pyruvate:ferredoxin oxidoreductase (PFOR) extends glycolysis by catalyzing the oxidative decarboxylation of pyruvate to acetyl-CoA using ferredoxin as an electron acceptor [73]. Acetate and ATP are then released from acetyl–CoA, ADP and P_i by the catalytic activity of ADP–forming acetyl–CoA synthetase (ACD). Parallel to ACD, the bifunctional aldehyde-alcohol dehydrogenase (ADHE) converts acetyl–CoA to ethanol (EtOH) by reducing two NADH molecules per EtOH produced (Figure 1.4).

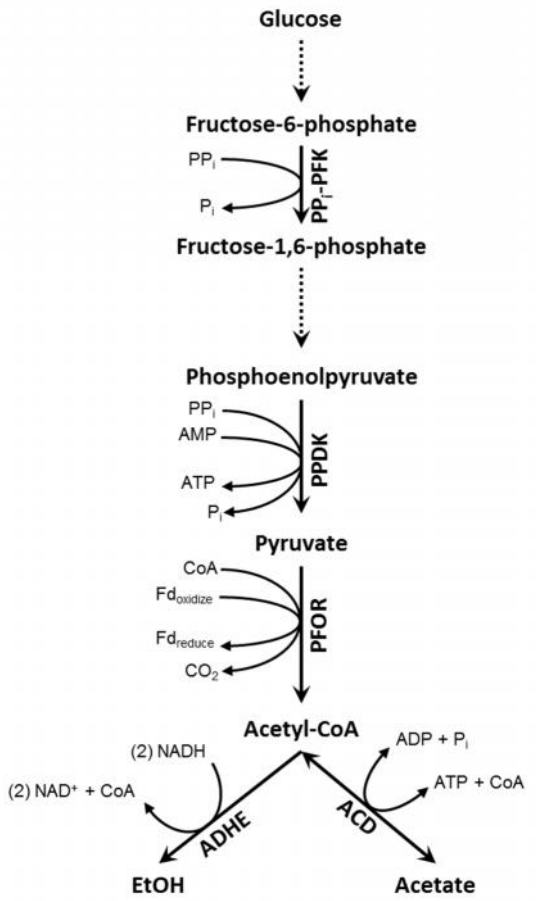

Figure 1.4: *E. histolytica* extended glycolytic pathway. PP_i-PFK: PP_i-dependent phosphofructokinase; PPDK: PP_i-dependent pyruvate phosphate dikinase; PFOR: pyruvate: ferredoxin oxidoreductase; ADHE: bifunctional alcohol-aldehyde dehydrogenase; ACD: ADP-forming acetyl-CoA synthetase; Fd: ferredoxin. Dashed arrows represent conversions carried out through several enzymatic steps.

In many organisms, glycogen metabolism contributes substantially to survival and energy metabolism during unfavorable conditions [124]. Electron microscopy revealed *E. histolytica* possesses dense glycogen granules [125]. Later NMR analyses showed a high concentration of glycogen in *E. histolytica* cell extract [126, 127]. Accordingly, *in vitro* analysis demonstrated active glycogen degradation activity from *E. histolytica* homogenate [128]. A recent report by Pineda *et al*. [129] indicates glycogen degradation can sustain cell viability for up to two hours before death occurs, suggesting glycogen plays a possible role as a source of reserve carbon in *E. histolytica.*

Amino acids catabolism has also been suggested to generate ATP in *E. hisotlytica*. In 1995, Zuo and Coombs [130] found that *E. histolytica* consumes five amino acids at a marked level: asparagine, arginine, leucine, threonine, and phenylalanine. Subsequently, genome sequences identified several enzymes capable of degrading amino acids such as asparagine, aspartate, methionine, threonine, and tryptophan to pyruvate or 2–oxobutanoate [118]. In addition to pyruvate, PFOR can also utilize 2–oxobutanoate to produce propionyl–CoA, which can then be used by ACD as a substrate for the generation of ATP and propionate (Figure 1.5) [118]. However, a recent study comparing the ATP level after incubating *E. histolytica* for two hours in PBS with and without an amino acid source concluded that amino acids do not contribute to *E. histolytica* ATP generation [129]. However, the long term influence of amino acids on ATP production remains unresolved.

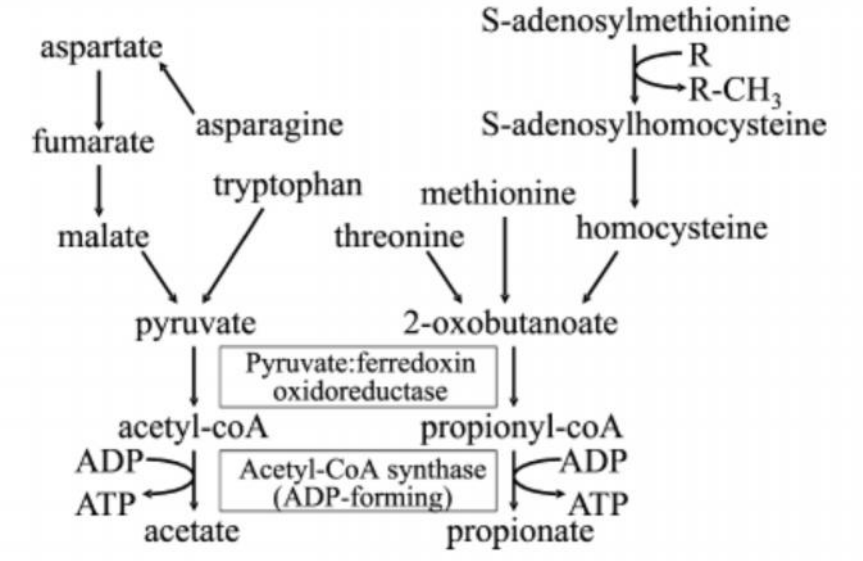

Figure 1.5: **Predicted amino acid degradation pathways in *E. histolytica*.** Several amino acids can be converted into useable substrate for pyruvate: ferredoxin oxidoreductase and ADP-forming acetyl-CoA synthetase for the generation of ATP. Figure obtained and modified with permission from [118].

Ultimately, acetate and ethanol are excreted as major end–products of energy metabolism in *E. histolytica* [73, 131]. Initial analysis indicated ethanol as the favorable product from monoxenic amoebas in anaerobic condition [131]. When exposed to oxidative stress however, acetate was shown to be the major end–product from axenic culture [73]. Pineda *et al.* (20 13) validated this finding and presented evidence pointing to ADHE inhibition by reactive oxygen species as the cause for the acetate shift.

Besides ACD, *E. histolytica* can also generate acetate from cysteine synthase and ACK (Figure 1.6). Cysteine synthase converts O-acetyl-L-serine to acetate and L-cysteine[132]. Multiple studies have shown the importance of cysteine synthesis in cellular attachment, motility, growth and oxidative stress tolerance in *E. histolytica* [133-137].

E. histolytica ACK (EhACK) is PP_i-dependent and primarily functions in the acetate/PP_i -producing direction [49, 50]. The physiological role of this enzyme still remains a mystery. One hypothesis is EhACK may act to supply PP_i for the PP_i-oriented glycolytic pathway in *E. histolytica.* To date though, a source of acetyl phosphate has not been identified and acetyl phosphate has not been detected in *E. histolytica.*

A recent study disputed this hypothesized role for EhACK. This study also argued against a possible role for EhACD in ATP production via the pyruvate to acetate pathway in *E. histolytica* [138]. However, the complete abolishment of acetate production in EhACD silenced cells indicated EhACD is the primary acetate producing pathway in E.

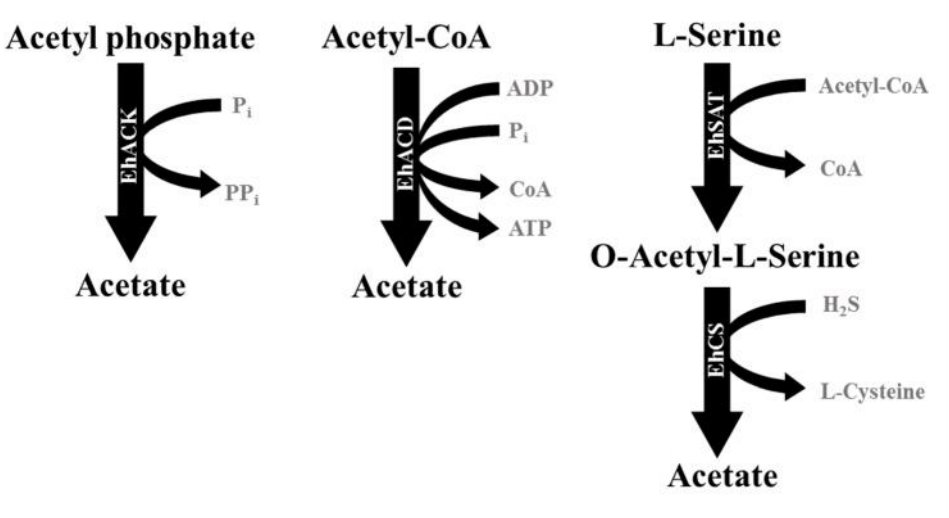

Figure 1.6: **Acetate producing pathways in *E. histolytica.*** EhACK: acetate kinase; EhACD: acetyl-CoA synthetase (ADP-forming); EhSAT: serine acetyltransferase; EhCS: cysteine synthase.

histolytica. Since EhACD converts one mole of acetyl-CoA, ADP, and P_i to one mole of CoA, ATP and acetate, an elimination of acetate production in EhACD silenced cells are expected to affect intracellular ATP concentration. Though, Pineda *et al.* [138] did not observed a change in ATP level and no glycolytic enzyme activities from cell lysate as accommodation in EhACD silenced cells. Thus, this presents an inconsistencies with existing data.

Nutrient acquisition and efficiency of energy metabolism are always proportional to fitness. Yet, our understanding regarding these topics in *E. histolytica* is still lacking and shrouded in mystery. Due to this gap in knowledge, glycolysis has long been believed to be the main ATP generating pathway even though the majority of infections reside in the glucose-limited environment of the colon. This presents a need for further studies into *E. histolytica* metabolism.

ACETATE KINASE:

Acetate kinase (ACK), a phosphotransferase, was discovered in 1944 [139] and first kinetically characterized in 1954 [140]. This enzyme catalyzes the reversible transfer of phosphate from acetyl phosphate to a phosphoryl acceptor (S), yielding acetate and a phosphorylated product (S-P) (Eq. 14).

Eq. 14: Acetyl phosphate + S ⇆ acetate + S-P

Previously, ACK's presence was believed to be limited only to microbes in the *Bacteria* and *Archaea* domains. However, in recent years ACK had also been identified in several eukaryotic microbes such as algae, some fungi, and *Entamoeba histolytica*[43]. Phosphoryl transfer is a common enzymatic occurrence within the cell, functioning from cellular signaling to energy metabolism and storage. Ordinarily, ACK produces ATP or ADP as an additional product to acetate, thus playing a role in energy conversion.

Currently, two types of ACK have been identified and characterized: ATP-dependent and pyrophosphate-dependent (PP_i) ACK. PP_i-dependent ACK is a rare isoform and at present, has only been identified in *Entamoeba histolytica*, whereas ATP-dependent ACK is widespread and found in all three domains of life.

ATP-Acetate Kinase

ACK is of major importance in prokaryote fermentative metabolism, providing an ATP-yielding pathway during anaerobic conditions. ATP-ACK converts acetyl phosphate to acetate by utilizing ADP as a phosphoryl acceptor to produce ATP (Eq. 1).

In 2001, Buss *et al.*[141] solved the first structure for the ACK from *Methanosarcina thermophila* and classified it to be a member of the acetate and sugar kinase-hsp70-actin (ASKHA) superfamily.

ACK forms a homodimer and is described to resemble a "bird with spreading wings" (Figure 1.7) [141]. The C-terminal domain of ACK composes the body of the bird and acts as the interface of dimerization between the two monomers. The N-terminal domain forms the wing portion of the bird. Both domains come together and form the active site cleft.

Members of the ASKHA superfamily are known to experience domain motion during catalysis. Gorrell *et al.* [142] previously used tryptophan fluorescence quenching to analyze MtACK domain closure upon substrate binding. Their study found domain motion only occurs upon nucleotide binding. The study also indicated that nucleotide binding to one monomer of MtACK affects nucleotide binding to the other monomer, suggesting a half-site mechanism where only one active site is substrate bound at a given time. The ACK catalytic reaction proceeds through a direct, in-line mechanism, though this has not always been the accepted truth. From early studies, two mechanisms were proposed: the direct, in-line and the triple displacement mechanisms of phosphoryl transfer.

Anthony and Spector [143] discovered *E. coli* ACK can be phosphorylated with [γ-^{32}P]-ATP or [^{32}P]-acetyl phosphate. Later, the same group demonstrated *E. coli* ACK

Figure 1.7: The structure of *Methanosarcina thermophila* acetate kinase. The two monomers are displayed in green and blue, forming a homodimer complex at the C-terminal interface. Sulfate and ADP are shown in space filling model, illustrating the active site. Figure obtained and modified from [141] with permission.

phosphoenzyme formation is dependent on the phosphorylating agent concentration and is chemically competent, being able to transfer the phosphate group to ADP to produce ATP or to acetate to produce acetyl phosphate [144]. Blattler and Knowles [145] further noted ACK phosphoryl transfer resulted in an inversion at the phosphorus atom. Based on these evidence, Spector [146] concluded ACK must proceed through multiple SN_2-displacements to be compatible with both a phosphoenzyme intermediate and an inverted phosphorus. Spector [146] proposed that ACK catalysis proceeds with two phosphoenzyme intermediates and three phosphoryl displacements, each causing a phosphate inversion event to yield a net inversion in the transfer of phosphate (Figure 1.8).

However, the phosphoenzyme transfer rate did not prove to be consistent with ACK steady state kinetics [140, 144, 147]. The triple displacement mechanism was further challenged when Fox and colleagues[148] reported the *E. coli* ACK phosphoenzyme can also reversibly transfer the phosphoryl group to Enzyme I of the phosphotransferase system. This suggested the true function of the ACK phosphoenzyme may not pertain to the conversion of acetyl phosphate to acetate.

In 1974, Todhunter and Purich [149] indicated an unspecified glutamate residue was the site of phosphorylation in *E. coli* ACK. Singh-Wissman *et al.* [150] identified five highly conserved glutamate residues (Glu-32, Glu-97, Glu-334, Glu-384, and Glu-385) in *M. thermophila* ACK (MtACK). Site-directed replacement of these residues and

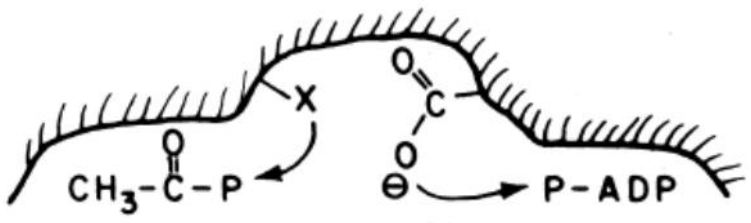

Figure 1.8: **Schematic of the proposed ACK triple displacement mechanism of phosphoryl transfer**. The γ-phosphate of ATP is transferred to a catalytic carboxyl group and is then transferred to an unknown group (X) prior to transfer to acetate. Figure obtained and modified from [146] with permission.

characterization of the variants indicated Glu-384 was essential for catalysis. Glu-385 and Glu-97, on the other hand, were found to have a role in substrate binding; alteration of Glu-385 affected both ATP and acetate binding but alteration of Glu-97 appeared to only affect acetate binding. Despite these studies, the site of glutamate phosphorylation remained unsettled.

A later study conducted by Miles *et al.* [151] confirmed the importance of Glu-384 in enzyme activity. Further analysis implicated Glu-384 in magnesium binding, as evidence by the 30-fold increase in magnesium concentration required for half-maximal activity for Glu-384-Ala variant. Additionally, Miles *et al.* noted the importance of Asn-7 and Asp-148 in catalysis [151]. Alterations at these two residues resulted in a 260 to 1800 fold reduction in k_{cat}.

The proposed direct in-line mechanism of transfer involves a single phosphate displacement event. In this mechanism, the substrates bind to ACK in a linear configuration that facilitates the direct transfer of phosphate from acetyl phosphate to ADP. This direct in-line transfer of phosphate is consistent with both steady state kinetic and stereochemistry data, providing initial support for this mechanism of transfer.

Additional studies later offered unambiguous evidence that ACK proceeds through a direct, in-line mechanism of phosphoryl transfer. Formation of an abortive complex from using ADP – AlF_3 – acetate to simulate the catalytic transition state in ACK acted as the most substantial evident for supporting this mode of transfer [152]. Employing aluminum fluoride to mimic the planar phosphoryl transition state, Miles *et*

al. [152] reported $MgCl_2$, ADP, $AlCl_3$, NaF, and acetate inhibit MtACK activity, demonstrating that the ACK catalytic transition state requires both ADP and acetate to form. Gorrell *et al.* [153] co-crystallized MtACK with acetate, ADP, Al^{3+} and F^-. The resulting structure showed ADP-AlF_3-acetate formed a linear array within the active site cleft [153]. This piece of evidence confirmed a direct in-line transfer mechanism and effectively ended the debate.

In the same study, Gorrell *et al.* [153] noted the importance of residues Arg-91 and Arg-241 in MtACK catalysis. Based on the crystal structure of MtACK, Buss *et al.* [141] proposed Arg-91 interacts with the phosphoryl group of acetyl phosphate and Arg-241 interacts with the carboxyl group of acetate. Analysis of MtACK Arg-91 and Arg-241 variants argued against a role for Arg-91 in acetyl phosphate binding [153]. A substantial increased in the K_m for acetate in both Arg-91 and Arg-241 variants supported the proposed role for Arg-241 in acetate binding and suggested Arg-91 may share a similar role. In all instances, replacing Arg-91 or Arg-241 reduced k_{cat} considerably, establishing the importance of these two residues in catalysis. These data are in accordance with a previous investigation to identify essential arginines in ACK by Singh-Wissman *et al.* [154].

Ingram-Smith *et al.* [155] identified two essential histidine residues in MtACK catalysis. Using a diethylpyrocarbonate (DEP) inactivation study, two to three histidine residues were correlated to have been modified and inactivated MtACK. Sequence alignment showed His-123, His-180, and His-208 are fully conserved in 56 ACK sequences. Structural analysis indicated His-123 and His-180 are located within MtACK

active site. Alanine variants at His-123 or His-180 showed only partial alleviation of enzyme inactivation by DEP, suggesting both sites are needed for full inactivation by DEP modification. Of the eight histidines present in MtACK, only the His-180-Ala variant proved detrimental to enzyme catalysis, reducing k_{cat} by 100 fold. Further investigation proved His-180 is important in catalysis but was not related to enzyme phosphorylation.

Based on the MtACK structure, Ingram-Smith *et al.* [156] later reported Val-93, Leu-122, Phe-179, and Pro-232 formed the hydrophobic site for acetate binding. The K_m for acetate increased 7 to 26 fold in alanine variants created at each of the four residues, indicating they do indeed play a role in acetate binding. Phe-179 also proved to be essential for catalysis, as evidence by a 480 fold decreased in k_{cat} when altered to alanine. Combined with structural modeling, hydrophobicity was reported to have a role in determining substrate selectivity, interacting with the methyl group and positioning the carboxyl group of acetate. Acetyl phosphate binding proved to not rely on hydrophobic interaction as for acetate but may depend more on the phosphoryl group interaction.

In phosphoryl substrate binding, Bork *et al.* [157] have identified three signature ATPase motifs, designated as ADENOSINE, PHOSPHATE1, and PHOSPHATE2, in the ASKHA superfamily. The PHOSPHATE2 and ADENOSINE motifs are positioned adjacent to one another on the C-terminal domain within the active site. The PHOSPHATE1 motif is located on the N-terminal domain across from the PHOSPHATE2 and ADENOSINE motifs in the active site. Together, these three motifs form the adenosine pocket and interact with ATP and ADP.

In 2014, Yoshioka *et al.* [158] examined four residues in the ADENOSINE motif and one residue in the PHOSPHATE 2 motif of *E. coli* ACK to examine their role in phosphoryl substrate determination. The candidate residues Asn-213, Gly-332, Gly-333, Ile-334 and Asn-337 were altered to the corresponding residues in EhACK (Thr, Asp, Gln, Met, and Glu, respectively). These variants displayed a rise in K_m for ATP and substantially decreased thermal stability when ATP was bound when compared to wild-type. Among 2625 ACK homologs, Yoshioka *et al.* [158] concluded Asn-337 (Glu-327 in EhACK) as the most significant out of the five sites in determining phosphoryl substrate specificity due to its high conservation in ACKs closely related to EhACK. Asp-337-Glu variant did displayed approximately 45-fold increase in K_m for ATP but only showed minor decreased in catalysis, demonstrating an inconsistency with their conclusion. Though, their data do support Gly-333 and Ile-334 playing an important role in ATP selectivity with Gly-333-Gln and Ile-334-Met variants demonstrating over a 7-fold and 9-fold increase in K_m for ATP and a 21-fold and 86-fold in k_{cat}, respectively.

Most recently, Ingram-Smith *et al.* [159] targeted Asn-211 in the PHOSPHATE2 motif, the highly conserved Gly-331 in the ADENOSINE motif, and Gly-239 to study the broad NTP utilization of MtACK. These residues were individually altered to alanine or residues present in the *E. histolytica* (Thr, Gln, Ser) or *Cryptococcus neoformans* (Ser, Gly, Gly) ACKs, respectively. The Gly-331-Gln variant displayed a notable 4.6-fold increase in the K_m for ATP and a 45-fold decrease in k_{cat}, evidence of steric hindrance impacting ATP binding and catalysis. To a lesser extent, the Gly-331-Ala alteration reduced catalysis by 8-fold and exhibited a relatively minor increase in K_m for ATP.

Alterations at Asn-211 and Gly-239 diminished enzymatic activity but did not considerably affect the K_m for ATP. The investigations by Yoshioka *et al.* [158] and Ingram-Smith *et al.*[159] demonstrated the vital role of the ADENOSINE and PHOSPHATE2 motifs in ATP binding to ACK. However, the source of phosphoryl substrate specificity determination remained unidentified.

PP_i – acetate kinase

As compare to the widespread ATP-dependent acetate kinase, *E. histolytica* possesses a more uncommon PP_i/P_i – dependent ACK. Instead of using ATP/ADP as the phosphoryl donor/acceptor, the *E. histolytica* ACK (EhACK) relies solely on PP_i/P_i as the phosphoryl donor/acceptor (Eq. 10) [49, 50]. This is the only known ACK that utilizes pyrophosphate and inorganic phosphate as a phosphoryl donor and acceptor.

EhACK was identified in 1962 and first described in 1975 by Reeves and colleagues to be PP_i/P_i – dependent [50, 160]. However, due to the molecular and biochemical limitations of the time, EhACK has only recently been thoroughly characterized biochemically and kinetically. EhACK activity was confirmed to exclusively depend on pyrophosphate and inorganic phosphate [49]. In addition, EhACK was described to also follow a direct, in-line mechanism of phosphoryl transfer and preferentially proceed in the acetate/PP_i forming direction with a k_{cat} several hundred – fold higher than that for the acetyl phosphate/P_i producing direction.

In 2013, Thaker *et al.* successfully solved the EhACK structure (Figure 1.9) [161]. The structure was compared to the well-studied, ATP–dependent MtACK. Overall, the

structure and active site of EhACK highly resembles MtACK, exhibiting a homodimeric form and resembling like a bird with spread wings [161]. However, upon closer inspection, Gly–331 and Ile–332 within the ATP binding pocket of MtACK were noted to be replaced by glutamine and methionine at the corresponding location in EhACK [161]. These differences were suggested to play a role in EhACK PP_i/P_i specificity by sterically reducing ATP binding. Furthermore, a salt bridge between aspartate–272 and arginine–274 in EhACK placed the arginine in a position that could further obstruct ATP binding (Figure 1.10). Surface representation of EhACK clearly illustrates an absent of the adenosine binding pocket due to this obstruction. However, this has not yet been experimentally examined and confirmed. Thus, the source of EhACK phosphoryl substrate selectivity remained to be confirmed.

In this thesis, I investigated the source of EhACK phosphoryl substrate specificity using the well-studied MtACK as a model for comparison. Additionally, acetate metabolism in *E. histolytica* was also explored. Specifically, I studied the physiological effects of silencing two acetate producing enzymes in this human parasite, acetate kinase and ADP-forming acetyl-CoA synthetase, to identify their roles in *E. histolytica* growth and survival. My results showed that ACD plays a role in utilization of several growth substrates in addition to glucose, whereas ACK plays a novel role unrelated to its previously proposed role in providing PPi for glycolysis.

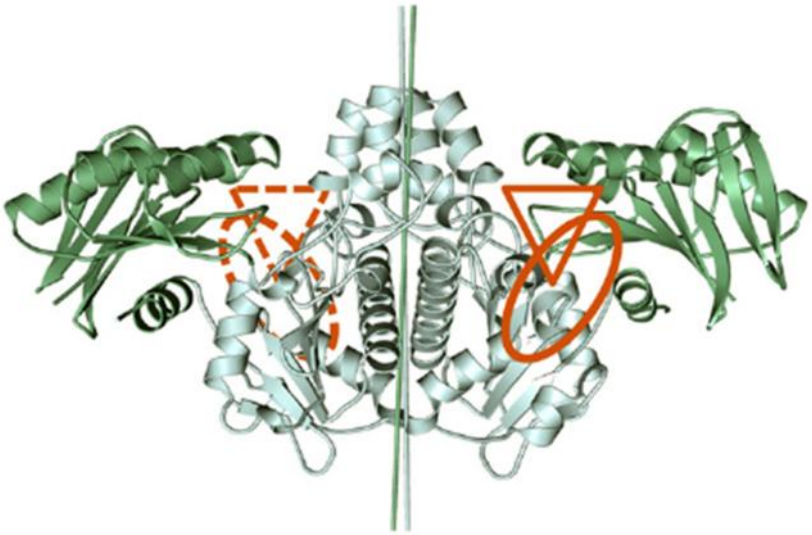

Figure 1.9: Crystal structure of *E. histolytica* ACK. The N-terminal domain is colored in green and the C-terminal domain is in cyan. The putative active site is marked by oval and triangle. Figure obtained and modified from [161] with permission.

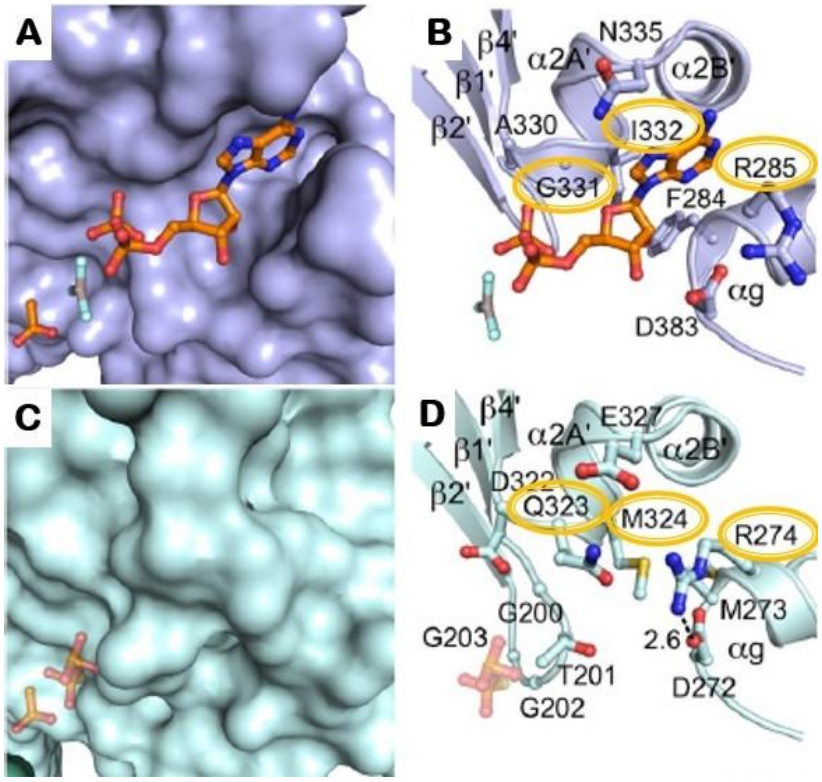

Figure 1.10: Active site architecture of MtACK and EhACK. A: Surface representation of the MtACK active site. **B:** Close up view of the ATP/ADP binding cleft of MtACK. **C:** Surface representation of the EhACK active site. **D:** Close up view of the PP_i/P_i binding site of EhACK. Residues proposed to obstruct ATP/ADP binding in EhACK are circled along with corresponding residues found in MtACK. Figure obtained and modified from [161] with permission.

REFERENCES

1. Wolfe, A. J. The acetate switch. *Microbiol Mol Biol Rev* **69**, 12-50 (2005).

2. Cummings, J. H., Pomare, E. W., Branch, W. J., Naylor, C. P. and Macfarlane, G. T. Short chain fatty acids in human large intestine, portal, hepatic and venous blood. *Gut* **28**, 1221-1227 (1987).

3. Topping, D. L. and Clifton, P. M. Short-chain fatty acids and human colonic function: Roles of resistant starch and nonstarch polysaccharides. *Physiol Rev* **81**, 1031-1064 (2001).

4. Wong, J. M., de Souza, R., Kendall, C. W., Emam, A. and Jenkins, D. J. Colonic health: Fermentation and short chain fatty acids. *J Clin Gastroenterol* **40**, 235-243 (2006).

5. Frost, G., *et al.* The short-chain fatty acid acetate reduces appetite via a central homeostatic mechanism. *Nat Commun* **5**, 3611 (2014).

6. Perry, R. J., *et al.* Acetate mediates a microbiome-brain-beta-cell axis to promote metabolic syndrome. *Nature* **534**, 213-217 (2016).

7. Comerford, S. A., *et al.* Acetate dependence of tumors. *Cell* **159**, 1591-1602 (2014).

8. Mashimo, T., *et al.* Acetate is a bioenergetic substrate for human glioblastoma and brain metastases. *Cell* **159**, 1603-1614 (2014).

9. Jaworski, D. M., Namboodiri, A. M. and Moffett, J. R. Acetate as a metabolic and epigenetic modifier of cancer therapy. *J Cell Biochem* **117**, 574-588 (2016).

10. Arpaia, N. and Rudensky, A. Y. Microbial metabolites control gut inflammatory responses. *Proc Natl Acad Sci U S A* **111**, 2058-2059 (2014).

11. Dittrich, C. R., Bennett, G. N. and San, K. Y. Characterization of the acetate-producing pathways in *Escherichia coli*. *Biotechnol Prog* **21**, 1062-1067 (2005).

12. Kumari, S., Tishel, R., Eisenbach, M. and Wolfe, A. J. Cloning, characterization, and functional expression of *acs*, the gene which encodes acetyl CoA synthetase in *Escherichia coli*. *J Bacteriol* **177**, 2878-2886 (1995).

13. Lawhon, S. D., Maurer, R., Suyemoto, M. and Altier, C. Intestinal short-chain fatty acids alter *Salmonella typhimurium* invasion gene expression and virulence through BarA/SirA. *Mol Microbiol* **46**, 1451-1464 (2002).

14. Lee, T. Y., Makino, K., Shinagawa, H. and Nakata, A. Overproduction of acetate kinase activates the phosphate regulon in the absence of the PhoR and PhoM functions in *Escherichia coli*. *J Bacteriol* **172**, 2245-2249 (1990).

15. Matsuyama, A., Yamamoto-Otake, H., Hewitt, J., MacGillivray, R. T. and Nakano, E. Nucleotide sequence of the phosphotransacetylase gene of *Escherichia coli* strain K12. *Biochim Biophys Acta* **1219**, 559-562 (1994).

16. Brown, T. D., Jones-Mortimer, M. C. and Kornberg, H. L. The enzymic interconversion of acetate and acetyl-CoA in *Escherichia coli*. *J Gen Microbiol* **102**, 327-336 (1977).

17. Bertagnolli, B. L. and Hager, L. P. Role of flavin in acetoin production by two bacterial pyruvate oxidases. *Arch Biochem Biophys* **300**, 364-371 (1993).

18. Posthuma, C. C., *et al.* Expression of the xylulose 5-phosphate phosphoketolase gene, *xpkA*, from *Lactobacillus pentosus* MD363 is induced by sugars that are fermented via the phosphoketolase pathway and is repressed by glucose mediated by CcpA and the mannose phosphoenolpyruvate phosphotransferase system. *Appl Environ Microbiol* **68**, 831-837 (2002).

19. Bruggemann, C., Denger, K., Cook, A. M. and Ruff, J. Enzymes and genes of taurine and isethionate dissimilation in *Paracoccus denitrificans*. *Microbiology* **150**, 805-816 (2004).

20. Denger, K., Ruff, J., Schleheck, D. and Cook, A. M. *Rhodococcus opacus* expresses the *xsc* gene to utilize taurine as a carbon source or as a nitrogen source but not as a sulfur source. *Microbiology* **150**, 1859-1867 (2004).

21. Ruff, J., Denger, K. and Cook, A. M. Sulphoacetaldehyde acetyltransferase yields acetyl phosphate: Purification from *Alcaligenes defragrans* and gene clusters in taurine degradation. *Biochem J* **369**, 275-285 (2003).

22. Taniai, H., *et al.* Concerted action of lactate oxidase and pyruvate oxidase in aerobic growth of *Streptococcus pneumoniae*: Role of lactate as an energy source. *J Bacteriol* **190**, 3572-3579 (2008).

23. Schäfer, T. and Schönheit, P. Pyruvate metabolism of the hyperthermophilic archaebacterium *Pyrococcus furiosus*. *Arch Microbiol* **155**, 366-377 (1991).

24. Schonheit, P. and Schafer, T. Metabolism of hyperthermophiles. *World J Microbiol Biotechnol* **11**, 26-57 (1995).

25. Schäfer, T., Selig, M. and Schönheit, P. Acetyl-CoA synthetase (ADP forming) in archaea, a novel enzyme involved in acetate formation and ATP synthesis. *Arch Microbiol* **159**, 72-83 (1993).

26. Labes, A. and Schonheit, P. Sugar utilization in the hyperthermophilic, sulfate-reducing archaeon *Archaeoglobus fulgidus* strain 7324: Starch degradation to acetate and CO_2 via a modified Embden-Meyerhof pathway and acetyl-CoA synthetase (ADP-forming). *Arch Microbiol* **176**, 329-338 (2001).

27. Brasen, C. and Schonheit, P. Unusual ADP-forming acetyl-CoA synthetases from the mesophilic halophilic euryarchaeon *Haloarcula marismortui* and from the hyperthermophilic crenarchaeon *Pyrobaculum aerophilum*. *Arch Microbiol* **182**, 277-287 (2004).

28. Musfeldt, M. and Schonheit, P. Novel type of ADP-forming acetyl CoA synthetase in hyperthermophilic archaea: Heterologous expression and characterization of isoenzymes from the sulfate reducer *Archaeoglobus fulgidus* and the methanogen *Methanococcus jannaschii*. *J Bacteriol* **184**, 636-644 (2002).

29. Awano, T., *et al.* Characterization of two members among the five ADP-forming acyl CoA synthetases reveals the presence of a 2-(imidazol-4-yl) acetyl-CoA synthetase in *Thermococcus kodakarensis*. *J Bacteriol* **196**, 140-147 (2014).

30. Schmidt, M. and Schonheit, P. Acetate formation in the photoheterotrophic bacterium *Chloroflexus aurantiacus* involves an archaeal type ADP-forming acetyl-CoA synthetase isoenzyme I. *FEMS Microbiol Lett* **349**, 171-179 (2013).

31. Fukuda, S., Toh, H., Taylor, T. D., Ohno, H. and Hattori, M. Acetate-producing bifidobacteria protect the host from enteropathogenic infection via carbohydrate transporters. *Gut Microbes* **3**, 449-454 (2012).

32. Fukuda, S., *et al.* Bifidobacteria can protect from enteropathogenic infection through production of acetate. *Nature* **469**, 543-547 (2011).

33. Nakamura, S., Morimoto, Y. V. and Kudo, S. A lactose fermentation product produced by *Lactococcus lactis* subsp. *lactis*, acetate, inhibits the motility of flagellated pathogenic bacteria. *Microbiology* **161**, 701-707 (2015).

34. McCleary, W. R., Stock, J. B. and Ninfa, A. J. Is acetyl phosphate a global signal in *Escherichia coli*? *J Bacteriol* **175**, 2793-2798 (1993).

35. Wanner, B. L. Gene regulation by phosphate in enteric bacteria. *J Cell Biochem* **51**, 47-54 (1993).

36. Lukat, G. S., McCleary, W. R., Stock, A. M. and Stock, J. B. Phosphorylation of bacterial response regulator proteins by low molecular weight phospho-donors. *Proc Natl Acad Sci USA* **89**, 718-722 (1992).

37. Feng, J., *et al.* Role of phosphorylated metabolic intermediates in the regulation of glutamine synthetase synthesis in *Escherichia coli*. *J Bacteriol* **174**, 6061-6070 (1992).

38. Xu, H., *et al.* Role of acetyl-phosphate in activation of the Rrp2-RpoN-RpoS pathway in *Borrelia burgdorferi*. *PLoS Pathogens* **6**, e1001104 (2010).

39. Gao, R., Mukhopadhyay, A., Fang, F. and Lynn, D. G. Constitutive activation of two-component response regulators: Characterization of VirG activation in *Agrobacterium tumefaciens*. *J Bacteriol* **188**, 5204-5211 (2006).

40. Wolfe, A. J., Conley, M. P. and Berg, H. C. Acetyladenylate plays a role in controlling the direction of flagellar rotation. *Proc Natl Acad Sci U S A* **85**, 6711-6715 (1988).

41. Dailey, F. E. and Berg, H. C. Change in direction of flagellar rotation in *Escherichia coli* mediated by acetate kinase. *J Bacteriol* **175**, 3236-3239 (1993).

42. Klein, A. H., Shulla, A., Reimann, S. A., Keating, D. H. and Wolfe, A. J. The intracellular concentration of acetyl phosphate in *Escherichia coli* is sufficient for direct phosphorylation of two-component response regulators. *J Bacteriol* **189**, 5574-5581 (2007).

43. Ingram-Smith, C., Martin, S. R. and Smith, K. S. Acetate kinase: Not just a bacterial enzyme. *Trends Microbiol* **14**, 249-253 (2006).

44. Mus, F., Dubini, A., Seibert, M., Posewitz, M. C. and Grossman, A. R. Anaerobic acclimation in *Chlamydomonas reinhardtii*: Anoxic gene expression, hydrogenase induction, and metabolic pathways. *J Biol Chem* **282**, 25475-25486 (2007).

45. Yang, W., *et al.* Alternative acetate production pathways in *Chlamydomonas reinhardtii* during dark anoxia and the dominant role of chloroplasts in fermentative acetate production. *Plant Cell* **26**, 4499-4518 (2014).

46. Taylor, T., Ingram-Smith, C. and Smith, K. S. Biochemical and kinetic characterization of the eukaryotic phosphotransacetylase class IIa enzyme from *Phytophthora ramorum*. *Eukaryot Cell* **14**, 652-660 (2015).

47. Ingram-Smith, C., Martin, S. R. and Smith, K. S. Acetate kinase: Not just a bacterial enzyme. *Trends Microbiol* **14,** pp 249-253 (2006).

48. Glenn, K., Ingram-Smith, C. and Smith, K. S. Biochemical and kinetic characterization of xylulose 5-phosphate/fructose 6-phosphate phosphoketolase 2 (XFP2) from *Cryptococcus neoformans*. *Eukaryot Cell* **13**, 657-663 (2014).

49. Fowler, M. L., Ingram-Smith, C. and Smith, K. S. Novel pyrophosphate-forming acetate kinase from the protist *Entamoeba histolytica*. *Eukaryot Cell* **11**, 1249-1256 (2012).

50. Reeves, R. E. and Guthrie, J. D. Acetate kinase (pyrophosphate). A fourth pyrophosphate-dependent kinase from *Entamoeba histolytica*. *Biochem Biophys Res Commun* **66**, 1389-1395 (1975).

51. Lyssiotis, C. A. and Cantley, L. C. Acetate fuels the cancer engine. *Cell* **159**, 1492-1494 (2014).

52. Watkins, P. A., Maiguel, D., Jia, Z. and Pevsner, J. Evidence for 26 distinct acyl-CoA synthetase genes in the human genome. *J Lipid Res* **48**, 2736-2750 (2007).

53. Luong, A., Hannah, V. C., Brown, M. S. and Goldstein, J. L. Molecular characterization of human acetyl-CoA synthetase, an enzyme regulated by sterol regulatory element-binding proteins. *J Biol Chem* **275**, 26458-26466 (2000).

54. Fujino, T., Kondo, J., Ishikawa, M., Morikawa, K. and Yamamoto, T. T. Acetyl-CoA synthetase 2, a mitochondrial matrix enzyme involved in the oxidation of acetate. *J Biol Chem* **276**, 11420-11426 (2001).

55. Van den Berg, M. A. and Steensma, H. Y. Acs2, a *Saccharomyces cerevisiae* gene encoding acetyl-CoA synthetase, essential for growth on glucose. *Eur J Biochem* **231**, 704-713 (1995).

56. Carman, A. J., Vylkova, S. and Lorenz, M. C. Role of acetyl CoA synthesis and breakdown in alternative carbon source utilization in *Candida albicans*. *Eukaryot Cell* **7**, 1733-1741 (2008).

57. Mazet, M., *et al.* Revisiting the central metabolism of the bloodstream forms of *Trypanosoma brucei*: Production of acetate in the mitochondrion is essential for parasite viability. *PLoS Negl Trop Dis* **7**, e2587 (2013).

58. Eisenberg, T., *et al.* Nucleocytosolic depletion of the energy metabolite acetyl-CoA stimulates autophagy and prolongs lifespan. *Cell Metab* **19**, 431-444 (2014).

59. Gao, X., *et al.* Acetate functions as an epigenetic metabolite to promote lipid synthesis under hypoxia. *Nat Commun* **7**, 11960 (2016).

60. Wellen, K. E., *et al.* ATP-citrate lyase links cellular metabolism to histone acetylation. *Science* **324**, 1076-1080 (2009).

61. Saint-Prix, F., Bonquist, L. and Dequin, S. Functional analysis of the ALD gene family of *Saccharomyces cerevisiae* during anaerobic growth on glucose: The $NADP^+$-dependent Ald6p and Ald5p isoforms play a major role in acetate formation. *Microbiology* **150**, 2209-2220 (2004).

62. Boubekeur, S., *et al.* A mitochondrial pyruvate dehydrogenase bypass in the yeast *Saccharomyces cerevisiae*. *J Biol Chem* **274**, 21044-21048 (1999).

63. Lee, F. J., Lin, L. W. and Smith, J. A. Acetyl-CoA hydrolase involved in acetate utilization in *Saccharomyces cerevisiae*. *Biochim Biophys Acta* **1297**, 105-109 (1996).

64. Chen, Y., Zhang, Y., Siewers, V. and Nielsen, J. Ach1 is involved in shuttling mitochondrial acetyl units for cytosolic C2 provision in *Saccharomyces cerevisiae* lacking pyruvate decarboxylase. *FEMS Yeast Res* **15**(2015).

65. Atteia, A., van Lis, R., Tielens, A. G. and Martin, W. F. Anaerobic energy metabolism in unicellular photosynthetic eukaryotes. *Biochim Biophys Acta* **1827**, 210-223 (2013).

66. Muller, M. and Lindmark, D. G. Respiration of hydrogenosomes of *Tritrichomonas foetus*. Ii. Effect of coa on pyruvate oxidation. *J Biol Chem* **253**, 1215-1218 (1978).

67. Steinbuchel, A. and Muller, M. Anaerobic pyruvate metabolism of *Tritrichomonas foetus* and *Trichomonas vaginalis* hydrogenosomes. *Mol Biochem Parasitol* **20**, 57-65 (1986).

68. Barrett, J., Coles, G. C. and Simpkin, K. G. Pathways of acetate and propionate production in adult *Fasciola hepatica*. *Int J Parasitol* **8**, 117-123 (1978).

69. van Vugt, F., van der Meer, P. and van den Bergh, S. G. The formation of propionate and acetate as terminal processes in the energy metabolism of the adult liver fluke *Fasciola hepatica*. *Int J Biochem* **10**, 11-18 (1979).

70. Saz, H. J., deBruyn, B. and de Mata, Z. Acyl-CoA transferase activities in homogenates of *Fasciola hepatica* adults. *J Parasitol* **82**, 694-696 (1996).

71. Van Hellemond, J. J., Opperdoes, F. R. and Tielens, A. G. Trypanosomatidae produce acetate via a mitochondrial acetate:Succinate CoA transferase. *Proc Natl Acad Sci U S A* **95**, 3036-3041 (1998).

72. Marvin-Sikkema, F. D., Pedro Gomes, T. M., Grivet, J. P., Gottschal, J. C. and Prins, R. A. Characterization of hydrogenosomes and their role in glucose metabolism of *Neocallimastix* sp. L2. *Arch Microbiol* **160**, 388-396 (1993).

73. Reeves, R. E., Warren, L. G., Susskind, B. and Lo, H. S. An energy-conserving pyruvate-to-acetate pathway in *Entamoeba histolytica*. Pyruvate synthase and a new acetate thiokinase. *J Biol Chem* **252**, 726-731 (1977).

74. Lindmark, D. G. Energy metabolism of the anaerobic protozoon *Giardia lamblia*. *Mol Biochem Parasitol* **1**, 1-12 (1980).

75. Sanchez, L. B. and Muller, M. Purification and characterization of the acetate forming enzyme, acetyl-CoA synthetase (ADP-forming) from the amitochondriate protist, *Giardia lamblia*. *FEBS Lett* **378**, 240-244 (1996).

76. Jones, C. P. and Ingram-Smith, C. Biochemical and kinetic characterization of the recombinant ADP-forming acetyl coenzyme a synthetase from the amitochondriate protozoan *Entamoeba histolytica*. *Eukaryot Cell* **13**, 1530-1537 (2014).

77. Sanchez, L. B., Galperin, M. Y. and Muller, M. Acetyl-CoA synthetase from the amitochondriate eukaryote *Giardia lamblia* belongs to the newly recognized superfamily of acyl-CoA synthetases (nucleoside diphosphate-forming). *J Biol Chem* **275**, 5794-5803 (2000).

78. Stechmann, A., *et al.* Organelles in *Blastocystis* that blur the distinction between mitochondria and hydrogenosomes. *Curr Biol* **18**, 580-585 (2008).

79. Fotedar, R., *et al.* Laboratory diagnostic techniques for *Entamoeba* species. *Clin Microbiol Rev* **20**, 511-532(2007).

80. CDC. Amebiasis. https://www.cdc.gov/dpdx/amebiasis/ (2010).

81. Verweij, J. J., *et al. Entamoeba histolytica* infections in captive primates. *Parasitol Res* **90**, 100-103 (2003).

82. Petri, W. A., Jr. and Singh, U. Diagnosis and management of amebiasis. *Clin Infect Dis* **29**, 1117-1125 (1999).

83. Lohia, A. The cell cycle of *Entamoeba histolytica*. *Mol Cell Biochem* **253**, 217-222 (2003).

84. Ghosh, S. K., *et al.* Chitinase secretion by encysting *Entamoeba invadens* and transfected *Entamoeba histolytica* trophozoites: Localization of secretory vesicles, endoplasmic reticulum, and golgi apparatus. *Infect Immun* **67**, 3073-3081 (1999).

85. Vazquezdelara-Cisneros, L. G. and Arroyo-Begovich, A. Induction of encystation of *Entamoeba invadens* by removal of glucose from the culture medium. *J Parasitol* **70**, 629-633 (1984).

86. Bailey, G. B. and Rengypian, S. Osmotic stress as a factor controlling encystation of *Entamoeba invadens*. *Arch Invest Med (Mex)* **11**, 11-16 (1980).

87. Avron, B., Stolarsky, T., Chayen, A. and Mirelman, D. Encystation of *Entamoeba invadens* IP-1 is induced by lowering the osmotic pressure and depletion of nutrients from the medium. *J Protozool* **33**, 522-525 (1986).

88. Sanchez, L., Enea, V. and Eichinger, D. Identification of a developmentally regulated transcript expressed during encystation of *Entamoeba invadens*. *Mol Biochem Parasitol* **67**, 125-135 (1994).

89. Coppi, A., Merali, S. and Eichinger, D. The enteric parasite *Entamoeba* uses an autocrine catecholamine system during differentiation into the infectious cyst stage. *J Biol Chem* **277**, 8083-8090 (2002).

90. Mi-ichi, F., *et al. Entamoeba* mitosomes play an important role in encystation by association with cholesteryl sulfate synthesis. *Proc Natl Acad Sci U S A* **112**, E2884-2890 (2015).

91. Singh, M., Sharma, S., Bhattacharya, A. and Tatu, U. Heat shock protein 90 regulates encystation in *Entamoeba*. *Front Microbiol* **6**, 1125 (2015).

92. Samanta, S. K. and Ghosh, S. K. The chitin biosynthesis pathway in *Entamoeba* and the role of glucosamine-6-P isomerase by RNA interference. *Mol Biochem Parasitol* **186**, 60-68 (2012).

93. Villagomez-Castro, J. C., Calvo-Mendez, C. and Lopez-Romero, E. Chitinase activity in encysting *Entamoeba invadens* and its inhibition by allosamidin. *Mol Biochem Parasitol* **52**, 53-62 (1992).

94. Segovia-Gamboa, N. C., *et al. Entamoeba invadens*, encystation process and enolase. *Exp Parasitol* **125**, 63-69 (2010).

95. Segovia-Gamboa, N. C., *et al.* Differentiation of *Entamoeba histolytica*: A possible role for enolase. *Exp Parasitol* **129**, 65-71 (2011).

96. Chadee, K., Petri, W. A., Innes, D. J. and Ravdin, J. I. Rat and human colonic mucins bind to and inhibit adherence lectin of *Entamoeba histolytica*. *J Clin Invest* **80**, 1245-1254 (1987).

97. Lidell, M. E., Moncada, D. M., Chadee, K. and Hansson, G. C. *Entamoeba histolytica* cysteine proteases cleave the Muc2 mucin in its C-terminal domain and dissolve the protective colonic mucus gel. *Proc Natl Acad Sci U S A* **103**, 9298-9303 (2006).

98. Bansal, D., *et al.* An ex-vivo human intestinal model to study *Entamoeba histolytica* pathogenesis. *PLoS Negl Trop Dis* **3**, e551 (2009).

99. Petri, W. A., Jr., Haque, R. and Mann, B. J. The bittersweet interface of parasite and host: Lectin-carbohydrate interactions during human invasion by the parasite *Entamoeba histolytica*. *Annu Rev Microbiol* **56**, 39-64 (2002).

100. Serrano-Luna, J., Pina-Vazquez, C., Reyes-Lopez, M., Ortiz-Estrada, G. and de la Garza, M. Proteases from *Entamoeba* spp. And pathogenic free-living amoebae as virulence factors. *J Trop Med* **2013**, 890603 (2013).

101. Reed, S. L., *et al.* The extracellular neutral cysteine proteinase of *Entamoeba histolytica* degrades anaphylatoxins C3a and C5a. *J Immunol* **155**, 266-274 (1995).

102. Braga, L. L., *et al.* Inhibition of the complement membrane attack complex by the galactose-specific adhesion of *Entamoeba histolytica*. *J Clin Invest* **90**, 1131-1137 (1992).

103. Guerrant, R. L., Brush, J., Ravdin, J. I., Sullivan, J. A. and Mandell, G. L. Interaction between *Entamoeba histolytica* and human polymorphonuclear neutrophils. *J Infect Dis* **143**, 83-93 (1981).

104. Davis, P. H., Zhang, X., Guo, J., Townsend, R. R. and Stanley, S. L., Jr. Comparative proteomic analysis of two *Entamoeba histolytica* strains with different virulence phenotypes identifies peroxiredoxin as an important component of amoebic virulence. *Mol Microbiol* **61**, 1523-1532 (2006).

105. Andra, J., Herbst, R. and Leippe, M. Amoebapores, archaic effector peptides of protozoan origin, are discharged into phagosomes and kill bacteria by permeabilizing their membranes. *Dev Comp Immunol* **27**, 291-304 (2003).

106. Berninghausen, O. and Leippe, M. Necrosis versus apoptosis as the mechanism of target cell death induced by *Entamoeba histolytica*. *Infect Immun* **65**, 3615-3621 (1997).

107. Bracha, R., Nuchamowitz, Y., Leippe, M. and Mirelman, D. Antisense inhibition of amoebapore expression in *Entamoeba histolytica* causes a decrease in amoebic virulence. *Mol Microbiol* **34**, 463-472 (1999).

108. Leippe, M., Andra, J., Nickel, R., Tannich, E. and Muller-Eberhard, H. J. Amoebapores, a family of membranolytic peptides from cytoplasmic granules of *Entamoeba histolytica*: Isolation, primary structure, and pore formation in bacterial cytoplasmic membranes. *Mol Microbiol* **14**, 895-904 (1994).

109. Zhang, X., *et al.* Expression of amoebapores is required for full expression of *Entamoeba histolytica* virulence in amebic liver abscess but is not necessary for the induction of inflammation or tissue damage in amebic colitis. *Infection and Immunity* **72**, 678-683 (2004).

110. Swami, B., Lavakusulu, D. and Devi, C. S. Tinidazole and metronidazole in the treatment of intestinal amoebiasis. *Curr Med Res Opin* **5**, 152-156 (1977).

111. Tandon, A., Jain, A. K., Dixit, V. K., Agarwal, A. K. and Gupta, J. P. Needle aspiration in large amoebic liver abscess. *Trop Gastroenterol* **18**, 19-21 (1997).

112. Marie, C. and Petri Jr, W. A. Regulation of virulence of *Entamoeba histolytica*. *Annu Rev Microbiol* (2014).

113. Loftus, B., *et al.* The genome of the protist parasite *Entamoeba histolytica*. *Nature* **433**, 865-868 (2005).

114. Rodriguez, M. A. and Orozco, E. Isolation and characterization of phagocytosis- and virulence-deficient mutants of *Entamoeba histolytica*. *J Infect Dis* **154**, 27-32 (1986).

115. Olivos-Garcia, A., *et al.* Cysteine proteinase activity is required for survival of the parasite in experimental acute amoebic liver abscesses in hamsters. *Parasitology* **129**, 19-25 (2004).

116. Meza, I. and Clarke, M. Dynamics of endocytic traffic of *Entamoeba histolytica* revealed by confocal microscopy and flow cytometry. *Cell Motil Cytoskeleton* **59**, 215-226 (2004).

117. Ralston, K. S., *et al.* Trogocytosis by *Entamoeba histolytica* contributes to cell killing and tissue invasion. *Nature* **508**, 526-530 (2014).

118. Anderson, I. J. and Loftus, B. J. *Entamoeba histolytica*: Observations on metabolism based on the genome sequence. *Exp Parasitol* **110**, 173-177 (2005).

119. Mi-ichi, F., Abu Yousuf, M., Nakada-Tsukui, K. and Nozaki, T. Mitosomes in *Entamoeba histolytica* contain a sulfate activation pathway. *Proc Natl Acad Sci U S A* **106**, 21731-21736 (2009).

120. Mi-ichi, F., Nozawa, A., Yoshida, H., Tozawa, Y. and Nozaki, T. Evidence that the *Entamoeba histolytica* mitochondrial carrier family links mitosomal and cytosolic pathways through exchange of 3'-phosphoadenosine 5'-phosphosulfate and ATP. *Eukaryot Cell* **14**, 1144-1150 (2015).

121. Nyvltova, E., *et al.* NIF-type iron-sulfur cluster assembly system is duplicated and distributed in the mitochondria and cytosol of *Mastigamoeba balamuthi*. *Proc Natl Acad Sci U S A* **110**, 7371-7376 (2013).

122. Reeves, R. E., South, D. J., Blytt, H. J. and Warren, L. G. Pyrophosphate:D-fructose 6-phosphate 1-phosphotransferase. A new enzyme with the glycolytic function of 6-phosphofructokinase. *J Biol Chem* **249**, 7737-7741 (1974).

123. Reeves, R. E. A new enzyme with the glycolytic function of pyruvate kinase. *J Biol Chem* **243**, 3202-3204 (1968).

124. Grundel, M., Scheunemann, R., Lockau, W. and Zilliges, Y. Impaired glycogen synthesis causes metabolic overflow reactions and affects stress responses in the cyanobacterium *Synechocystis* sp. Pcc 6803. *Microbiology* **158**, 3032-3043 (2012).

125. Rosenbaum, R. M. and Wittner, M. Ultrastructure of bacterized and axenic trophozoites of *Entamoeba histolytica* with particular reference to helical bodies. *J Cell Biol* **45**, 367-382 (1970).

126. Bakker-Grunwald, T., Martin, J. B. and Klein, G. Characterization of glycogen and amino acid pool of *Entamoeba histolytica* by 13C-NMR spectroscopy. *J Eukaryot Microbiol* **42**, 346-349 (1995).

127. Saavedra, E., *et al.* Kinetic modeling can describe *in vivo* glycolysis in *Entamoeba histolytica*. *FEBS J***274**, 4922-4940 (2007).

128. Werries, E., Franz, A. and Geisemeyer, S. Detection of glycogen-debranching system in trophozoites of *Entamoeba histolytica*. *J Protozool* **37**, 576-580 (1990).

129. Pineda, E., *et al. In vivo* identification of the steps that control energy metabolism and survival of *Entamoeba histolytica*. *FEBS J* **282**, 318-331 (2015).

130. Zuo, X. and Coombs, G. H. Amino acid consumption by the parasitic, amoeboid protists *Entamoeba histolytica* and *Entamoeba invadens. FEMS Microbiol Lett* **130**, 253-258 (1995).

131. Montalvo, F. E., Reeves, R. E. and Warren, L. G. Aerobic and anaerobic metabolism in *Entamoeba histolytica*. *Exp Parasitol* **30**, 249-256 (1971).

132. Nozaki, T., *et al.* Molecular cloning and characterization of the genes encoding two isoforms of cysteine synthase in the enteric protozoan parasite *Entamoeba histolytica*. *Mol Biochem Parasitol* **97**(1998).

133. Fahey, R. C., Newton, G. L., Arrick, B., Overdank-Bogart, T. and Aley, S. B. *Entamoeba histolytica*: A eukaryote without glutathione metabolism. *Science* **224**, 70-72 (1984).

134. Gillin, F. D. and Diamond, L. S. Attachment of *Entamoeba histolytica* to glass in a defined maintenance medium: Specific requirement for cysteine and ascorbic acid. *J Protozool* **27**(1980).

135. Gillin, F. D. and Diamond, L. S. *Entamoeba histolytica* and *Giardia lamblia*: Effects of cysteine and oxygen tension on trophozoite attachment to glass and survival in culture media. *Exp Parasitol* **52**(1981).

136. Jeelani, G., *et al.* Two atypical L-cysteine-regulated NADPH-dependent oxidoreductases involved in redox maintenance, L-cystine and iron reduction, and metronidazole activation in the enteric protozoan *Entamoeba histolytica*. *J Biol Chem* **285**, 26889-26899 (2010).

137. Husain, A., Jeelani, G., Sato, D. and Nozaki, T. Global analysis of gene expression in response to L-cysteine deprivation in the anaerobic protozoan parasite *Entamoeba histolytica*. *BMC Genomics* **12**, 275 (2011).

138. Pineda, E., *et al.* Roles of acetyl-CoA synthetase (ADP-forming) and acetate kinase (PP_i-forming) in ATP and PP_i supply in *Entamoeba histolytica*. *Biochim Biophys Acta* **1860**, 1163-1172 (2016).

139. Lipmann, F. Enzymatic synthesis of acetyl phosphate. *J Biol Chem* **155**, 55-70 (1944).

140. Rose, I. A., Grunberg-Manago, M., Korey, S. R. and Ochoa, S. Enzymatic phosphorylation of acetate. *J Biol Chem* **211**, 737-756 (1954).

141. Buss, K. A., *et al.* Urkinase: Structure of acetate kinase, a member of the ASKHA superfamily of phosphotransferases. *J Bacteriol* **183**, 680-686 (2001).

142. Gorrell, A. and Ferry, J. G. Investigation of the *Methanosarcina thermophila* acetate kinase mechanism by fluorescence quenching. *Biochemistry* **46**, 14170-14176 (2007).

143. Anthony, R. S. and Spector, L. B. A phosphoenzyme intermediary in acetate kinase action. *J Biol Chem* **245**, 6739-6741 (1970).

144. Anthony, R. S. and Spector, L. B. Exchange reactions catalyzed by acetate kinase. *J Biol Chem* **246**, 6129-6135 (1971).

145. Blattler, W. A. and Knowles, J. R. Stereochemical course of phosphokinases. The use of adenosine [gamma-(s)-16O,17O,18O] triphosphate and the mechanistic consequences for the reactions catalyzed by glycerol kinase, hexokinase, pyruvate kinase, and acetate kinase. *Biochemistry* **18**, 3927-3933 (1979).

146. Spector, L. B. Acetate kinase: A triple-displacement enzyme. *Proc Natl Acad Sci U S A* **77**, 2626-2630 (1980).

147. Janson, C. A. and Cleland, W. W. The inhibition of acetate, pyruvate, and 3-phosphogylcerate kinases by chromium adenosine triphosphate. *J Biol Chem* **249**, 2567-2571 (1974).

148. Fox, D. K., Meadow, N. D. and Roseman, S. Phosphate transfer between acetate kinase and Enzyme I of the bacterial phosphotransferase system. *J Biol Chem* **261**, 13498-13503 (1986).

149. Todhunter, J. A. and Purich, D. L. Evidence for the formation of a γ-phosphorylated glutamyl residue in the *Escherichia coli* acetate kinase reaction. *Biochem Biophys Res Commun* **60**, 273-280 (1974).

150. Singh-Wissmann, K., Ingram-Smith, C., Miles, R. D. and Ferry, J. G. Identification of essential glutamates in the acetate kinase from *Methanosarcina thermophila*. *J Bacteriol* **180**, 1129-1134 (1998).

151. Miles, R. D., Iyer, P. P. and Ferry, J. G. Site-directed mutational analysis of active site residues in the acetate kinase from *Methanosarcina thermophila*. *J Biol Chem* **276**, 45059-45064 (2001).

152. Miles, R. D., Gorrell, A. and Ferry, J. G. Evidence for a transition state analog, MgADP-aluminum fluoride-acetate, in acetate kinase from *Methanosarcina thermophila*. *J Biol Chem* **277**, 22547-22552 (2002).

153. Gorrell, A., Lawrence, S. H. and Ferry, J. G. Structural and kinetic analyses of arginine residues in the active site of the acetate kinase from *Methanosarcina thermophila*. *J Biol Chem* **280**, 10731-10742 (2005).

154. Singh-Wissmann, K., Miles, R. D., Ingram-Smith, C. and Ferry, J. G. Identification of essential arginines in the acetate kinase from *Methanosarcina thermophila*. *Biochemistry* **39**, 3671-3677 (2000).

155. Ingram-Smith, C., Barber, R. D. and Ferry, J. G. The role of histidines in the acetate kinase from *Methanosarcina thermophila*. *J Biol Chem* **275**, 33765-33770 (2000).

156. Ingram-Smith, C., *et al.* Characterization of the acetate binding pocket in the *Methanosarcina thermophila* acetate kinase. *J Bacteriol* **187**, 2386-2394 (2005).

157. Bork, P., Sander, C. and Valencia, A. An ATPase domain common to prokaryotic cell cycle proteins, sugar kinases, actin, and hsp70 heat shock proteins. *Proc Natl Acad Sci U S A* **89**, 7290-7294 (1992).

158. Yoshioka, A., Murata, K. and Kawai, S. Structural and mutational analysis of amino acid residues involved in ATP specificity of *Escherichia coli* acetate kinase. *J Biosci Bioeng* **118**, 502-507 (2014).

159. Ingram-Smith, C., *et al.* The role of active site residues in ATP binding and catalysis in the *Methanosarcina thermophila* acetate kinase. *Life (Basel)* **5**, 861-871 (2015).

160. Bragg, P. D. and Reeves, R. E. Pathways of glucose dissimilation in Laredo strain of *Entamoeba histolytica*. *Exp Parasitol* **12**, 393-400 (1962).

161. Thaker, T. M., *et al.* Crystal structures of acetate kinases from the eukaryotic pathogens *Entamoeba histolytica* and *Cryptococcus neoformans*. *J Struct Biol* **181**, 185-189 (2013).

CHAPTER II

INVESTIGATION OF PYROPHOSPHATE VERSUS ATP SUBSTRATE SELECTION IN THE *ENTAMOEBA HISTOLYTICA* ACETATE KINASE

Thanh Dang and Cheryl Ingram-Smith

ABSTRACT:

Acetate kinase (ACK; E.C. 2.7.2.1), which catalyzes the interconversion of acetate and acetyl phosphate, is nearly ubiquitous in bacteria but is present only in one genus of archaea and certain eukaryotic microbes. All ACKs utilize ATP/ADP as the phosphoryl donor/acceptor in the respective directions of the reaction (acetate + ATP ⇆ acetyl phosphate + ADP), with the exception of the *Entamoeba histolytica* ACK (EhACK) which uses pyrophosphate (PP_i)/inorganic phosphate (P_i) (acetyl phosphate + P_i ⇆ acetate + PP_i. Structural analysis and modeling of EhACK indicated steric hindrance by active site residues constricts entry to the adenosine pocket as compared to ATP-utilizing *Methanosarcina thermophila* ACK (MtACK). Reciprocal alterations were made to enlarge the adenosine pocket of EhACK and reduce that of MtACK. The EhACK variants showed a step-wise increase in ADP and ATP binding but were still unable to use these as substrates, and enzymatic activity with P_i/PP_i was negatively impacted. Consistent with this, ATP utilization by MtACK variants was negatively affected but the alterations were not sufficient to convert this enzyme to P_i/PP_i utilization. Our results suggest that controlling access to the adenosine pocket can contribute to substrate specificity but is not the sole determinant.

INTRODUCTION:

Acetate kinase (ACK; E.C. 2.7.2.1) catalyzes the reversible transfer of phosphate from acetyl phosphate to a phosphoryl acceptor (S), yielding acetate and a phosphorylated product (S–P) [Eq.1]. ACK, nearly ubiquitous in bacteria, has been identified in just a single genus of archaea, *Methanosarcina*. In recent years, ACK has also been identified in certain eukaryotic microbes including the green algae *Chlamydomonas*, euascomycete and basidiomycete fungi, and certain protists, namely *Entamoeba histolytica* [(1)].

[Eq. 1] Acetyl phosphate + S ⇆ acetate + S-P

This enzyme was discovered in 1944 [(2)] and the first kinetic characterization was reported in 1954 [(3)]. In 2001, Buss *et al.* solved the structure for the *Methanosarcina thermophila* ACK (MtACK), and subsequent studies with this archaeal enzyme determined that ACK proceeds through a direct in-line mechanism of phosphoryl transfer [(4-6)]. Acyl substrate selection in ACK has been studied in the *Methanosarcina* enzyme. Four key residues, Val^{93}, Leu^{122}, Phe^{179}, and Pro^{232}, have been shown to form a hydrophobic pocket for acetate binding [(7)] which were implicated in acyl substrate selection in this enzyme. In particular, Val^{93} appears to play an important role in limiting substrate length.

Ordinarily, ACK utilizes ATP/ADP as phosphoryl donor/acceptor; however, the *E. histolytica* enzyme is unusual in that it is PP_i–dependent. Instead of using ATP/ADP as the phosphoryl donor/acceptor [Eq. 2], *E. histolytica* ACK (EhACK) can only use pyrophosphate (PP_i)/inorganic phosphate (P_i) as the phosphoryl donor/acceptor [Eq.3] [(8-10)].

[Eq. 2] Acetyl phosphate + ADP ⇆ acetate + ATP

[Eq. 3] Acetyl phosphate + P_i ⇆ acetate + PP_i

Whereas most ATP-dependent ACKs function in both directions of the reaction, the *E. histolytica* enzyme strongly prefers the acetate-forming direction [8-10]. Double reciprocal plots of substrate concentration versus enzyme activity indicated EhACK follows a ternary–complex mechanism [8-10], supporting a direct in-line mechanism of phosphoryl transfer as seen for MtACK [4-6]. Currently, EhACK is the only known ACK to utilize pyrophosphate or inorganic phosphate as a phosphoryl donor or acceptor instead of ATP/ADP.

ACK belongs to the ASKHA (acetate, sugar kinase, heat shock and actin) enzyme superfamily. In 1992, Bork *et al.* identified PHOSPHATE1, PHOSPHATE2 and ADENOSINE as three signature ATPase motifs shared by members of this superfamily [11]. These three conserved motifs form part of the adenosine binding pocket and are directly involved in ATP binding. Thaker *et al.* solved the EhACK structure and noted two amino acids substitutions in the ADENOSINE motif versus MtACK that may sterically hinder ATP binding [12].

Here, we investigated the role of residues in the ADENOSINE and PHOSPHATE2 motifs in phosphoryl substrate selection and utilization in ACK. Our results indicated that the adenosine pocket and the ADENOSINE motif play a critical role in ATP binding. However, ATP binding alone did not lead to utilization. Thus, although EhACK shares

strong similarities with ATP-dependent ACKs, subtle differences have dramatically shaped its identity and function.

MATERIALS AND METHODS:

Materials

Chemicals were purchased from Sigma-Aldrich, VWR International, Gold Biotechnology, Fisher Scientific, and Life Technologies. Oligonucleotide primers were purchased from Integrated DNA Technologies.

Site-directed mutagenesis

Site-directed mutagenesis of the *E. histolytica ack (ehack)* and *M. thermophila ack (mtack)* genes was performed according to manufacturer's instructions with the QuikChange II kit (Agilent Technologies, CA, USA). The altered sequences were confirmed by sequencing at the Clemson University Genomics Institute. Mutagenesis primers used are shown in Table 2.1.

Recombinant protein production

EhACK and its variants were produced in *Escherichia coli* strain YBS121 Δ*ack* Δ*pta* carrying the pREP4 plasmid containing the *lacI* gene and purified as described in Fowler *et al*. [(9)]. MtACK and its variants were produced in *E. coli* Rosetta2 (DE3) pLysS and purified as described in Fowler *et al*. [(9)]. Purified enzymes were dialyzed overnight in 25 mM Tris–HCl, 150 mM NaCl, and 10% glycerol (pH 7.4), aliquoted, and stored at -80ºC. Recombinant enzymes were examined by SDS–PAGE and estimated to be greater than 95% pure. Protein concentration was measured by absorbance at 280nm using Take3 micro–volume plate (Biotek, VT, USA).

EhACK primers	
$Q^{323}G$-$M^{324}I$ F	5’GATCTTTTAGTATTTACTGATGGCATCGGATTAGAAGTTTGGCAAGTACG
$Q^{323}G$-$M^{324}I$ R	5’CGTACTTGCCAAACTTCTAATCCGATGCCATCAGTAAATACTAAAAGATC
$Q^{323}A$-$M^{324}A$ F	5’GATCTTTTAGTATTTACTGATGCCGCGGGATTAGAAGTTTGGCAAGTACG
$Q^{323}A$-$M^{324}A$ R	5’CGTACTTGCCAAACTTCTAATCCCGCGGCATCAGTAAATACTAAAAGATC
$D^{272}A$-$R^{274}A$ F	5’GGTGTTAGTGAATTATCTAGTGCTATGGCAGATATTTTACATGAAATAG
$D^{272}A$-$R^{274}A$ R	5'CTATTTCATGTAAAATATCTGCCATAGCACTAGATAATTCACTAACACC
G^{203} Deletion F	5’GCTTGTCATCTTGGAACAGGTTCTAGTTGTTGTGGCATTGTTAATGG
G^{203} Deletion R	5’CCATTAACAATGCCACAACAACTAGAACCTGTTCCAAGATGACAAGC

MtACK primers	
$G^{331}Q$-$I^{332}M$ F	5’ GCAGTGGTCTTTACTGCACAGATGGGAGAAAACAGCGCAAGC
$G^{331}Q$-$I^{332}M$ R	5’ GCTTGCGCTGTTTTCTCCCATCTGTGCAGTAAAGACCACTGC

Table 2.1: Primers used for mutagenesis.

Determination of kinetic parameters

Kinetic parameters for the EhACK enzymes were determined using the colorimetric hydroxamate assay for the acetyl phosphate-forming direction [2, 3, 17] and the reverse modified hydroxamate assay [9, 22] for the acetate-forming direction as previously described [9]. In the acetyl phosphate-forming direction, activities for EhACK and its variants were assayed in a mixture containing 100mM morpholinoethanesulfonic acid (pH 5.5), 5 mM $MgCl_2$, and 600 mM hydroxylamine hydrochloride (pH 7.5) with varying concentrations of acetate and sodium pyrophosphate. Reactions were performed at 45°C. For the acetate-forming direction, kinetic parameters were determined in a mixture of 100 mM Tris–HCl (pH 7.0) and 10 mM $MgCl_2$ with varying concentrations of sodium phosphate and acetyl phosphate. Enzymatic reactions were performed at 37°C.

The acetyl phosphate produced (acetyl phosphate-forming direction) or remaining (acetate-forming direction) was reacted with hydroxylamine to produced acetyl hydroxamate, which was then was converted to a ferric hydroxamate complex by reaction with an acidic ferric chloride solution, making the solution change from a yellow to brownish red color that can detected spectrophotometrically at 540 nm. Acetyl phosphate formation or depletion was determined by measuring the absorbance at 540 nm with an Epoch microplate spectrophotometer (Biotek) and comparison to an acetyl phosphate standard curve. Kinetic data were fit to the Michaelis-Menten equation by nonlinear regression using KaleidaGraph (Synergy Software) for determination of apparent kinetic parameters.

Similarly, kinetic parameters for MtACK and its variants were determined using the hydroxamate assay [2, 3, 17] and the reverse modified hydroxamate assay [9, 22] as previously described. In the acetate-forming direction, enzyme activities were determined in 100 mM Tris (pH 7.5) with varying concentrations of MgADP and acetyl phosphate. For the acetyl phosphate-forming direction, kinetic parameters were determined in 100 mM Tris (pH 7.5) and 600 mM hydroxylamine (pH 7.5) with varying concentrations of acetate and MgATP. Enzymatic reactions were performed at 37°C.

Acetyl phosphate formation and depletion were determined by measuring the absorbance at 540 nm with an Epoch microplate spectrophotometer (Biotek) and comparison to an acetyl phosphate standard curve. Kinetic data were fit to the Michaelis-Menten equation by nonlinear regression using KaleidaGraph (Synergy Software) for determination of apparent kinetic parameters.

Determination of inhibition parameters

Inhibition of EhACK by ATP and ADP and of MtACK by PP_i was determined using the hydroxamate and reverse modified hydroxamate assays as described above. All inhibition assays were performed using substrates at their K_m concentrations, with the exception of acetyl phosphate which was used at a concentration of 2 mM for all reactions in the acetate–forming direction. The half maximal inhibitory concentrations (IC_{50} values) were determined using PRISM 5 (Graphpad Software). ATP's mode of inhibition of wild-type EhACK was determined by measuring enzymatic activity in the

acetate forming direction in a four by seven matrix of varied ATP and P_i concentrations, with other substrate concentrations kept constant.

ACK sequence alignment, ConSurf analysis, and structural modeling

ACK sequences were obtained from NCBI. Accession numbers are as follows: *E. histolytica*, PDB ID 4H0O; *Methanosarcina thermophila*, PDB ID 1TUY; *Cryptococcus neoformans*, PDB ID 4H0P; *Salmonella typhimurium*, PDB ID 3SLC; *Thermotoga maritima*, PDB ID 2IIR; Mycobacterium smegmatis, PDB ID 4IJN; *Mycobacterium avium*, PDB ID 3P4I; *Mycobacterium paratuberculosis*, PDB ID 3R9P; *Mycobacterium marinum* PDB ID 4DQ8. Sequences alignments were performed using Clustal Omega [23-25]. ACK structures were downloaded from Protein Data Bank (PDB): 4H0O (*Entamoeba histolytic*a), 1TUY (*M. thermophila*), 4H0P (*C. neoformans*), and 3SLC (*S. typhimurium*). Structure superposition and modeling were performed using Accelrys Discovery Studio 3.5 (Biovia). ConSurf analysis [26-28] (http://consurf.tau.ac.il) was used to examine evolutionary conservation of ACK sequence and identify amino acids likely to play important structural and functional roles.

RESULTS:

Structures have been solved for six bacterial (four of which are from Mycobacterium), one archaeal, and two eukaryotic ACKs [4, 12-14]. Although the global structures are similar, the percent identity and similarity between these ACK sequences showed that the eukaryotic ACKs are less related to the bacterial and archaeal enzymes (Table 2.2). Previous phylogenetic analysis revealed that fungal ACKs belong to a distinct clade but the *E. histolytica* and other eukaryotic sequences group with the bacterial and archaeal ACKs [1]. Thus, the unique P_i/PP_i-dependence of EhACK must be due to localized differences in the active site.

Structural differences between the adenosine binding pocket of PP_i- and ATP-ACKs

In addition to the PHOSPHATE1, PHOSPHATE2, and ADENOSINE sequence motifs, Ingram-Smith *et al.* [15] defined two other regions designated as LOOP3 and LOOP4 that also influence ATP binding in ACK. Inspection of the active site in the MtACK structure showed that these regions surround the ATP binding site, with ADENOSINE forming a hydrophobic pocket for the adenosine moiety of ADP/ATP [4, 7, 10, 12, 15]. ConSurf analysis, which estimates the evolutionary conservation at each position based on phylogenetic and structural analysis, indicated that the central positions in the ADENOSINE motif have the highest conservation level (Figure 2.1). Positions 322-327 of EhACK are of particular note as this region of the ADENOSINE motif is strongly conserved in other ACKs but not EhACK.

	E.hist	*M.therm*	*C.neo*	*S.typh*	*T.mari*	*M.smeg*	*M.avium*	*M.para*	*M.mari*
E.hist		35/53	29/44	34/50	38/57	34/50	31/46	32/46	30/47
M.therm	35/53		31/49	44/62	57/76	41/59	41/59	41/58	41/58
C.neo	29/44	31/49		33/49	32/48	31/47	33/47	33/47	33/48
S.typh	34/50	44/62	33/49		46/67	44/58	40/55	41/55	41/55
T.mari	38/57	57/76	32/48	46/67		47/61	45/60	45/59	43/59
M.smeg	34/50	41/59	31/47	44/58	47/61		67/77	67/77	67/78
M.avium	31/46	41/59	33/47	40/55	45/60	67/77		98/98	73/84
M.para	32/46	41/58	33/47	41/55	45/59	67/77	98/98		73/84
M.mari	30/47	41/58	33/48	41/55	43/59	67/78	73/84	73/84	

Table 2.2: Percent identity and similarity between ACKs.

```
                             PHOSPHATE2
E.hist     193  KIIACHLGTGGSSCCGIV  210
M.therm    203  KIITCHLGNG-SSITAVE  219
C.neo      215  NVVVAHLGSG-SSSCCIK  231
S.typh     205  NIITCHLGNG-GSVSAIR  221
T.mari     202  KIITCHIGNG-ASVAAVK  218
M.smeg     184  NQIVLHLGNG-ASASAVA  200
M.avium    192  KQIVLHLGNG-CSASAIA  208
M.para     192  KQIVLHLGNG-CSASAIA  208
M.mari     192  NQIVLHLGNG-ASASAVA  208
                : :. *:*.*  *   :
CONSURF         857879899696923951

                             ADENOSINE
E.hist     317  LLVFTDQMGLEVWQVRKA  334
M.therm    325  AVVFTAGIGENSASIRKR  342
C.neo      355  GLVFSGGIGEKGAELRRD  372
S.typh     327  AVVFTGGIGENAAMVREL  344
T.mari     325  AIVFTAGVGENSPITRED  342
M.smeg     305  VISFTAGVGENVPPVRRD  322
M.avium    313  VISFTAGIGENDAAVRRD  330
M.para     313  VISFTAGIGENDAAVRRD  330
M.mari     313  VVSFTAGIGEHDAAVRRD  330
                 : *:  :* .    *.
CONSURF         456998969996111911
```

Figure 2.1: Partial alignment of ACK amino acid sequences. Sequences of ACKs for which the structure have been solved were aligned and ConSurf analysis was performed to examine sequence conservation. The PHOSPHATE2 and ADENOSINE motifs are shown. The full alignment is provided in the Figure 2.2. Abbreviations and PDB accession numbers: *E.hist*, *E. histolytica*, PDB ID 4H0O; *M.therm*, *Methanosarcina thermophila*, PDB ID 1TUY; *C.neo*, *Cryptococcus neoformans*, PDB ID 4H0P; *S.typhi*, *Salmonella typhimurium*, PDB ID 3SLC; *T.mari*, *Thermotoga maritima*, PDB ID 2IIR; *M.smeg*, *Mycobacterium smegmatis*, PDB ID 4IJN; *M.avium*, *Mycobacterium avium*, PDB ID 3P4I; *M.para*, *Mycobacterium paratuberculosis*, PDB ID 3R9P; *M.mari*, *Mycobacterium marinum* PDB ID 4DQ8.

```
                    ____PHOSPHATE1_____
T.mari          -------MRVLVINSGSSSIKYQLIEMEGEKVLC-------KGIAERIGIEGSRLVHRVG 46
M.therm         -------MKVLVINAGSSSLKYQLIDMTNESALA-------VGLCERIGIDNSIITQKKF 46
M.avium         MDGSDGARRVLVINSGSSSLKFQLVDPESGVAAS-------TGIVERIGEESS------- 46
M.para          MDGSDGARRVLVINSGSSSLKFQLVDPEFGVAAS-------TGIVERIGEESS------- 46
M.smeg          ------MVTVLVVNSGSSSLKYAVVRPASGEFLA-------DGIIEEIG--SG------- 38
S.typh          ----MSSKLVLVLNCGSSSLKFAIIDAVNGDEYL-------SGLAECFHLPEARIKWKMD 49
E.hist          ------MSNVLIFNVGSSSLTYKVFCSDNIVCSG-------KSNRVNVTGTEKPFIEHHL 47
C.neo           --MPDKAEYLLAINCGSSSIKGKLFAIPSFELLANLAVTNISSSDERVKIKTTWEEGKGK 58
                        :* .* ****:.  :.                .    .

T.mari          DEKHVIER-ELPDHEEALKLILNTLVDEKLGVIKDLKEIDAVGHRVVHGGERFKESVLVD 105
M.therm         DGKKLEKLTDLPTHKDALEEVVKALTDDEFGVIKDMGEINAVGHRVVHGGEKFTTSALYD 106
M.avium         ---------PVPDHDAALRRAFDMLAGD--GVDLNTAGLVAVGHRVVHGGNTFYRPTVLD 95
M.para          ---------PVPDHDAALRRAFDMLAGD--GVDLNTAGLVAVGHRVVHGGNTFYRPTVLD 95
M.smeg          ---------AVPDHDAALRAAFDELAAA--GLHLEDLDLKAVGHRMVHGGKTFYKPSVVD 87
S.typh          GSKQEAALGAGAAHSEALNFIVNTILAQ---KPELSAQLTAIGHRIVHGGEKYTSSVVID 106
E.hist          NGQIIKIETPILNHPQAAKLIIQFLKEN-------HISIAFVGHRFVHGGSYFKKSAVID 100
C.neo           DSEEEADYGDKIRYASLVPILLDHLTNS---THVKKEEIKYVCHRVVHGGMHDKGIRVVK 115
                             :       .. :             :  : **.****       : .

T.mari          --EEVLKAIEEVSPLAPLHNPANLMGIKAAMKLLPGVP--NVAVFDTAFHQTIPQKAYLY 161
M.therm         --EGVEKAIKDCFELAPLHNPPNMMGISACAEIMPGTP--MVIVFDTAFHQTMPPYAYMY 162
M.avium         --DAVIARLHELSELAPLHNPPALLGIEVARRLLPGIA--HVAVFDTGFFHDLPPAAATY 151
M.para          --DAVIARLHELSELAPLHNPPALQGIEVARRLLPDIA--HVAVFDTGFFHDLPPAAATY 151
M.smeg          --DELIAKARELSPLAPLHNPPAIKGIEVARKLLPDLP--HIAVFDTAFFHDLPAPASTY 143
S.typh          --ESVIQGIKDSASFAPLHNPAHLIGIAEALKSFPQLKDKNVAVFDTAFHQTMPEESYLY 164
E.hist          --EVVLKELKECLPLAPIHNPSSFGVIEISMKELPTTR--QYVAIDTAFHSTISQAERTY 156
C.neo           GHEEGLMEMDKLSEFAPLHNHRAVLAVKSCIDALPHHT--SLLLFDTIFHRTIAPEVYTY 173
                  :       .   :**:**   .  :  .   :*         :** *.  :.     *

                                                        ____PHOSPHATE2____
T.mari          AIP-YEYYEKYKIRRYGFHGTSHRYVSKRAAEILGKKLEELKIITCHIGNG-ASVAAVKY 219
M.therm         ALP-YDLYEKHGVRKYGFHGTSHKYVAERAALMLGKPAEETKIITCHLGNG-SSITAVEG 220
M.avium         AID-RELADRWQIRRYGFHGTSHRYVSEQAAAFLDRPLRGLKQIVLHLGNG-CSASAIAG 209
M.para          AID-RELADRWQIRRYGFHGTSHRYVSEQAAAFLDRPLRGLKQIVLHLGNG-CSASAIAG 209
M.smeg          AID-RELAETWHIKRYGFHGTSHEYVSQQAAIFLDRPLESLNQIVLHLGNG-ASASAVAG 201
S.typh          ALP-YSLYKEHGVRRYGAHGTSHFYVTQEAAKMLNKPVEELNIITCHLGNG-GSVSAIRN 222
E.hist          AIP-QPYQSQY--LKFGFHGLSYEYVINSLKNVID--VSHSKIIACHLGTGGSSCCGIVN 211
C.neo           ALPPPDTELTMPLRKYGFHGLSYASIVQSLAEHLKKPSDQINVVVAHLGSG-SSSCCIKN 232
                *:            ::* ** *:  : :     :       : :. *:*.*  *   :

                     _________LOOP3_________
T.mari          GKCVDTSMGFTPLEGLVMGTRSGDLDPAIPFFIMEKEG-------ISPQEMYDILNKKSG 272
M.therm         GKSVETSMGFTPLEGLAMGTRCGSIDPAIVPFLMEKEG-------LTTREIDTLMNKKSG 273
M.avium         TRPLDTSMGLTPLEGLVMGTRSGDIDPSVVSYLCHTAG-------MGVDDVESMLNHRSG 262
M.para          TRPLDTSMGLTPLEGLVMGTRSGDIDPSIVSYLCHTAG-------MGVDDVESMLNHRSG 262
M.smeg          GKAVDTSMGLTPMEGLVMGTRSGDIDPGVIMYLWRTAG-------MSVDDIESMLNRRSG 254
S.typh          GKCVDTSMGLTPLEGLVMGTRSGDIDPAIIFHLHDTLG-------MSVDQINKMLTKESG 275
E.hist          GKSFDTSMGNSTLAGLVMSTRCGDIDPTIPIDMIQQVG-------IEK--VVDILNKKSG 262
C.neo           GKSIDTSMGLTPLEGLLGGTRSGTIDPTAIFHHTEDAASDANVGDFTVSKAEIILNKNSG 292
                 : .:**** :.: **  .**.* :**          .       :       ::.:.**
```

```
                    ___LOOP4____
T.mari          VYGLSKGFSSDMRDIEEAALKG------DEWCKLVLEIYDYRIAKYIGAYAAAMN----- 321
M.therm         VLGVS-GLSNDFRDLDEAASKG------NRKAELALEIFAYKVKKFIGEYSAVLN----- 321
M.avium         VVGLS--GVRDFRRLRELIESG------DGAAQLAYSVFTHRLRKYIGAYLAVLG----- 309
M.para          VVGLS--GVRDFRRLRELIESG------DGAAQLAYSVFTHRLRKYIGAYLAVLG----- 309
M.smeg          VLGLG--GASDFRKLRELIESG------DEHAKLAYDVYIHRLRKYIGAYMAVLG----- 301
S.typh          LLGLT-EVTSDCRYVEDNYAT-------KEDAKRAMDVYCHRLAKYIGSYTALMDG---- 323
E.hist          LLGVS-ELSSDMRDILHEIETRGP---KAKTCQLAFDVYIKQLAKTIGGLMVEIG----- 313
C.neo           FKALA--GTTNFGHIIQNLDPSKCSEEDHEKAKLTYAVFLDRLLNFVAQYLFKLLSEVPI 350
                . .:      :   : .             .: .  ::  :: : :.     :

                     _____ADENOSINE____
T.mari          -GVDAIVFTAGVGENSPITREDVCSYLEFLGVKLDKQKNEETIRGKEGIISTPDSRVKVL 380
M.therm         -GADAVVFTAGIGENSASIRKRILTGLDGIGIKIDDEKNK--IRGQEIDISTPDAKVRVF 378
M.avium         -HTDVISFTAGIGENDAAVRRDAVSGMEELGIVLDERRNLPGAKGAR-QISADDSPITVL 367
M.para          -HTDVISFTAGIGENDAAVRRDAVSGMEELGIVLDERRNLAGGKGAR-QISADDSPITVL 367
M.smeg          -RTDVISFTAGVGENVPPVRRDALAGLGGLGIEIDDALNSAKSDEPR-LISTPDSRVTVL 359
S.typh          -RLDAVVFTGGIGENAAMVRELSLGKLGVLGFEVDHERNLAARFGKSGFINKEGTRP-AV 381
E.hist          -GLDLLVFTDQMGLEVWQVRKAICDKMKFLGIELDDSLNEKSMGKKIEFLTMPSSKVQVC 372
C.neo           ESIDGLVFSGGIGEKGAELRRDVLKKLAWLGAEVDEEANNSNSGGAVKCITKEGSKLKGW 410
                   * : *:  :* :    *.     :  :*  :*.  *          :.  .:

T.mari          VVPTNEELMIARDTKEIVEKIGR------- 403
M.therm         VIPTNEELAIARETKEIVETEVKLRSSIPV 408
M.avium         VVPTNEELAIARDCVRVLGG---------- 387
M.para          VVPTNEELAIARDCVRVLGG---------- 387
M.smeg          VVPTNEELAIARACVGVV------------ 377
S.typh          VIPTNEELVIAQDASRLTA----------- 400
E.hist          VAPNDEELVILQKGKELFQF---------- 392
C.neo           VVETDEEGWMARMAKEEFGF---------- 430
                *  .:**  : :
```

Figure 2.2: ACK sequence alignment. The full ACK sequence alignment from which Figure 2.1 was derived is shown.

ADP/ATP-utilizing ACKs have a highly conserved Gly residue and an adjacent Ile/Val within the ADENOSINE motif (positions 331 and 332 in MtACK). Inspection of the MtACK structure revealed a large opening to the adenosine binding pocket (Figure 2.3A) that is also evident in the structures of other ATP-ACKs. Occlusion of the adenosine pocket is evident in the surface representation of EhACK (Figure 2.3B). Thaker *et al.* [12] postulated that $Gln^{323}Met^{324}$ within the ADENOSINE motif of EhACK may sterically prevent ADP/ATP binding.

Role of the ADENOSINE motif in ATP/ADP versus PP_i/P_i utilization.

To investigate the role of the ADENOSINE motif in determining substrate selection, EhACK variants were created that simulate the open adenosine pocket observed in ATP-dependent ACKs. Gln^{323} and Met^{324} were altered to Gly and Ile, respectively, to mimic the residues found at equivalent positions in MtACK. These positions were also both altered to Ala to minimize side chain intrusions into the opening of the adenosine pocket. The reverse alterations were made in MtACK, converting Gly^{331}–Ile^{332} to Gln–Met, respectively, to determine the effect of closing the entry to the adenosine pocket. The EhACK and MtACK variants were purified (Figure 2.4) and kinetic parameters were determined in both directions of the reaction (Table 2.3).

The $Q^{323}G$–$M^{324}I$ and $Q^{323}A$–$M^{324}A$ EhACK variants displayed similar K_m values for acetyl phosphate and slightly decreased K_m values for phosphate as the unaltered enzyme but the k_{cat} values were decreased 8.3-fold for the $Q^{323}G$–$M^{324}I$ variant and 19-fold for $Q^{323}A$–$M^{324}A$ variant, resulting in ~7 and 11-fold reduced catalytic efficiency,

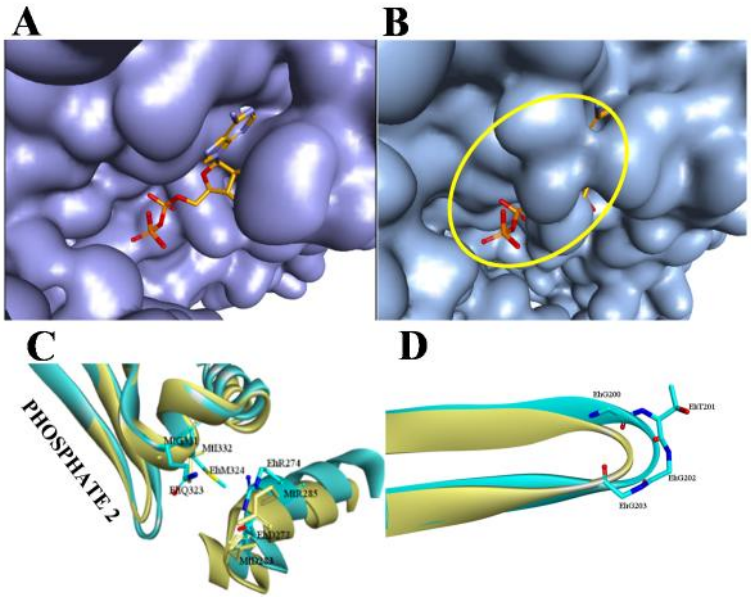

Figure 2.3: The ACK adenosine binding pocket. (**A**) Surface representation of MtACK with bound ADP. (**B**) Surface representation of EhACK. The constricted opening to the adenosine pocket is circled. The position of bound ADP in MtACK was superimposed into the EhACK structure. (**C**) Superimposition of the adenosine pocket from MtACK (yellow) and EhACK (cyan) showing the positions of targeted residues. (**D**) Superimposed PHOSPHATE2 motifs from MtACK (yellow) and EhACK (cyan), showing the position of the additional Gly in the EhACK PHOSPHATE2 motif.

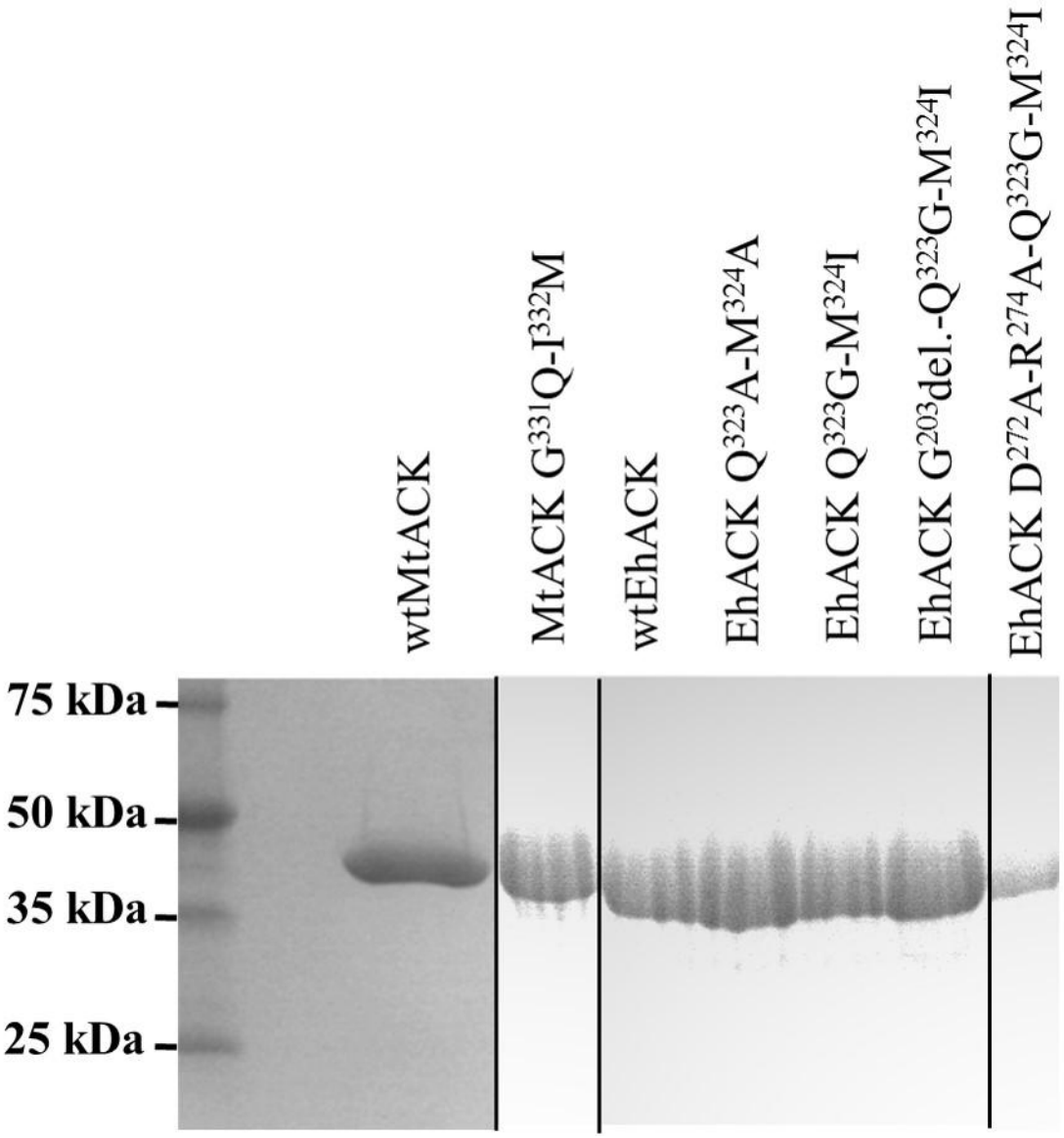

Figure 2.4 SDS-PAGE analysis of purified enzymes. Black vertical lines represent separate gels.

Enzyme	Substrate	K_m (mM)	k_{cat} (sec^{-1})
EhACK		Acetate-forming direction	
Wild-type	AcP	0.57 ± 0.03	266 ± 12
$Q^{323}G$-$M^{324}I$		0.47 ± 0.04	32 ± 1.0
$Q^{323}A$-$M^{324}A$		0.34 ± 0.07	14 ± 1.2
G^{203}deletion-$Q^{323}G$-$M^{324}I$		No detectable activity	
$D^{272}A$-$R^{274}A$-$Q^{323}G$-$M^{324}I$		0.66 ± 0.11	0.052 ± 0.005
Wild-type	P_i	14 ± 1.2	196 ± 5
$Q^{323}G$-$M^{324}I$		7.3 ± 0.5	28 ± 1.2
$Q^{323}A$-$M^{324}A$		8.2 ± 1.1	20 ± 0.8
G^{203}deletion-$Q^{323}G$-$M^{324}I$		No detectable activity	
$D^{272}A$-$R^{274}A$-$Q^{323}G$-$M^{324}I$		18 ± 1.2	0.076 ± 0.004
		Acetyl phosphate-forming direction	
Wild-type	Acetate	166 ± 7	1.4 ± 0.05
$Q^{323}G$-$M^{324}I$		372 ± 40	0.51 ± 0.02
$Q^{323}A$-$M^{324}A$		566 ± 44	0.51 ± 0.03
G^{203}deletion-$Q^{323}G$-$M^{324}I$		No detectable activity	
$D^{272}A$-$R^{274}A$-$Q^{323}G$-$M^{324}I$		No detectable activity	
Wild-type	PP_i	2.1 ± 0.33	0.90 ± 0.03
$Q^{323}G$-$M^{324}I$		2.0 ± 0.37	0.45 ± 0.03
$Q^{323}A$-$M^{324}A$		2.3 ± 0.41	0.36 ± 0.01
G^{203}deletion-$Q^{323}G$-$M^{324}I$		No detectable activity	
$D^{272}A$-$R^{274}A$-$Q^{323}G$-$M^{324}I$		No detectable activity	
MtACK		Acetate-forming direction	
Wild-type	AcP	1.2 ± 0.09	1550 ± 54
$G^{331}Q$-$I^{332}M$		1.7 ± 0.14	12 ± 0.7
Wild-type	ADP	1.8 ± 0.13	1915 ± 15
$G^{331}Q$-$I^{332}M$		5.7 ± 0.56	12 ± 0.5
		Acetyl phosphate-forming direction	
Wild-type	Acetate	20 ± 0.3	789 ± 16
$G^{331}Q$-$I^{332}M$		302 ± 11	17 ± 4.2
Wild-type	ATP	1.7 ± 0.03	711 ± 23
$G^{331}Q$-$I^{332}M$		9.4 ± 0.27	14 ± 0.2

Table 2.3: Apparent kinetic parameters for wild-type and variant EhACKs and MtACKs.

respectively. In the direction of acetyl phosphate formation, these variants displayed slightly increased K_m for acetate but no increase in K_m for PP_i and only mild decrease in k_{cat}. No activity was observed with either variant using ATP or ADP as substrate in the respective direction of the reaction.

The $G^{331}Q–I^{332}M$ alteration in MtACK resulted in substantial reductions in k_{cat} (Table 2.3). In the acetate-forming direction, catalysis was reduced over 100-fold, and in the acetyl phosphate-forming direction, k_{cat} was reduced ~50-fold. This alteration resulted in ~5-fold increase in K_m for ADP and ATP, and a 15-fold increase in K_m for acetate but no substantial change in the K_m for acetyl phosphate. As with wild-type MtACK, no activity was observed with P_i or PP_i as substrate in the respective directions of the reaction for the MtACK variant.

Additional structural elements may contribute to occlusion of the ATP/ADP binding pocket

A salt bridge between Arg^{274} and Asp^{272} on LOOP4 of EhACK may cause further constriction of the adenosine pocket by positioning the Arg side chain toward the pocket [12]. These two residues are conserved in MtACK but the side chain of Arg is positioned away from the adenosine pocket. These residues are not conserved among all ACKs though and LOOP4 does not impinge upon the adenosine pocket. The PHOSPHATE2 motif, which interacts with the β phosphate of ATP and was suggested to have a role in substrate positioning [4, 11, 15], is longer in EhACK and protrudes farther into the active site than in the ATP-dependent enzymes (Figure 2.3C). Sequence alignment and structural

superposition of the PHOSPHATE2 motif illustrate that this difference arises from addition of a single residue, Gly^{203} (Figures 2.1 and 2.3D).

To examine whether this salt bridge and the extended PHOSPHATE2 motif influence substrate selection, EhACK $Q^{323}G–M^{324}I$ variants in which the salt bridge has been eliminated ($D^{272}A–R^{274}A–Q^{323}G–M^{324}I$) or in which the PHOSPHATE2 motif has been shortened ($\Delta G^{203}– Q^{323}G–M^{324}I$) were analyzed. The $D^{272}A–R^{274}A–Q^{323}G–M^{324}I$ replacement decreased k_{cat} in the acetate-forming direction by ~2,500–5,000 fold but had little effect on K_m for either substrate (Table 2.3). This variant had no detectable activity in the acetyl phosphate-forming direction (Table 2.3). The $\Delta G^{203}– Q^{323}G–M^{324}I$ variant was inactive in either direction of the reaction, and thus the effect of the Gly^{203} deletion compounded onto the $D^{272}A–R^{274}A–Q^{323}G–M^{324}I$ alteration was not examined. No enzymatic activity was observed with either of these variants using ATP or ADP as the substrate in place of PP_i or P_i.

Inhibition of EhACK and MtACK by alternative phosphoryl donors and acceptors.

Since wild-type EhACK and MtACK cannot utilize ATP/ADP or PP_i/P_i, respectively, as alternative phosphoryl donor/acceptor, inhibition assays were performed to determine whether these compounds can bind and inhibit activity even if they cannot be used productively as substrate. EhACK activity was measured in the favored acetate-forming direction in the presence or absence of 10 mM AMP, ADP, or ATP (Figure 2.5A). Although AMP had no effect, both ADP and ATP were found to inhibit EhACK activity

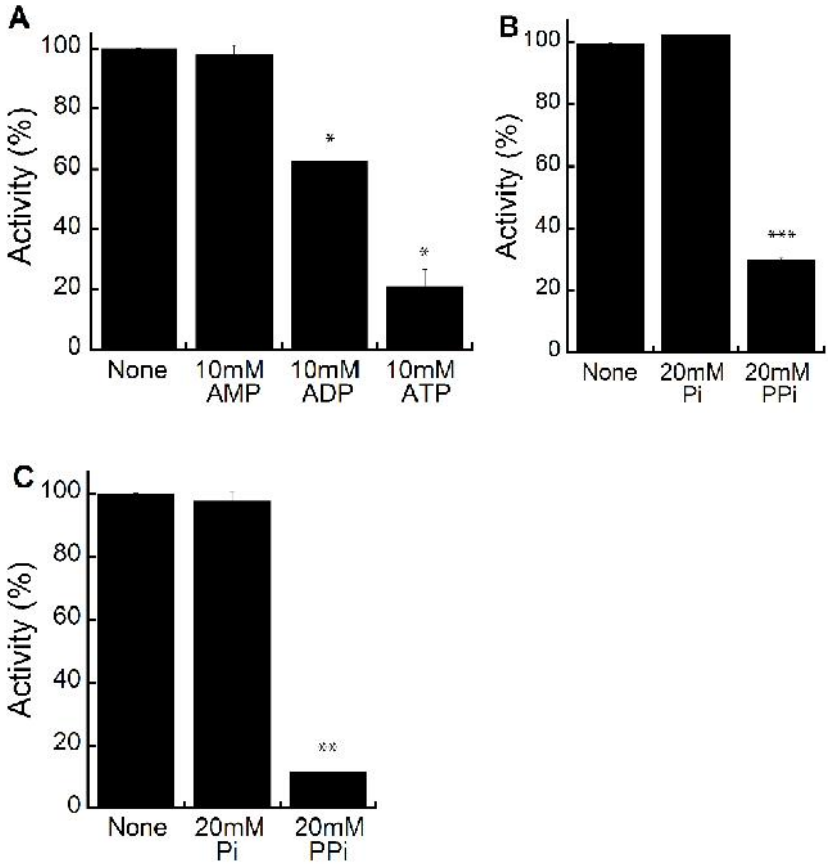

Figure 2.5: Inhibition of EhACK and MtACK by alternative phosphoryl donors and acceptors. (**A**) Inhibition of wild-type EhACK in the presence of 10 mM AMP, ADP, or ATP in the acetate-forming direction of the reaction. (**B**) Inhibition of wild-type MtACK in the presence of 20 mM P_i or PP_i in the acetate-forming direction. (**C**) Inhibition of wild-type MtACK in the presence of 20 mM P_i or PP_i in the acetyl phosphate-forming direction. Significant difference between inhibitions compared to wild-type enzyme activity is tested using an unpaired Welch t-test with R. * = p-value < 0.001, ** = p-value < 0.00003, *** = p-value < 0.000008. Activities are the mean ± SD of three replicates.

but to differing extents. The presence of ATP resulted in nearly 80% inhibition versus ~30% inhibition by ADP. The presence of P_i or PP_i with AMP was not sufficient to mimic the effect of inhibition by ADP or ATP, respectively (data not shown). For MtACK, P_i had no effect on enzymatic activity. PP_i inhibited the enzyme in both directions of the reaction to differing extents, producing ~70% inhibition in the acetate-forming direction and ~90% inhibition in the acetyl phosphate-forming direction (Figures 2.5B and 2.5C).

The mode of inhibition of EhACK by ATP was determined by kinetic analysis using a matrix of reactions in which the ATP concentration was varied versus P_i concentration with the acetate concentration held constant. ATP was found to be a competitive inhibitor of EhACK, as demonstrated by the results in Figure 2.6. Further examination of ATP inhibition of the EhACK variants in the favored acetate-forming direction of the reaction revealed that a similar final level of inhibition of ~85-90% was achieved for the variants and wild-type enzyme by 15 mM ATP (Figure 2.7A).

The IC_{50} value for ATP, defined as the concentration of ATP required to cause 50% inhibition of enzymatic activity, was reduced for the EhACK variants versus the wild-type enzyme (Table 2.4). The IC_{50} values were reduced 20-30% for the two Q^{323}-M^{324} variants versus the wild-type enzyme, whereas the quadruple variant in which both the Q^{323}-M^{324} residues and the D^{272}-R^{274} salt bridge were altered had an IC_{50} value that was reduced by over 60%. Since ATP is a competitive inhibitor of EhACK activity, this increase in inhibition suggests that the D^{272}A-R^{274}A-Q^{323}G-M^{324}I variant binds ATP more efficiently than wild-type enzyme even though it cannot use it as a substrate.

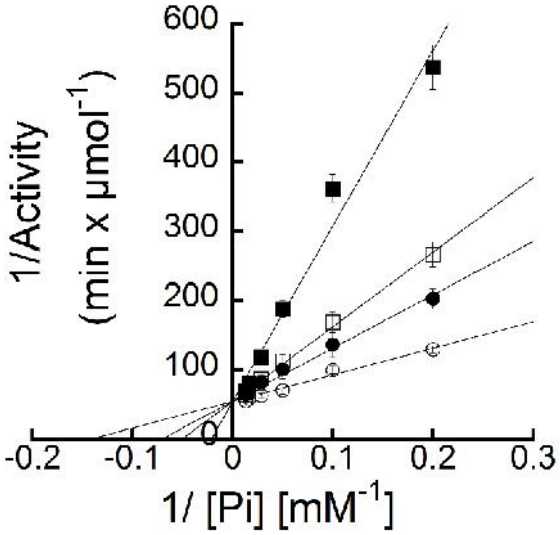

Figure 2.6: ATP is a competitive inhibitor of EhACK. Double reciprocal plot of EhACK activity versus P_i concentration in the absence (○) or presence of 2.5mM (●), 5mM (□), or 7.5mM ATP (■). Activities are the mean ± SD of three replicates.

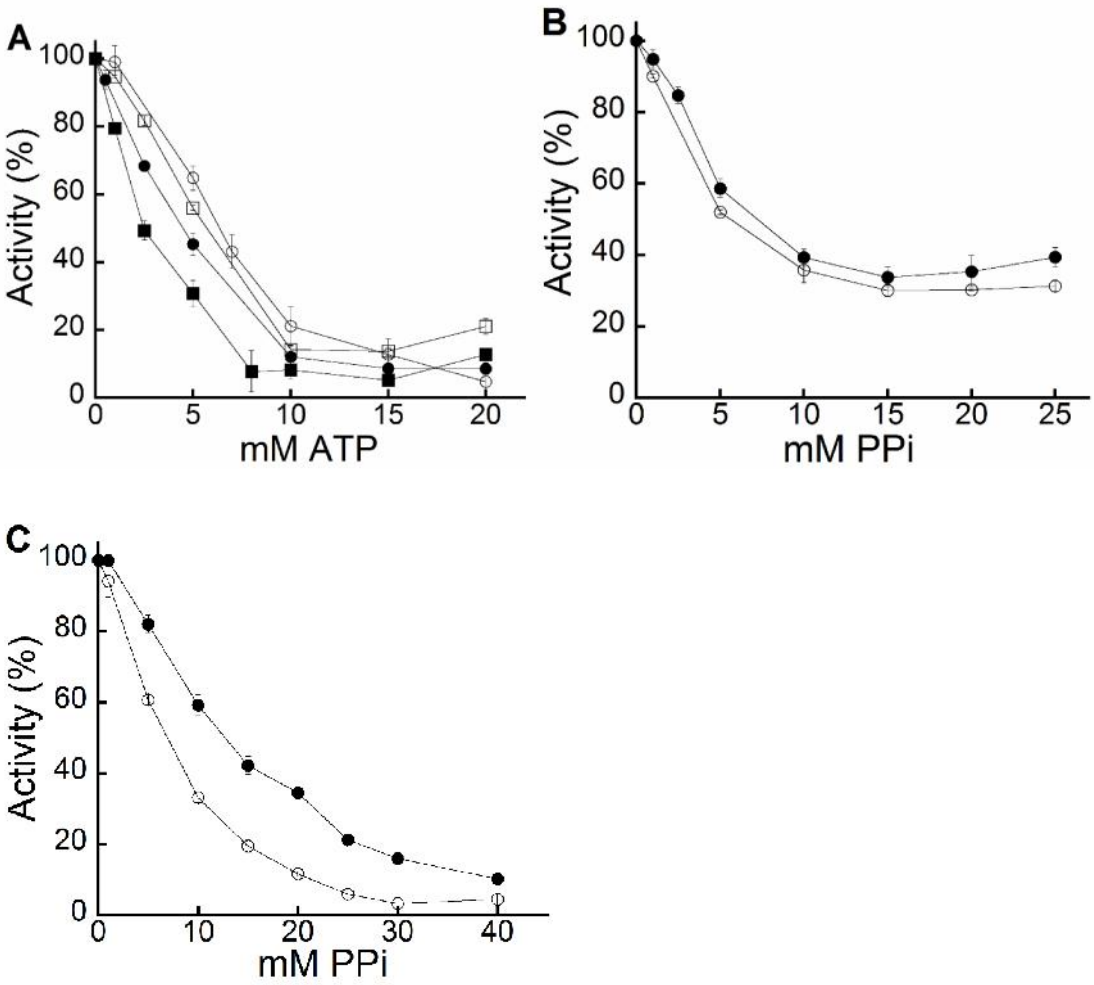

Figure 2.7: Inhibition curves for EhACK and MtACK wild-type and variant enzymes. Enzymatic activity was determined for each enzyme in the presence of the indicated concentration of ATP or PP_i. Activities were plotted as a percentage of the activity observed for the wild-type enzyme in the absence of inhibitor. Activities are the mean ± SD of three replicates. (**A**) ATP inhibition of EhACK and its variants in the acetate-forming direction. EhACK wild-type, (○); EhACK $Q^{323}G$-$M^{324}I$ variant (●); EhACK $Q^{323}A$-$M^{324}A$ variant, (□); EhACK $D^{272}A$-$R^{274}A$-$Q^{323}G$-$M^{324}I$ variant (■). (B) and (C) PP_i inhibition of

MtACK and its variants in the acetate-forming (**B**) and acetyl phosphate-forming (**C**) directions. MtACK wild-type, (○); MtACK $G^{331}Q$-$I^{332}M$ variant (●)

	ATP IC_{50} (mM)
EhACK	**Acetate-forming direction**
Wild-type	6.1 ± 0.05
$Q^{323}G$-$M^{324}I$	4.2 ± 0.30
$Q^{323}A$-$M^{324}A$	4.8 ± 0.09
$D^{272}A$-$R^{274}A$-$Q^{323}G$-$M^{324}I$	2.4 ± 0.19

	PP_i IC_{50} (mM)	
MtACK	**Acetate-forming direction**	**Acetyl phosphate-forming direction**
Wild-type	3.3 ± 0.06	7.5 ± 0.28
$G^{331}Q$-$I^{332}M$	4.0 ± 0.28	14 ± 1.1

ND, not determined because the enzyme was inactive in this direction.

Table 2.4: IC_{50} values for ATP inhibition of EhACK and PP_i inhibition of MtACK

For MtACK, inhibition by PP_i in the acetate-forming direction was similar for the wild-type enzyme and the $G^{331}Q$-$I^{332}M$ variant, with ~70% maximum inhibition observed (Figure 2.7B). The IC_{50} values for PP_i were similar for both enzymes (Table 2.4). PP_i inhibition in the acetyl phosphate-forming direction was much stronger, reaching greater than 90% for both the wild-type and variant enzymes. However, maximum inhibition for the wild-type enzyme was achieved at lower ATP concentration (20-25 mM versus 40 mM for the variant). This is reflected in the IC_{50} value, which is nearly two-fold higher for the $G^{331}Q$-$I^{332}M$ variant than for the wild-type.

DISCUSSION:

Substrate selection in ATP-utilizing ACKs

Thaker *et al.* [12], in analysis of the MtACK and EhACK structures, predicted that P_i/PP_i binding does not involve the adenosine pocket and PP_i likely binds in a position corresponding to the position of the β- and γ-phosphates of ATP in MtACK. Our inspection of structures for the four *Mycobacterium* ACKs and the *S. enterica* ACKs in addition to those for MtACK and *C. neoformans* ACK showed that the opening to the adenosine pocket is not occluded in ATP-utilizing ACKs, only in the EhACK structure. Thus, we investigated whether phosphoryl donor selection by ACK is based primarily on accessibility of the adenosine pocket.

Alterations were made to MtACK to determine if the substrate specificity could be changed from ATP to PP_i if the adenosine pocket was occluded. Catalysis was greatly reduced (~50-150 fold) in the enzyme variants and this was accompanied by increases in the K_m values for both acetate and ATP in the acetyl phosphate-forming direction of the reaction. Gorrell *et al.* [16], using tryptophan fluorescence quenching, found that domain closure occurs upon nucleotide binding. Thus, the effects of these alterations on MtACK activity may be complicated to interpret as reduced catalysis could be due to inefficient utilization of ATP and to an influence in domain closure. Notably though, substrate specificity did not change and the MtACK variant was unable to utilize PP_i as a substrate. Thus, conversion of ATP-dependent MtACK to a P_i/PP_i-dependent enzyme could not be achieved by simple closure of the adenosine pocket.

MtACK has a broad NTP substrate range [15, 17] with a preference for ATP and is highly active in both the acetate- and acetyl phosphate-forming directions. Ingram-Smith *et al.* [15] examined the roles of conserved active site residues in NTP substrate selection in MtACK, and found that Gly^{331} in the ADENOSINE motif exerted a strong influence. Asn^{211} in the PHOSPHATE2 motif and Gly^{239} in the LOOP3 motif were found to be important for enzymatic activity but did not play a substantial role in NTP preference.

Yoshioka *et al.* [10] studied four residues in the ADENOSINE motif and one residue in the PHOSPHATE2 motif of *E. coli* ACK for their role in ATP versus PP_i substrate determination. The candidate residues Asn^{213}, Gly^{332}, Gly^{333}, Ile^{334} and Asn^{337} were altered to the respective residues present in EhACK (Thr, Asp, Gln, Met, and Glu, respectively) and the ability of the enzyme variants to utilize PP_i in place of ATP was examined. All five variants displayed increased K_m for ATP and decreased catalysis but none was able to utilize PP_i.

Yoshioka *et al.* [10] also examined the distribution of the *E. coli* ACK candidate residues and the corresponding residues in EhACK among 2625 ACK homologs. They suggested that Asn^{337} (Glu^{327} of EhACK) is most important in determining substrate selection as it is present in the ten ACK sequences most closely related to EhACK. However, their kinetic results with the Asn^{337} variants are inconclusive in this regard, although the kinetic results for this and other variants do strongly support a major role in ATP binding for the ADENOSINE motif but do not delineate specific residues responsible for determining ATP versus PP_i utilization.

Substrate selection in PP_i-dependent EhACK

As a converse to our experiments with MtACK, we altered residues blocking the opening to the adenosine pocket in EhACK to reduce the occlusion and evaluated the enzyme's ability to utilize P_i/PP_i versus ATP/ADP. The EhACK variants exhibited decreased activity with P_i and PP_i, much as we expected. Although catalysis was reduced for the Q^{323}G-M^{324}I and Q^{323}A-M^{324}A variants, further opening of the entrance to the adenosine pocket in the D^{272}A-R^{274}A-Q^{323}G-M^{324}I variant almost completely eliminated activity. This suggested that as the opening to the adenosine pocket increases, P_i and PP_i may still bind but their positioning may be suboptimal.

Although the enzyme variants were still unable to utilize ATP as a substrate, ATP and ADP did inhibit enzyme activity. The level of inhibition increased as the opening to the adenosine pocket was expanded, especially for the D^{272}A-R^{274}A-Q^{323}G-M^{324}I variant. This suggested that ATP and ADP could now enter the adenosine pocket and interfere with P_i binding. Such an interpretation of these results is supported by the observation that ATP inhibition is competitive versus P_i.

The similar behavior of the Q^{323}G-M^{324}I and Q^{323}A-M^{324}A variants with respect to inhibition by ATP indicated that the increased binding (as judged by IC_{50} values) must be due to expanding the entrance to the adenosine pocket rather than a specific interaction between the altered residues and ATP. Models of the enzyme variants indicated that these alterations to the adenosine pocket would result in decreased impairment of ATP binding (Figure 2.8). In particular, deletion of G^{203} to shorten the PHOSPHATE2 loop combined

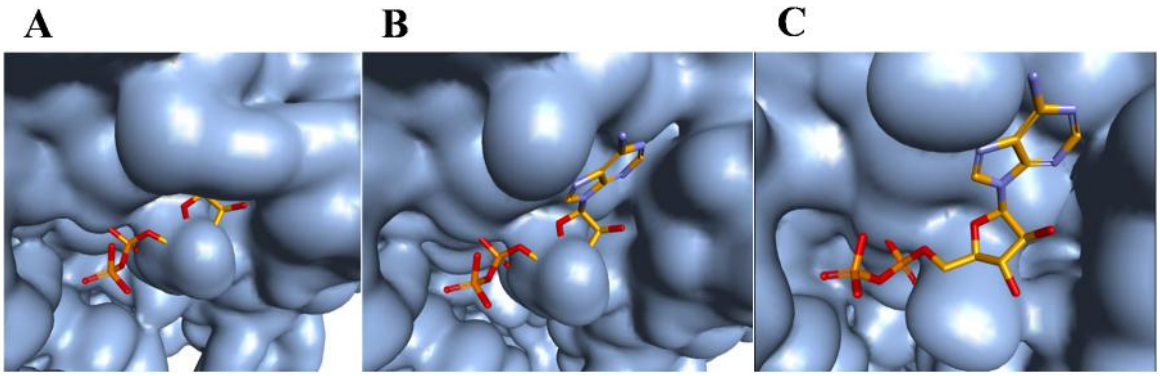

Figure 2.8: *In silico* modeling of the adenosine binding pocket of EhACK variants. Models were built using Accelrys Discovery Studio version 3.5 (Biovia). ADP binding in MtACK was superimposed into the EhACK structure models. (**A**) Q^{323}G-M^{324}I variant. (**B**) D^{272}A-R^{274}A-Q^{323}G-M^{324}I variant. (**C**) ΔG^{203}- D^{272}A-R^{274}A-Q^{323}G-M^{324}I variant.

with alteration of the ADENOSINE motif and removal of the D^{272}-R^{274} salt bridge should allow the pocket to accommodate ATP well (Figure 2.8C). Although the alterations made to EhACK appeared to increase the enzyme's ability to bind ATP, as indicated by the inhibition results, ATP was still not an effective substrate.

Other possible PP_i-dependent ACKs

Using a BLASTp search of the non-redundant protein sequence database at NCBI with EhACK as the query sequence, we identified a small number of putative ACK sequences that may also be PP_i-dependent or require a substrate other than ATP or PP_i. Several of these putative ACK sequences came from metagenome analyses of anaerobic digestors. However, there were four putative ACK deduced amino acid sequences that came from draft genomes for the bacteria *Ornatilinea apprima*, *Longilinea arvoryzae*, *Flexilinea flocculi*, and *Leptolinea tardivitalis* [18-21]. These bacteria are all obligate anaerobes from the phylum *Chloroflexi* within the family *Anaerolineaceae*. Three of the four produce acetate as a main product from glucose fermentation; *L. arvoryzae* also produces acetate as a primary fermentation product but from growth on sucrose instead of glucose. Little else is known about these bacteria beyond their initial characterization for recognition as new species.

Alignment of these putative ACK sequences with those of the four *Entamoeba* ACK sequences (those from *E. histolytica*, *Entamoeba nuttalli*, *Entamoeba dispar*, and *Entamoeba invadens*) revealed two key findings. Within the PHOSPHATE2 motif, all eight of these sequences have the extended loop containing the second Gly residue (Figure

2.9). These are the only putative ACK sequences identified to have this extended PHOSPHATE2 loop (see Figure 1 for comparison). Within the ADENOSINE motif, all of these sequences have a conserved Asp residue (immediately adjacent to Q^{323}-M^{324} of EhACK) that is not conserved in any other ACK sequences (all of which have Ala or Gly at the equivalent position, as shown in Figure 2.1). Interestingly, these bacterial ACKs have a conserved Asp at the equivalent position to Gln^{323} of PP_i-dependent EhACK and the other *Entamoeba* ACKs. A completely conserved Gly resides at this position (Gly^{331} of MtACK) in all ATP-dependent ACKs. Whether this indicates that these enzymes are neither ATP-dependent nor PP_i-dependent, or whether there is some flexibility in the identity of the residue at this position in PP_i-dependent ACKs is unknown.

```
                    PHOSPHATE2
E.his      193 KIIACHLGTGGSSCCGIV 210
E.nut      193 KIIACHLGTGGSSCCGIV 210
E.dis      193 KIIACHLGTGGSSCCGIV 210
E.inv      193 KIVACHLGTGGSSCCAIL 210
O.app      201 KIIACHLGTGGSSAVALK 218
L.arv      201 KLILCHLGTGGSSVVAMK 218
F.flo      201 KFILCHLGSGGSSITAVR 218
L.tar      201 KLILCHLGTGGSSVTAMK 218
               *   **** ****

                    ADENOSINE
E.his      317 LLVFTDQMGLEVWQVRKA 334
E.nut      317 LLVFTDQMGLEVWQVRRA 334
E.dis      317 LLVFTDQMGLEVWQVRKA 334
E.inv      317 MLVFTDQVGLEVPEVRKA 334
O.app      322 ALIFTDDIGLWSWQLRES 339
L.arv      323 AIVFTDDVGLKSWKLRAK 340
F.flo      323 AIVFTDDIGETSWKLREK 340
L.tar      323 AIVFTDDVGLKSWKLREK 340
                  ***  *      *
```

Figure 2.9: Partial alignment of putative PP_i-ACK amino acid sequences. Sequences were aligned using Clustal Omega. The PHOSPHATE2 and ADENOSINE motifs are shown. The full alignment is provided in the Figure 2.10. Abbreviations and sequence accession numbers: *E.his*, *E. histolytica*, XP_655990.1; *E.nut*, *Entamoeba nuttalli*, XP_008860710.1; *E.dis*, *Entamoeba dispar*, XP_001741606.1; *E.inv*, *Entamoeba invadens*, XP_004254504.1; *O.app*, *Ornatilinea apprima*, WP_075061087.1; *L.arv*, *Longilinea arvoryzae*, WP_075074878.1; *F.flo*, *Flexilinea flocculi*, WP_062279690.1; *L.tar*, *Leptolinea tardivitalis*; WP_062422928.1.

```
                ____PHOSPHATE1_____
E.his     MSNVLIFNVGSSSLTYKVFCSDN-----IVCSGKSNRVNVTGTEKPFIEHHLNGQIIKIE 55
E.nut     MSNVLIFNVGSSSLTYKVFCSDN-----IVCNGKANRVNVTGTEKPFIEHHLNGKIIKIE 55
E.dis     MSNVLIFNVGSSSLTYKVFCSDK-----IVCSGKANRVNVTGTTKPFIEHHLNGKVIKVE 55
E.inv     MPHILVFNVGSSSLTYKLFENTK-----EIIKGKANRVNVTGAELPFIEHHINGKTITIE 55
O.app     -MNLLVFNCGSSSLNYKVFSGDSNSTAQITAKGKAHRVGVKGSDPSFIEHHLSNQTVKET 59
L.arv     -MNILIFNCGSSSQGFKVYQTSGHDQPVVLVSGKAKNVATQTRADAFIEWKSKISAGSQK 59
F.flo     -MNILVFNCGSSSQGFKVYEVDQNHAEKVVISGKAKNVAARTQSQPYLFWNMNDKTEQKF 59
L.tar     -MNILIFNCGSSSQGFKLYQKEYGTTPILVAAGKARNVATKTRADSCLDWTAGSQKGSVN 59
            ::*:** ****  :*::             **:..* .     . :      .

E.his     TPILNHPQAAKLIIQFLKENHISIAFVGHRFVHGGSYFKKSAVIDEVVLKELKECLPLAP 115
E.nut     TPILNHPQAAKLIIQFLKENHISIAFVGHRFVHGGSYFKKSAIIDEVVLKELKECLPLAP 115
E.dis     TPTLNHQQAAEFIIQFLKENHVSIAFVGHRFVHGGSYFKRSAIIDEAVLKELKECLPLAP 115
E.inv     TGPLNHQEAARLIIKFLKENKFTIDIVGHRFVHGGSYFKTSAVIEGPVLKELKSCIPLAP 115
O.app     QPLETHAQAAERVLQNLRDHQIPIDAVGHRFVHGGAYFKESALLTEDTLARLTECLPLAP 119
L.arv     TDLSSHRQAAGKIIAILKELQVSVDAIGHRFVHGGTFFDKTVQIDPPVLQKLQQCLPFAP 119
F.flo     CDLSSHRLAAQEIIGILNAKGIQPDAIGHRFVHGGKLFQQTTRIDTNTRNLLIQCLPLAP 119
L.tar     VELPSHREAARQILALLRKSNLSVDAIGHRFVHGGDVFQHTTRIDKAVLAGLKGCFPLAP 119
              .*  **  ::  *.   .    :********  *. :. :   .   *  *:*:**

E.his     IHNPSSFGVIEISMKELPTTRQYVAIDTAFHSTISQAERTYAIPQPYQS--QYLKFGFHG 173
E.nut     IHNPSSFGVIEMSMKELPTTRQYVAIDTAFHSTISQAERTYAIPQPYQS--QYLKFGFHG 173
E.dis     IHNPSSFSVIEVSMKELPTTKQYVAIDTAFHSTISQAERTYAIPQPYQS--QYLKFGFHG 173
E.inv     IHNPASYSVIEVALTELPNTKQYVAIDTAFHSTINKTQRTYAIPEPFQS--QYLKFGFHG 173
O.app     IHNPNSMSVIYTCLEHQPGCPQYVTFDTAFHAALPPEAYTYAVPQSIRDTHTYRRFGFHG 179
L.arv     IHNPNSYSVIEVCLEQFPDVPQFAVFDTAFHARMPEVSKQYAIPRDLVEKYGYYKYGFHG 179
F.flo     IHNPNSFSVIEVCEQLLPSIPQYAVFDTAFHSQMPESSARYAIPGSIAEKFGFRKYGFHG 179
L.tar     IHNPNSYSVIEVCRELLPDAAQFAVFDTAFHANMPAESRQYALPRELVQENGYRKYGFHG 179
          **** * .**  .    *   *:..:*****: :      **:*    .   : ::****

                                ____PHOSPHATE2____      ________LOOP3___
E.his     LSYEYVINSLKNVID--VSHSKIIACHLGTGGSSCCGIVNGKSFDTSMGNSTLAGLVMST 231
E.nut     LSYEYVINSLKNVID--VSHSKIIACHLGTGGSSCCGIVNGKSFDTSMGNSTLAGLVMST 231
E.dis     LSYEYVINSLKNVID--VSHSKIIACHLGTGGSSCCGIVNGKSFDTSMGNSTLAGLVMST 231
E.inv     LSYEFVLTSLKERMD--VDKLKIVACHLGTGGSSCCAILNGKSYDTSMGNSTLAGLVMST 231
O.app     LSYHFVTQAAGPFLETPFSESKIIACHLGTGGSSAVALKNGVPLDTSMGFTPLPGLIMST 239
L.arv     LSYQYVSSRMLELMGKPLEELKLILCHLGTGGSSVVAMKNGLPLDTSMGYSPLAGLVMST 239
F.flo     LSYQYVSTKTAQLIGKPLQNSKFILCHLGSGGSSITAVRDGKSIDTSMGYSPLAGLVMSS 239
L.tar     LSYQYVSARTAEYLGRPLEELKLILCHLGTGGSSVTAMKDGRSMDSSMGYSPLPGLVMST 239
          ***.:*       :   ... *:: ****:****  .: :* . *:*** :.*.**:**:

          _______                                   ___LOOP4____
E.his     RCGDIDPTIPIDMIQQVGIEKVVD-ILNKKSGLLGVSELSSDMRDILHEIETRGPKAKTC 290
E.nut     RCGDIDPTIPIDMIQQVGIEKVVD-ILNKKSGLLGVSELSSDMRDILHEIEIRGPKAKTC 290
E.dis     RCGDIDPTIPIDMIQQVGVERVVD-ILNKRSGLLGVSELSSDMRDILHEIEIKGPKAKTC 290
E.inv     RCGDIDPSIPINIVEQIGIQKTVD-LLNKRSGLFGVSETSCDIRDLLKEIKENGQKAEKC 290
O.app     RTGDLDAQIPIQLLKEGKSPKEIETLLNKKSGLLGISQFSSDLRDILARVE----QDPNA 295
L.arv     RSGDIDPEIVLEMIRNGSSPDEVSQILNNRSGLIGLSGFSSSLPEIIEASE---KGNADC 296
F.flo     RSGDLDPEIILDLVRSGYSADEVSRILNRESGLIGLSGFSSNLAEIIDAAE---SGNVSC 296
L.tar     RCGDLDPEIVLEMIRRGSSVDDVEFILNNQSGLIGLSGYSSNLEEVIAEGE---KGNEDC 296
          * **:*. * ::::.       :. :**..***:*:*  *..: :::   :        .
```

```
                                      _____ADENOSINE____
E.his     QLAFDVYIKQLAKTIGGLMVEIGGLDLLVFTDQMGLEVWQVRKAICDKMKFLGIELDDSL 350
E.nut     QLAFDVYIKQLAKTIGGLMVEIGGLDLLVFTDQMGLEVWQVRRAICDKMKFLGIELDDSI 350
E.dis     QLAFDVYIKQLAKTIGGLMVEIRGLDLLVFTDQMGLEVWQVRKAICDKMKFLGIELDNSL 350
E.inv     ALAFDLYINQLTKTIGGLMVEIGGLDMLVFTDQVGLEVPEVRKAVCNKLEFLGVELDSEK 350
O.app     HLAFEMAVHRLVKYIGAYAVLLGGLDALIFTDDIGLWSWQLRESVCQGLTWCGIAIDPTA 355
L.arv     QLAYDVYAHRLETYLGAYTWLLDGADAIVFTDDVGLKSWKLRAKVCGGVQNLGVEIDAAK 356
F.flo     QIAFDVYAQRLMEYMGAFYWLLNGADAIVFTDDIGETSWKLREKLFGGKDLLGVKLDQEL 356
L.tar     RLAFDVYAHRLQLYLGAFFWLLNDADAIVFTDDVGLKSWKLREKVCRGVENLGILLDADA 356
           :*:::  ::*   :*.    : . * ::***::*    ::*  :       *: :*

E.his     NEKSMGKKIEFLTMPSSKVQVCVAPNDEELVILQKGKELFQF------ 392
E.nut     NEKSMGKKIEFLTMPSSKVQVCVAPNDEELVILQKGKELFQF------ 392
E.dis     NEKSMGKKIEFLTTPSSKVQVCVAPNDEELVILQKGKELFQF------ 392
E.inv     NEKSRGKEIEFISTEKSRMKICVVPNDEELVILKKGSELFQFCN---- 394
O.app     NREAPYDRITPIEAPDSRARVLVIPTDEEWVIGQEGFALLQEGRHAYH 403
L.arv     NVNAPLDRASRVSSARSKTQIWVMPTDEESVILQEILAQFCLA----- 399
F.flo     NRQATGSKPSCISQEGSKTQIWVIPTDEEIVILNEVRAIIG------- 397
L.tar     NRLALPDQITCFSSPASRTRLLTVPTDEEQVILQEVLSQLEQA----- 399
          *  :  ..   .    *: :: . *.*** ** ::    :
```

Figure 2.10: Alignment of putative PP_i-ACK sequences. The full ACK sequence alignment from which Figure 2.9 was derived is shown.

CONCLUSIONS:

Our results demonstrate that phosphoryl donor specificity in ACK is mediated not just by access to the adenosine binding pocket but by other elements as well, as simple opening or occlusion of the entrance to this pocket was not sufficient to alter substrate specificity. This suggests that the active sites of the ADP/ATP-dependent and P_i/PP_i-dependent enzymes have evolved to optimize utilization of their preferred substrate at the expense of the ability to use alternative substrates, and thus better suit their biological function.

ACKNOWLEDGEMENTS:

We thank Kerry Smith (Clemson University) for beneficial discussions regarding this work. This work was supported by a grant from the National Institutes of Health (R15GM114759) and Clemson University.

AUTHOR CONTRIBUTIONS:

CIS conceived and supervised the work and co-wrote the manuscript. TD designed and performed the experiments, analyzed the data, interpreted the results, and co-wrote the manuscript. Both authors reviewed the results and approved the final version of the manuscript.

REFERENCES:

1. Ingram-Smith, C., Martin, S. R. and Smith, K. S. Acetate kinase: Not just a bacterial enzyme. *Trends Microbiol* **14**, pp 249-253 (2006).

2. Lipmann, F. Enzymatic synthesis of acetyl phosphate. *J Biol Chem* **155**, 55-70 (1944).

3. Rose, I. A., Grunberg-Manago, M., Korey, S. R. and Ochoa, S. Enzymatic phosphorylation of acetate. *J Biol Chem* **211**, 737-756 (1954).

4. Buss, K. A., *et al.* Urkinase: Structure of acetate kinase, a member of the ASKHA superfamily of phosphotransferases. *J Bacteriol* **183**, 680-686 (2001).

5. Gorrell, A., Lawrence, S. H. and Ferry, J. G. Structural and kinetic analyses of arginine residues in the active site of the acetate kinase from *Methanosarcina thermophila*. *J Biol Chem* **280**, 10731-10742 (2005).

6. Miles, R. D., Gorrell, A. and Ferry, J. G. Evidence for a transition state analog, MgADP-aluminum fluoride-acetate, in acetate kinase from *Methanosarcina thermophila*. *J Biol Chem* **277**, 22547-22552 (2002).

7. Ingram-Smith, C., *et al.* Characterization of the acetate binding pocket in the *Methanosarcina thermophila* acetate kinase. *J Bacteriol* **187**, 2386-2394 (2005).

8. Reeves, R. E. and Guthrie, J. D. Acetate kinase (pyrophosphate). A fourth pyrophosphate-dependent kinase from *Entamoeba histolytica*. *Biochem Biophys Res Commun* **66**, 1389-1395 (1975).

9. Fowler, M. L., Ingram-Smith, C. and Smith, K. S. Novel pyrophosphate-forming acetate kinase from the protist *Entamoeba histolytica*. *Eukaryot Cell* **11**, 1249-1256 (2012).

10. Yoshioka, A., Murata, K. and Kawai, S. Structural and mutational analysis of amino acid residues involved in atp specificity of *Escherichia coli* acetate kinase. *J Biosci Bioeng* **118**, 502-507 (2014).

11. Bork, P., Sander, C. and Valencia, A. An ATPase domain common to prokaryotic cell cycle proteins, sugar kinases, actin, and hsp70 heat shock proteins. *Proc Natl Acad Sci U S A* **89**, 7290-7294 (1992).

12. Thaker, T. M., *et al.* Crystal structures of acetate kinases from the eukaryotic pathogens *Entamoeba histolytica* and *Cryptococcus neoformans*. *J Struct Biol* **181**, 185-189 (2013).

13. Baugh, L., *et al.* Increasing the structural coverage of tuberculosis drug targets. *Tuberculosis (Edinb)* **95**, 142-148 (2015).

14. Chittori, S., Savithri, H. S. and Murthy, M. R. Structural and mechanistic investigations on *Salmonella typhimurium* acetate kinase (acka): Identification of a putative ligand binding pocket at the dimeric interface. *BMC Struct Biol* **12**, 24 (2012).

15. Ingram-Smith, C., *et al.* The role of active site residues in atp binding and catalysis in the *Methanosarcina thermophila* acetate kinase. *Life (Basel)* **5**, 861-871 (2015).

16. Gorrell, A. and Ferry, J. G. Investigation of the *Methanosarcina thermophila* acetate kinase mechanism by fluorescence quenching. *Biochemistry* **46**, 14170-14176 (2007).

17. Aceti, D. J. and Ferry, J. G. Purification and characterization of acetate kinase from acetate-grown *Methanosarcina thermophila*. Evidence for regulation of synthesis. *J Biol Chem* **263**, 15444-15448 (1988).

18. Yamada, T., *et al. Anaerolinea thermolimosa* sp. nov., *Levilinea saccharolytica* gen. nov., sp. nov. and *Leptolinea tardivitalis* gen. nov., sp. nov., novel filamentous anaerobes, and description of the new classes *Anaerolineae classis* nov. and *Caldilineae classis* nov. in the bacterial phylum *Chloroflexi*. *Int J Syst Evol Microbiol* **56**, 1331-1340 (2006).

19. Yamada, T., *et al. Bellilinea caldifistulae* gen. nov., sp. nov. And *Longilinea arvoryzae* gen. nov., sp. nov., strictly anaerobic, filamentous bacteria of the phylum *Chloroflexi* isolated from methanogenic propionate-degrading consortia. *Int J Syst Evol Microbiol* **57**, 2299-2306 (2007).

20. Podosokorskaya, O. A., Bonch-Osmolovskaya, E. A., Novikov, A. A., Kolganova, T. V. and Kublanov, I. V. *Ornatilinea apprima* gen. nov., sp. nov., a cellulolytic representative of the class *Anaerolineae*. *Int J Syst Evol Microbiol* **63**, 86-92 (2013).

21. Sun, L., *et al.* Isolation and characterization of *Flexilinea flocculi* gen. nov., sp. nov., a filamentous anaerobic bacterium belonging to the class *Anaerolineae* in the phylum *Chloroflexi*. *Int J Syst Evol Microbiol* (2015).

22. Fowler, M. L., Ingram-Smith, C. J. and Smith, K. S. Direct detection of the acetate-forming activity of the enzyme acetate kinase. *J Vis Exp* (2011).

23. Sievers, F., *et al.* Fast, scalable generation of high-quality protein multiple sequence alignments using Clustal Omega. *Molecular Systems Biology* **7**, 539-539 (2011).

24. McWilliam, H., *et al.* Analysis tool web services from the EMBL-EBI. *Nucleic Acids Res* **41**, W597-600 (2013).

25. Li, W., *et al.* The EMBL-EBI bioinformatics web and programmatic tools framework. *Nucleic Acids Res* **43**, W580-584 (2015).

26. Armon, A., Graur, D. and Ben-Tal, N. Consurf: An algorithmic tool for the identification of functional regions in proteins by surface mapping of phylogenetic information. *J Mol Biol* **307**, 447-463 (2001).

27. Glaser, F., *et al.* Consurf: Identification of functional regions in proteins by surface-mapping of phylogenetic information. *Bioinformatics* **19**, 163-164 (2003).

28. Landau, M., *et al.* Consurf 2005: The projection of evolutionary conservation scores of residues on protein structures. *Nucleic Acids Res* **33**, W299-302 (2005).

CHAPTER III

THE ROLE OF ADP-FORMING ACETYL-COA SYNTHETASE AND ACETATE KINASE IN *ENTAMOEBA HISTOLYTICA*

Thanh Dang, Diana Nguyen, Cheryl Jones, and Cheryl Ingram-Smith

ABSTRACT:

Entamoeba histolytica is a human pathogenic protozoan that causes approximately 90 million cases of amoebic dysentery, resulting in 50,000 – 100,000 deaths annually. This amitochondriate parasite lacks many essential biosynthetic pathways including the TCA cycle and oxidative phosphorylation. As a result, substrate level phosphorylation plays a necessary and important role in ATP production. *E. histolytica* produces ethanol and acetate as the major end products during growth, of which acetate can be generated by acetate kinase (EhACK) and ADP–forming acetyl–CoA synthetase (EhACD). ACK converts acetyl phosphate + orthophosphate to acetate + pyrophosphate (PP_i). Biochemical and kinetic characterization of recombinant EhACK showed that it strongly prefers the acetate/PP_i forming direction. On the other hand, recombinant EhACD displays high activity in both directions to convert acetyl-CoA + orthophosphate + ADP to acetate + ATP + CoA. Using reverse genetics, both EhACK and EhACD were shown to play a role in *E. histolytica* proliferation. An *acd* knockdown strain displayed a growth defect in normal high glucose media, or when exposed to bovine serum starvation. Metabolite analysis substantiated EhACD's role to extend glycolysis for ATP generation and linked reduced growth of the *acd* knockdown to ATP availability. Moreover, EhACD was found to be essential for growth on propionate,

suggesting a role in propionate activation as carbon source. EhACK also shared signs of involving in growth during stress conditions; the *ack* knockdown strain showed enhanced growth in medium lacking tryptone and low in glucose. Thus, EhACK may play a role in growth under stress conditions and unlikely plays a role in glycolysis.

INTRODUCTION:

Entamoeba histolytica is an amoebic parasite that infects an estimated 90 million people worldwide and causes approximately 100,000 deaths per year [1-3]. Infection proceeds through an oral-fecal route, resulting in *E. histolytica* colonization within the large intestine. This amitochondriate parasite lacks many essential biosynthesis pathways including the TCA cycle and oxidative phosphorylation; thus, ATP generation is limited to glycolysis [4-6].

Unlike the standard glycolytic pathway, *E. histolytica* glycolysis is pyrophosphate (PP_i)-dependent. Instead of ATP–dependent phosphofructokinase and pyruvate kinase, *E. histolytica* possesses pyrophosphate–dependent phosphofructokinase (PP_i-PFK) and pyruvate phosphate dikinase (PPDK) (Figure 3.1). Pyrophosphate, therefore, plays an important role in energy conservation. Ultimately, *E. histolytica* produces ethanol and acetate as the major end products during growth on glucose, of which acetate can generated by acetate kinase (EhACK) and ADP–forming acetyl–CoA synthetase (EhACD).

Acetate kinase (ACK; EC 2.3.1.8) is a phosphotransferase that interconverts acetyl phosphate and acetate. Widespread in bacteria, acetate kinase primarily function to generate ATP or activate acetate by partnering with another enzyme, commonly phosphotransacetylase (PTA) [7, 8]. ACK has also been identified in one genus of archaea,

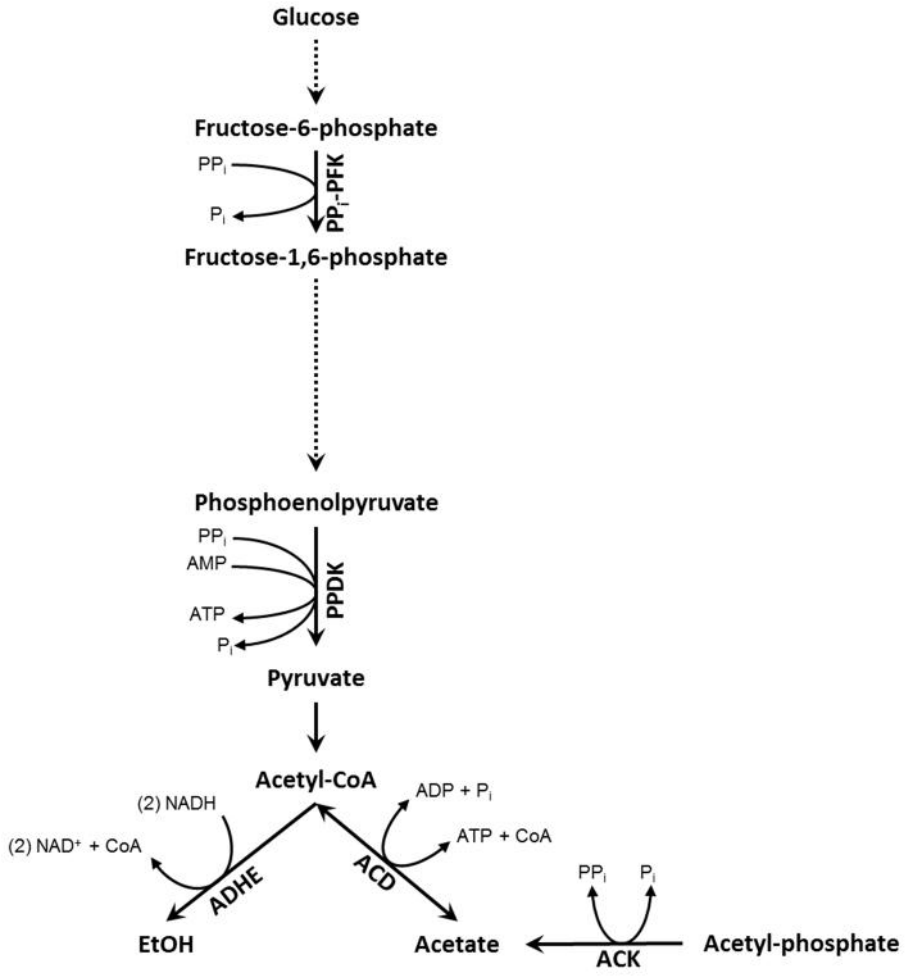

Figure 3.1: ***Entamoeba histolytica*** **extended glycolytic pathway.** This schematic depicts *E. histolytica* PP_i-dependent glycolysis in which phosphofructokinase (PFK) and pyruvate kinase (PK) are replaced with PP_i-dependent PFK and pyruvate phosphate dikinase (PPDK). ACD and the bifunctional aldehyde-alcohol dehydrogenase (ADHE) extend the glycolytic pathway to produce ethanol (EtOH) and acetate, which can also be produced by ACK.

other eukaryotic microbes, several fungi, and *E. histolytica* [9, 10]. EhACK was shown to be pyrophosphate and inorganic phosphate dependent, a stark contrast to all other characterized ACKs which are ATP and ADP dependent [9, 11]. Kinetic analysis also demonstrated that EhACK operates primarily in the acetate-producing direction *in vitro.* Consistent with this, activity was detected only in the acetate/PP_i – direction in cell extract, supporting this as the physiological direction of EhACK [11]. However, ACK's role in *E. histolytica* remains undefined.

EhACK was hypothesized to provide supplemental pyrophosphate for the pyrophosphate-dependent glycolysis in *E. histolytica* [11]. In a comparison between the transcriptome of the virulent HM–1:IMSS and the nonvirulent Rahman strains, several glycolytic enzymes including PP_i–PFK were found to be highly upregulated in HM–1:IMSS in both axenic culture and during contact with human colon explant [12]. This upregulation was thought to reflect the carbon metabolism needs during colonic mucosa degradation and tissue destruction during intestinal amoebiasis. EhACK was constitutively expressed in active trophozoites and at a slightly higher level in HM–1:IMSS versus the Rahman strain [13, 14]. These findings supported the possibility that EhACK could work in unison with PP_i–dependent phosphofructokinase and pyruvate phosphate dikinase to drive glycolysis.

ACD (EC 6.2.1.13) catalyzes the conversion of acetyl-CoA to acetate to generate ATP. Current knowledge of ACD comes from *in vitro* biochemical and kinetic characterization of eukaryotic ACDs from *E. histolytica* [15], *Giardia lamblia* [16] and the archaeal *Pyrococcus furiosus* ACD [17, 18]. ACD is believed to play a critical role in

conservation of energy by extending the glycolytic pathway, generating additional ATP and recycling CoA[19]. *In vitro* kinetic analysis of recombinant EhACD also showed this enzyme catalyzes a reversible reaction, indicating potential alternative roles *in vivo* [15]. Based on these kinetic analyses, this enzyme may function in acetate activation during nutrient limiting conditions as seen with AMP-forming acetyl-CoA synthetase [7, 15]. *Acd* also appears to be constitutively expressed [14], suggesting that this enzyme may be essential in energy metabolism, survival, or proliferation. However, its significance has yet to be investigated in depth.

A majority of *E. histolytica* infections reside within the human colon, where glucose is limiting. Alternative carbon sources and energy conservation thus can be plausibly seen as an essential part of *E. histolytica* survival and growth. Here, we investigated the functional role and contribution of EhACK and EhACD in growth, survival and adaptation to nutrient limiting environments. Our study showed that EhACD enhanced *E. histolytica* proliferation and suggested EhACK may hold a novel role *in vivo*.

MATERIALS AND METHODS:

Chemicals and reagents

Chemicals were purchased from Qiagen, Promega, Sigma-Aldrich, VWR International, Gold Biotechnology, Fisher Scientific, Gemini Bio-products, EMD Millipore, and Life Technologies. Penicillin-streptomycin and Diamond vitamins from Life Technologies (Carlsbad, CA) and heat inactivated adult bovine serum from Gemini (Sacramento, CA) were used for all *Entamoeba* media culture. Restriction enzymes were purchased from New England Biolabs (Ipswich, MA). Primers were purchased from Integrated DNA Technologies (Coralville, IA).

Strains and culture conditions

E. histolytica HM-1:IMSS was grown axenically in Diamond's TYI-S-33 medium[20] (17.95 g tryptone, 9.66 g yeast extract, 9.2 g glucose, 1.84 g NaCl, 0.92 g K_2HPO_4, 1.15 g cysteine, 0.178 g ascorbic acid, 0.0194 g ammonium ferric chloride, 15% v/v adult bovine serum, 1.73% v/v penicillin-streptomycin, and 2.62% v/v Diamond vitamins per liter at pH 6.8) under standard conditions at 37°C. Log phase trophozoites were harvested and used for all experiments. Modifications to TYI-S-33 medium were as follows: reduced glucose, 10 mM glucose; tryptone exclusion, no added tryptone; tryptone exclusion + low glucose, no added tryptone and glucose; reduced adult bovine serum, 3.85% adult bovine serum; and adult bovine serum excluded. Growth on acetate, propionate, or butyrate was performed in TYI-S-33 medium with no added glucose and supplemented with 63 mM acetate, 24 mM propionate, or 23 mM butyrate.

Growth curves were determined for wild-type (WT), pKT3M-luciferase (LUC), EhACK knockdown (EhACKkd) and EhACD knockdown (EhACDkd) strains. Trypan blue exclusion [28] was used to distinguish viable from dead cells and viable cells were counted every 24 hours using a Luna Automated counter (Logos Biosystem, Annandale, VA). Cultures for growth determinations were grown at 37°C in base TYI-S-33 medium with the following alterations: normal high glucose, reduced glucose, low glucose, tryptone exclusion, tryptone exclusion + low glucose, reduced adult bovine serum, and adult bovine serum exclusion (Table 3.1).

Construct cloning and transfection

Primers used are listed in Table 3.2. The full length *Entamoeba histolytica* ACK (EHI_170010) and ACD (EHI_178960) coding sequences were PCR-amplified from *E. histolytica* genomic DNA using KOD hot start polymerase (EMD Millipore, Billerica, MA). *E. hisotlytica* genomic DNA was isolated from 2 x 10^6 trophozoites using Wizard genomic DNA isolation kit (Promega, Madison, WI). EhACK and EhACD RNAi constructs were created by cloning the amplified products into the modified pKT3M vector in place of the resident luciferase gene using the AvrII and XhoI restriction enzymes [21]. All final constructs were confirmed by Sanger sequencing at the Clemson University Genomics Institute (CUGI). *E. histolytica* trophozoites were transfected with the RNAi constructs by electroporation as described previously [22, 23]. Briefly, a total of 2.4 x 10^6 cells were electroporated with 100µg of DNA using two consecutive pulses at 1.2kV and 25uF. Transfectants were selected after two days by adding 6µg/mL G418 into the medium. Stable transfectants were maintained under G418 selection.

Conditions	*Glucose (mM)*	*Tryptone (% w/v)*	*Adult bovine serum (% v/v)*
Normal high glucose	50	2.2	15
Reduced glucose	**10**	2.2	15
Low glucose	**Not added**	2.2	15
Tryptone exclusion	50	**Not added**	15
Tryptone exclusion + low glucose	**Not added**	**Not added**	15
Reduced adult bovine serum	50	2.2	**3.85**
Adult bovine serum exclusion	50	2.2	**Not added**

Table 3.1: List of glucose, tryptone, and adult bovine serum alterations to standard TYI-S-33 medium. Bolded texts illustrate the alteration within the specific condition.

	Primer Sequences
Cloning primers	
EhACK RNAi Forward	5’ CTACCTAGGATGTCTAACGTACTAATATTCAAC G
EhACK RNAi Reverse	5’ CTACTCGAGTTAAAACTGAAATAATTCTTTTCCTTT TTGTAA
EhACD RNAi Forward	5’ACACCTAGGATGCAATTTGAGCCACTCTTCAATCC
EhACD RNAi Reverse	5’ ACACTCGAGTTATGGTTGGATGACGAGGTGAGAG
RT-PCR primers	
EhACK RTPCR Forward	5’ AGGGTAAATGTTACAGGAACAGA
EhACK RTPCR Reverse	5’ TGGTGCCACACAAACTTGAAC
EhACD RTPCR Forward	5’ AGTGCCGGTTATTGGTGCAT
EhACD RTPCR Reverse	5’ AGCTTCAGCAACTGCTTCGT
ssrRNA Forward	5′-AGGCGCGTAAATTACCCACTTTCG
ssrRNA Reverse	5′-CACCAGACTTGCCCTCCAATTGAT

Table 3.2: **List of primers used for RNAi construct generation and RT-PCR confirmation.**

Reverse transcriptase-PCR (RT-PCR)

Primers are listed in Table 3.1. RNA was isolated from 2 x 10^6 trophozhoites using the RNeasy mini kit (Qiagen, Valencia, CA). RT-PCR was employed to determine whether the *Ehack* and *Ehacd* were silenced by the respective RNAi constructs. RT-PCR was performed using the One-step RT-PCR kit (Qiagen). RNA levels were normalized for comparison using the small subunit ribosomal RNA gene (accession number: X61116) as previously described [(24)].

Enzyme assays

Ehack and *Ehacd* knockdowns were confirmed by measuring ACK and ACD activity, respectively, in cell lysates. A total of 4 x 10^6 cells were harvested by centrifugation and washed twice in phosphate buffered saline (PBS). Cells were resuspended in 25 mM Tris, 150 mM NaCl (pH 7.4). Cells were lysed by vortexing with acid-washed beads for one minute, followed by 1 minute on ice. This cycle was repeated 3 times. The lysates were centrifuged at 5000 x g for 15 minutes and the supernatant was retained.

ACK activity was measured using the reverse hydroxamate assay as previously described [(25)]. Enzyme activity was assessed in a 300 µl reaction containing 50 mM sodium phosphate, 2 mM acetyl phosphate, 100 mM Tris-HCl (pH 7), and 10 mM $MgCl_2$ and 50 µl cell lysate for 30 minutes at 37^{o}C before quantification. Reactions were terminated by adding 100 µl of the development solution (0.92 M trichoroacetic acid, 250

mM $FeCl_2$, and 2.5 N HCl). Absorbance at 540 nM was measured using a Synergy Epoch microplate reader (Biotek, Winooski, VT).

ACD activity in the acetyl-CoA forming-direction and acetate forming-direction were measured as described by Jones and Ingram-Smith [15]. ACD activity was quantitated using 10 µl of cell lysate at 37°C for 15 minutes. For the acetyl-CoA forming-direction, the hydroxamate assay was used at substrate saturating concentrations. Reaction contained 1 mM CoA, 20 mM Mg:ATP, 100 mM acetate, and 50 mM Tris-HCl (7.3). Absorbance at 540 nm was measured using a Synergy Epoch microplate reader. For the acetate forming-direction, the DNTB assay was employed. Reactions contained 50 mM Tris-HCl (pH 7.3), 300 µM 5,5-dithio-bis-2-nitrobenzoic acid (DNTB), 300 µM acetyl-CoA, 8 mM potassium phosphate, and 5 mM Mg:ATP. Assays were performed using 96-wells plate in 200 µl reaction volume. The change in absorbance at 412 nm was determined using Synergy H1 microplate reader.

Total protein concentration in cell lysates was measured using the Bradford assay [26, 27] with bovine serum albumin as the standard.

Intracellular metabolite analysis

E. histolytica intracellular metabolites were extracted using an adapted methanol extraction method [29] from 1 x 10^6 log phase trophozoites. Cells were harvested by centrifugation, washed three times in ice cold 5% mannitol solution, and resuspended in 1500 µl of 100% methanol (-20°C). Trophozoites were lysed using a freeze-thaw method. Cells were frozen in liquid nitrogen for 5 minutes and thawed on dry ice for 10 minutes.

This cycle was repeated 3 times. The lysate was centrifuged at 13,000 rpm for 5 minutes and the supernatant isolated. Samples were analyzed at Clemson Multi-Users Analytic Lab via LC-MS/MS. Intracellular metabolite concentrations were calculated by assuming *E. histolytica* trophozoites have an intracellular volume of 1.3 µl per 1 x 10^6 cells as previously reported [30, 31].

RESULTS:

Ehacd silencing affects growth on glucose but Ehack silencing does not

To examine the roles of EhACK and EhACD, reverse genetics was employed. The *ack* and *acd* genes were individually silenced using the trigger-RNAi gene silencing system developed by Morf *et al.* [21]. The *ack* and *acd* coding regions were cloned into the modified pKT3M trigger-derived antisense small RNA vector. The pKT3M vector containing a luciferase gene (*luc*) was used as a transfection control. RNA was isolated from wild type, *luc* control, and the *ack* and *acd* silenced strains and RT-PCR was performed to examine RNA levels for the silenced genes. *ack* and *acd* mRNA levels were undetectable in the respective silenced strains (Figure 3.2A and B) but were unaffected in the wild-type and *luc* control strains. In addition, ACK and ACD enzyme activity was considerably reduced or abolished in *ack* and *acd* silenced cells, respectively (Figure 3.2C-E). Taken together, this confirmed the successful silencing of these two genes.

The *ack* and *acd* gene silenced strains, hereafter referred to as EhACKkd and EhACDkd, both remained viable. EhACDkd grew slower than control cells (WT and LUC) in standard TYI-S-33 medium containing 50 mM glucose (Figure 3.3A); This difference in growth was statistically significant by 72 and 96 hours. However, the EhACKkd strain grew at a comparable rate to the WT and LUC strains.

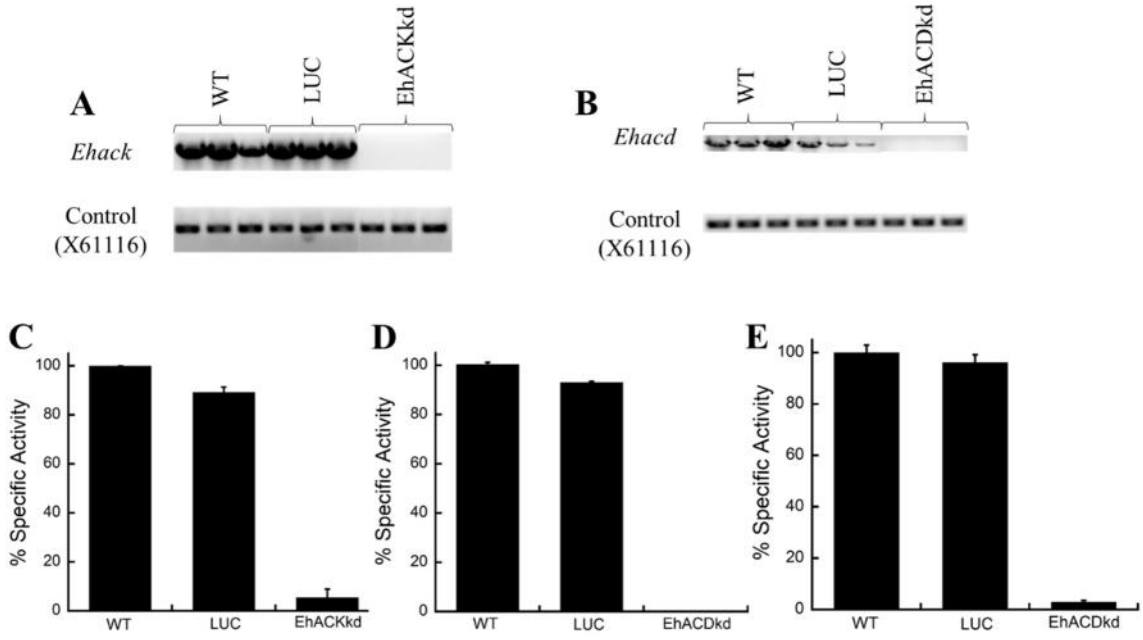

Figure 3.2: **EhACK and EhACD silencing by trigger antisense-derived RNA interference.** RT-PCR depicting *Ehack* mRNA levels (**A**) and *Ehacd* mRNA levels (**B**). Control (X61116) shows RT-PCR of the small subunit RNA gene and indicates equivalent mRNA in all lanes. **C**: EhACK activity from cell extracts in the acetate-forming direction. **D**: EhACD activity from cell extracts in the acetyl-CoA forming direction. **E**: EhACD activity from cell extracts in the acetate-forming direction. WT: untransfected cells; LUC: luciferase control cells; EhACKkd: ACK knockdown cells; EhACDkd: ACD knockdown cells. Enzyme activities are the mean ± SD of at least three replicates. Specific activities are represented as a percentage of the activity observed from the wild-type strain.

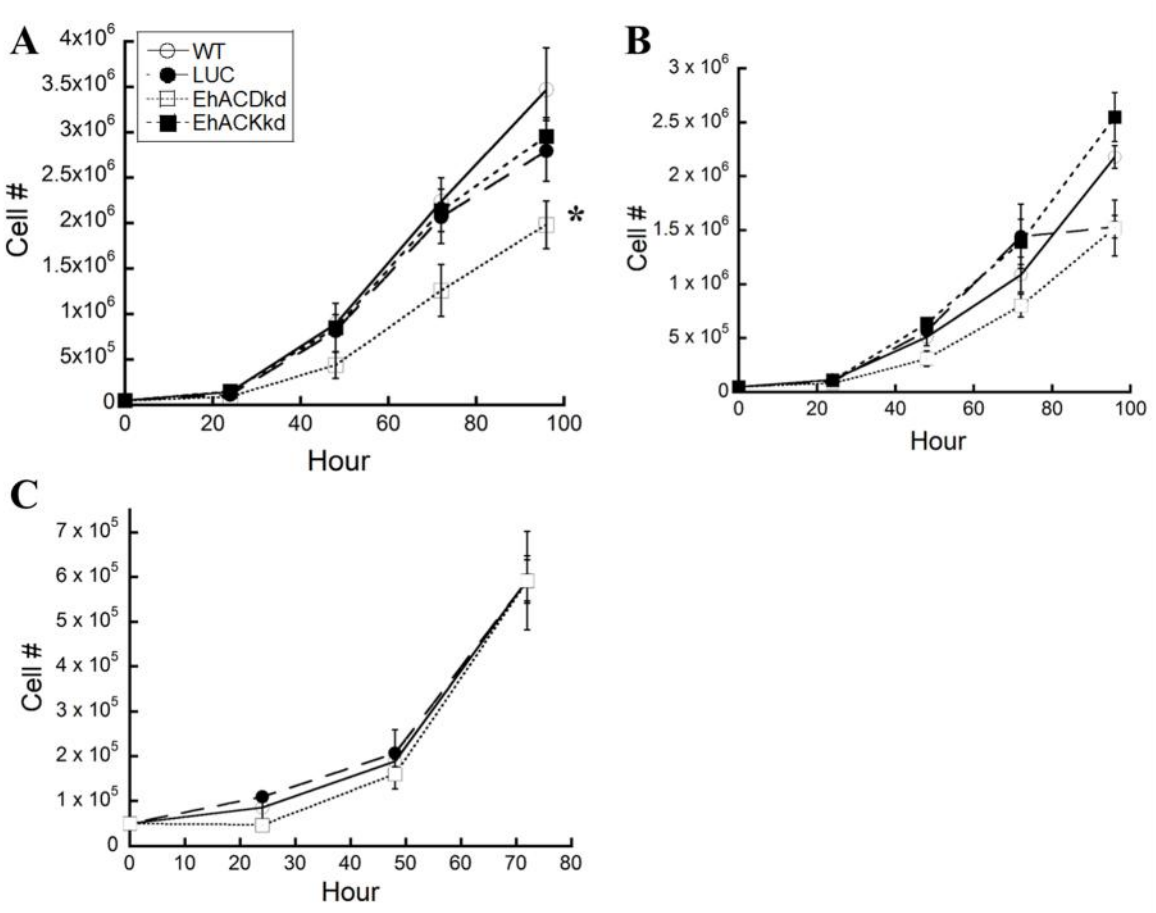

Figure 3.3: ***E. histolytica*** **growth in varying glucose concentration**. Growth was assessed by direct cell counting, using tryphan blue exclusion to indicate live versus dead cells. Growth curves were initiated with 5 x 10^4 cells per tube. Cells were grown in TYI-S-33 medium containing (**A**) 50 mM glucose (the standard glucose concentration in this medium), (**B**) 10 mM glucose, or (**C**) no added glucose. Cell numbers are the mean ± SD of at least three biological replicates. The significance of the growth deficiency for the ACDkd strain versus the WT and LUC strains was tested using a one-way ANOVA and TUKEY separation of means with R. * = p-value ≤ 0.05.

We next tested whether this difference in growth for the EhACDkd strain would persist at lower glucose concentrations. The EhACDkd strain still showed the slowest growth when the glucose concentration was reduced to 10 mM (Figure 3.3B). However, this growth defect disappeared when EhACDkd cells were grown in TYI-S-33 medium in the absence of added glucose (Figure 3.3C). The EhACKkd strain showed no difference in growth from the WT and LUC control cells in the presence of 10 mM glucose (Figure 3.3B) and therefore growth was not assessed in the absence of added glucose.

Intracellular metabolite levels are affected in EhACDkd and EhACKkd strains

Intracellular acetyl-CoA and ATP concentrations were measured for the WT, LUC control, EhACDkd, and EhACKkd strains after growth in TYI-S-33 medium containing 50 mM glucose. Both the EhACDkd and EhACKkd strains showed an accumulation of acetyl-CoA of approximately 172% vs. WT or LUC (Figure 3.4). Consistent with the proposed role of ACD in acetate production from acetyl-CoA, the EhACDkd strain proved to have a substantially reduced ATP pool that was approximately 20% that observed for the EhACKkd, LUC, and WT strains.

Since the EhACDkd phenotype changed with glucose concentration, we examined whether ACD activity in wild-type cells varied with changes in glucose concentration in the growth medium. EhACD activity was examined in WT cells grown in TYI-S-33 medium containing 50 mM (standard), 10 mM, or no added glucose. ACD activity remained constant in both the acetate-forming and acetyl-CoA-forming direction regardless of glucose concentration (Figure 3.5).

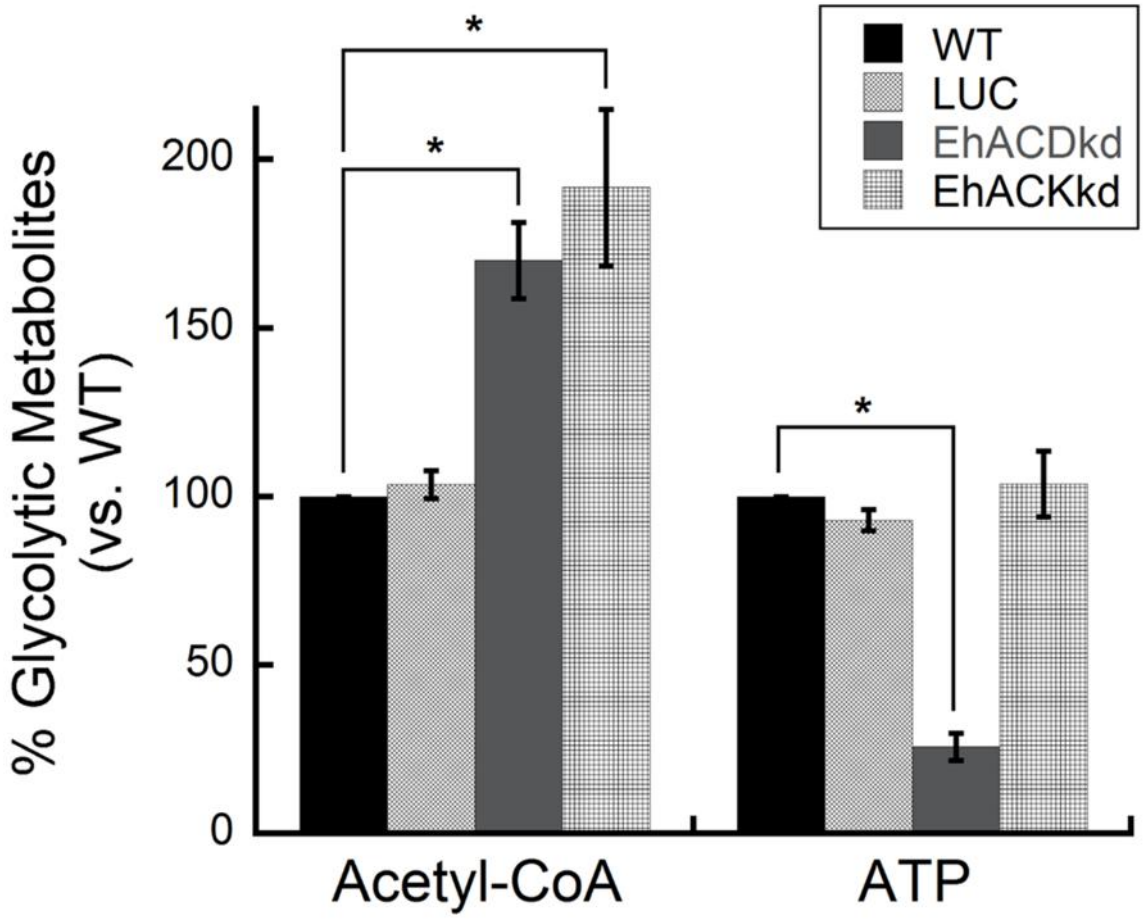

Figure 3.4: **Acetyl-CoA and ATP level comparison between each *E. histolytica* cell line.** Cell extracts were prepared from 1 x 10^6 cells at 72 hours of growth. Samples were analyzed via LC-MS/MS. Intracellular metabolite concentrations were normalized to the concentration in WT cells which are ATP 0.86 ± 0.09 mM and acetyl-CoA 0.22 ± 0.03 mM (n = 6). The statistical significance of metabolite concentration vs. WT cell intracellular concentration were tested using a Welch two samples T-test in R. * = p-value < 0.001.

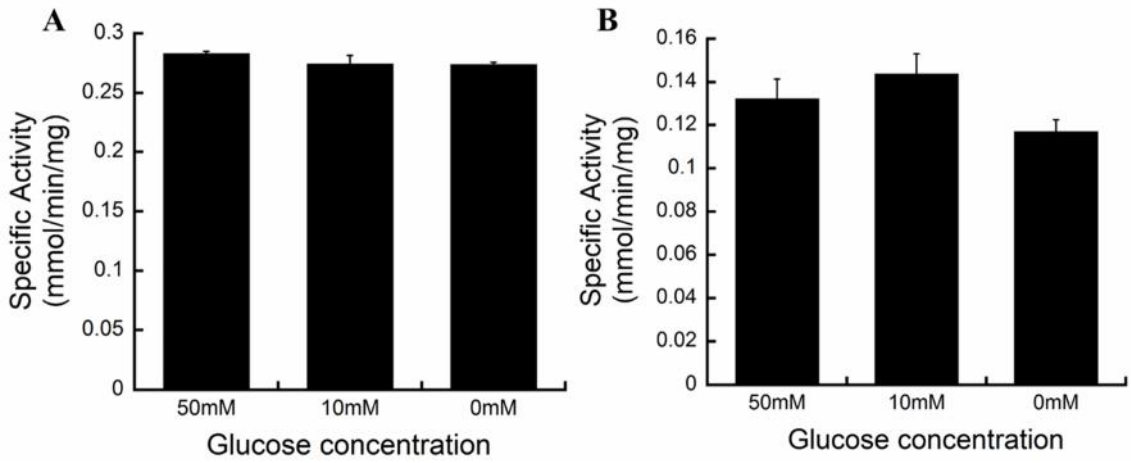

Figure 3.5: **ACD activity from WT cells grown at varying glucose concentrations**. Cells were grown for 48 hours in TYI-S-33 medium and cell extracts were prepared for measurement of enzymatic activity. **A**: ACD activity in the acetyl-CoA forming direction. **B**: ACD activity in the acetate-forming direction. Enzyme activity was measured at saturating substrate concentration. Activities are the mean ± SD of at least three replicates.

EhACK and EhACD expression and activity are independent from each other

If EhACK and EhACD have related roles, changes in expression or activity of one might be expected to influence expression or activity of the other. To this end, EhACK and EhACD activities were compared between the wild-type, LUC control, EhACKkd, and EhACDkd strains. Enzyme activity in cell extract from each strain showed no change in ACK activity when *acd* was silenced and vice versa (Figure 3.6). Thus, EhACK and EhACD do not appear to be co-regulated.

EhACD plays a role in propionate utilization

The human colon, where *E. histolytica* colonizes, contains low to no glucose but does have abundant level of short chain fatty acids (110-120mM), mainly as acetate, propionate and butyrate with relative molar mass ratio of 57:22:21 [(32)], respectively. Certain anaerobic microbes can switch from producing acetate to utilizing acetate as a carbon source when necessary, termed the "acetate switch" [(7)]. Kinetic analysis of EhACD showed it can interconvert acetyl-CoA and acetate at relatively similar rates for each direction of the reaction [(15)], suggesting EhACD may be able to utilize acetate as a growth substrate under some conditions as well as produce it during growth on glucose.

WT, LUC, EhACDkd, and EhACKkd strains were grown in low glucose and the presence of 63 mM acetate, 24 mM propionate, or 23 mM butyrate for 72 hours.

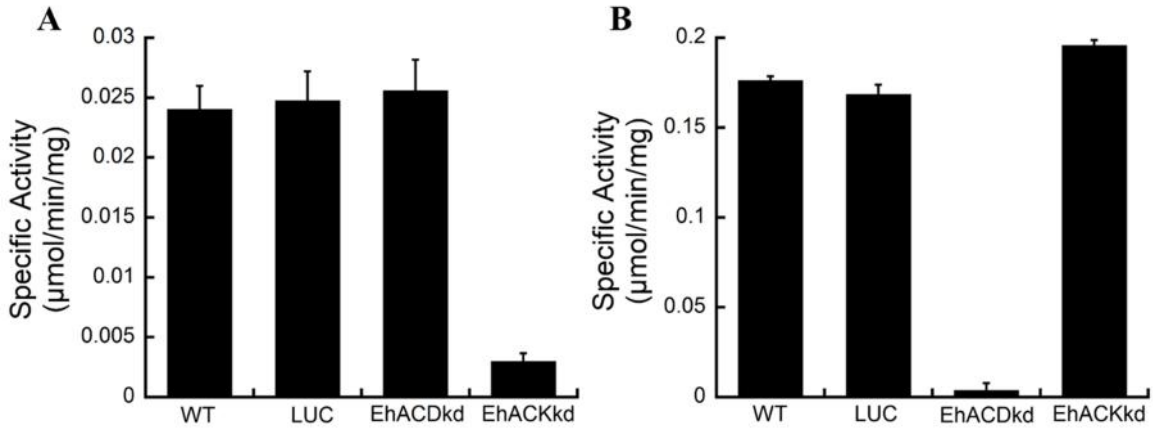

Figure 3.6: **ACK and ACD activity in WT and gene silenced strains**. The wild-type, LUC control, and ACDkd and ACKkd strains were grown in standard TYI-S-33 medium for 72 hours and ACD and ACK activities were determined in cell lysates. **A**: ACK activity from cell lysate in the acetate -forming direction. **B**: ACD activity from cell lysate in the acetyl-CoA forming direction. Activities are the mean ± SD of at least three replicates.

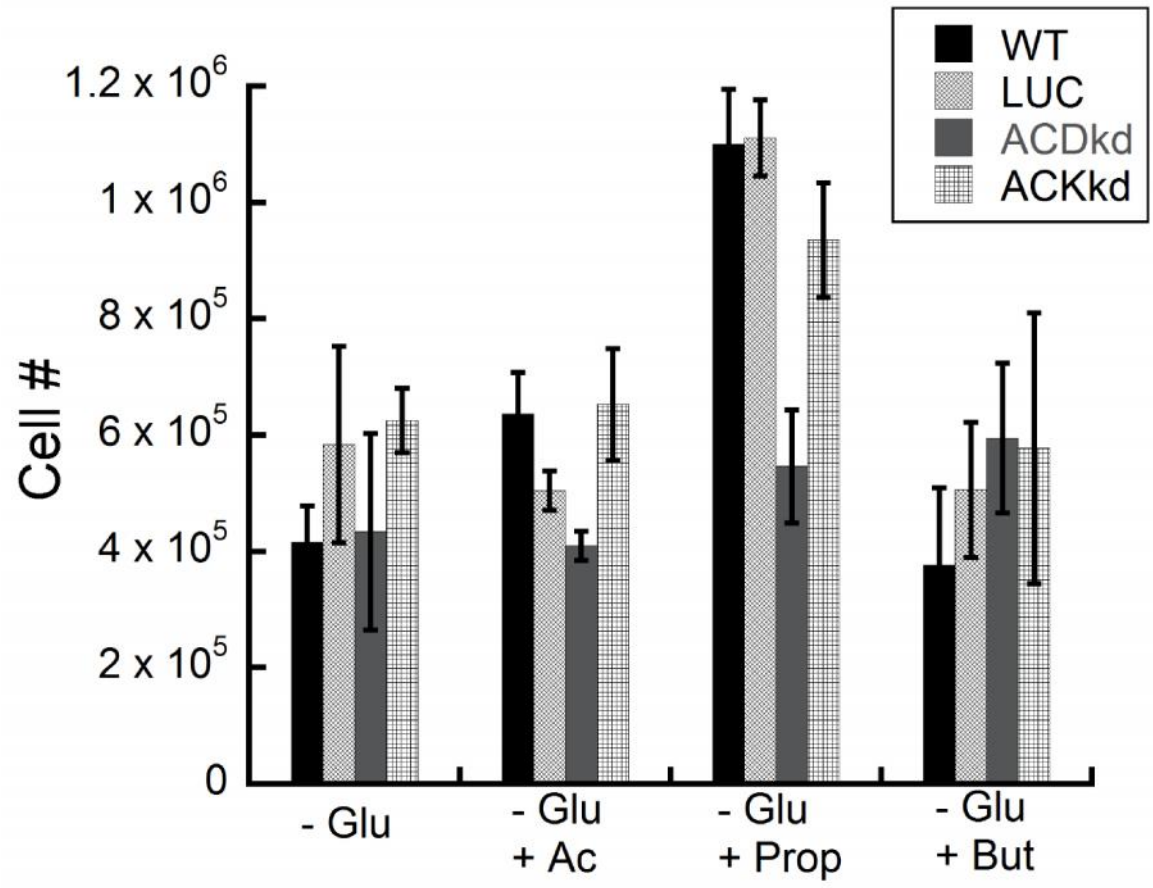

Figure 3.7: **Growth in low glucose (Glu) TYI-S-33 media with or without short chain fatty acid supplementation**. Cells were grown 72 hours in media without supplementation or supplemented with 63 mM acetate (Ac), 23 mM propionate (Prop), or 24 mM butyrate (But). Growth was initiated with 5 x 10^4 cells. Cell numbers are the mean ± SD of at least three biological replicates.

For each strain, growth in butyrate or acetate supplemented media was comparable to that observed in the absence of glucose or short chain fatty acid. Intriguingly, strains showed improved growth on propionate supplemented media improved growth, with the exception of the EhACDkd strain (Figure 3.7).

The EhACKkd strain grows in medium lacking glucose and tryptone

Studies have shown amino acids may also act as a substrate for energy metabolism in *E. histolytica* [5, 6]. To investigate this, we examined growth in TYI-S-33 media lacking tryptone, which is a source of free amino acids. As expected, omission of tryptone resulted in substantial reduction in growth of the WT and control LUC strains as well as the EhACKkd and EhACDkd strains (Figure 3.8A). Surprisingly, when glucose was also omitted from the medium, EhACKkd cells showed a significant growth advantage versus WT, LUC control, and EhACDkd strains (Figure 3.8B). Minimal growth of these latter strains was observed and cell death was observed by 96 hours.

Growth under other nutrient limiting conditions is also affected

Since *E. histolytica* encounters various environments during infection, growth was also examined under several other nutrient limited conditions. *E. histolytica* exposure to serum in the colon, which is the primary site of infection, is unlikely. Therefore, we examined growth in the absence of adult bovine serum and found that all strains died (data not shown), indicating a requirement for adult bovine serum for *in vitro* growth in culture. Next, growth in medium containing reduced serum levels of 3.85% (v/v) instead of the 15% (v/v) serum concentration in standard TYI-S-33 medium was measured. Slow

growth was observed for the WT, LUC, and EhACKkd strains cultured in the reduced serum medium (Figure 3.9). However, the EhACDkd strain did not proliferate and showed signs of death by 48 hours (Figure 3.9).

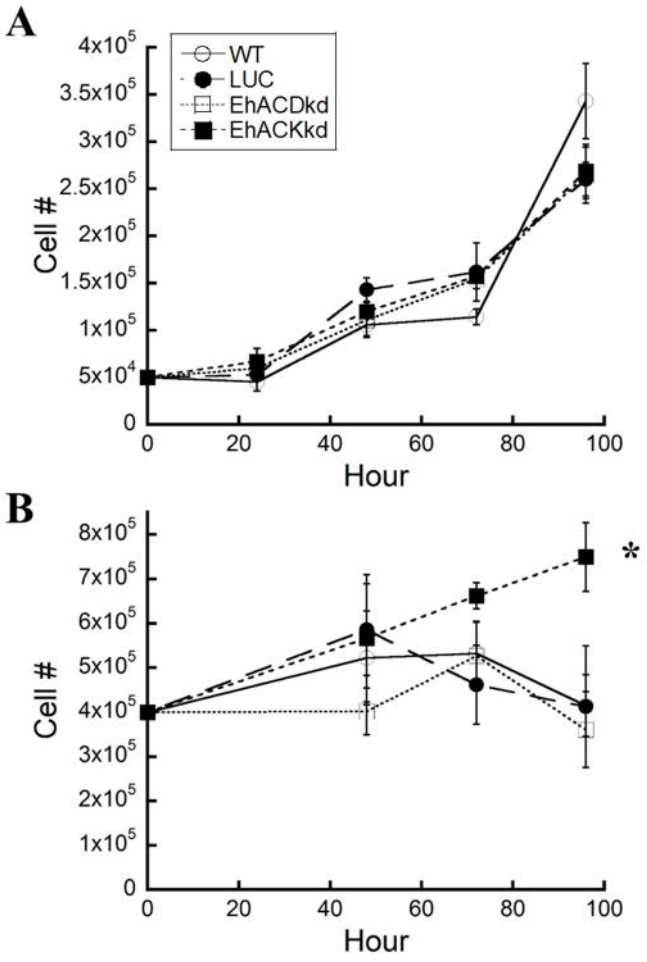

Figure 3.8: Growth of *E. histolytica* WT and gene silenced strains in TYI-S-33 medium lacking tryptone or glucose and tryptone. **A**: Growth in medium lacking tryptone. **B**: Growth in medium lacking tryptone and glucose. Cell counts are the mean ± SD of at least three biological replicates. The statistical significance of differences in growth between the EhACKkd versus WT and LUC control strains was tested using a one-way ANOVA and TUKEY separation of means in R. * = p-value ≤ 0.01.

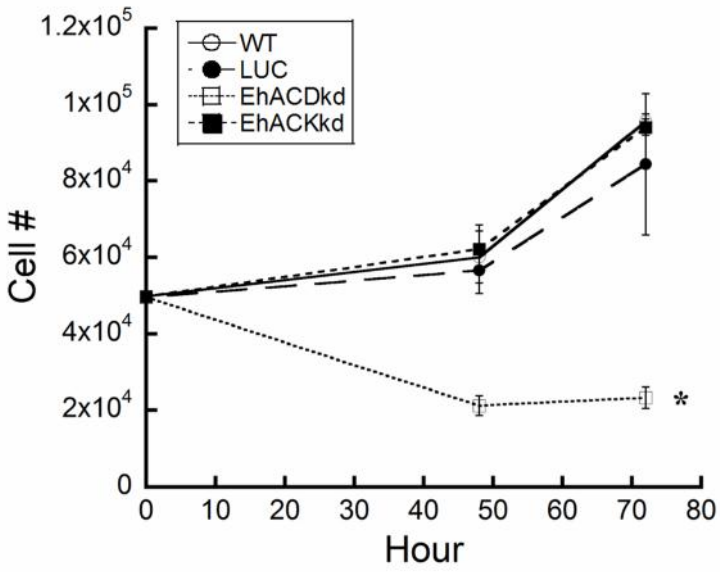

Figure 3.9: **Growth during serum starvation.** Strains were cultured in TYI-S-33 medium containing reduced (3.85% versus standard 15%) adult bovine serum. Growth was initiated with 5 x 10^4 cells. Cell counts are the mean ± SD of at least three biological replicates. The significance of the growth deficiency for the EhACDkd strain versus the WT and LUC strains was tested using a one-way ANOVA and TUKEY separation of means with R. * = p-value < 0.00001.

DISCUSSION:

The two major metabolites produced during *E. histolytica* axenic growth on glucose are ethanol and acetate. In the colon, the main site for *E. histolytica* infection, glucose concentrations are low; however, short chain fatty acids are abundant with acetate having the highest molar mass ratio [32]. Acetate metabolism has been extensively studied in prokaryotes, most notably in *Escherichia coli,* to have a role in ATP generation, coenzyme A recycling, and acetate activation for utilization as a carbon source when necessary [7]. In bacteria, ACK typically partners with the enzyme phosphotransacetylase to interconvert acetate and acetyl-CoA. The other common enzyme which interconverts acetate and acetyl-CoA is AMP-forming acetyl-CoA synthethase (ACS), which is thought to operate only in the acetyl-CoA forming direction. These two pathways form the "acetate switch" [7] where interchange between acetate production and utilization occurs to accommodate the cell's needs [8, 33-36].

In *E. histolytica*, ACK and ACD are two acetate-producing enzymes and ACS is not present. Even though ACD and ACS are not related, the fact that both are capable of activating acetate to acetyl-CoA makes it plausible that ACD plays an analogous physiological role to ACS. In the same manner, although EhACK deviates from other ACKs in phosphoryl substrate usage (PP_i versus ATP), it may still retain a parallel role to other ACKs. Gene expression studies have shown that both *ACD* and *ACK* are constitutively expressed in *E. histolytica* at moderate and low levels, respectively [14, 37]. This suggests these two enzymes may be an essential part of *E. histolytica* biology.

The role of EhACD in growth on glucose

Gene silencing of *EhACD* indicated this enzyme is involved in *E. histolytica* growth and proliferation. The EhACDkd strain exhibited significant growth reduction in normal high glucose media versus the wild-type (Fig. 3.3A). Metabolite analysis revealed that intracellular ATP levels decreased and acetyl-CoA increased, consistent with our previous hypothesized role for ACD in extending the glycolytic pathway to produce ATP by converting acetyl-CoA to acetate.

A previous study by Pineda *et al.* also looked at the effects of ACD gene silencing in *E. histolytica* [(31)]. Although they did detect reduced acetate production and a decrease in intracellular CoA levels, there was no effect on intracellular ATP levels. The authors concluded that ACD plays a role in CoA recycling during oxidative exposure but rejected a role for ACD in ATP production. These results conflict with our current results. However, this difference may be explained by the fact that Pineda *et al*. only achieved partial gene silencing of ACD (~10-50%) [(31)] as compared to our current study in which the *ACD* gene was effectively silenced and neither *acd* RNA nor enzymatic activity was detectable. In addition, they neglected to measure growth differences in the gene silenced strains versus the WT.

Although the EhACDkd strain grew more slowly than the wild-type at high (50 mM) glucose, both strains exhibited similar growth as the glucose concentration in the medium was decreased (Fig. 3.3). ACD activity in extracts of wild-type cells grown in varying glucose concentrations was found to be unchanged. This indicated that ACD was

not regulated by glucose availability and the reduced growth of the wild-type strain at low glucose was not due to changes in ACD activity. Instead, the impact of the reduced glucose concentration on growth must be due to other reasons. One possible explanation is that less acetyl-CoA is produced under these conditions, thus reducing substrate availability for ACD and subsequently reducing ATP production via this route.

Role of EhACD in growth on other substrates

Another important aspect of acetate metabolism is acetate utilization. *In vitro* characterization of EhACD showed this enzyme can function equally well in both directions and can also utilize propionate and propionyl-CoA as substrates [(15)]. Moreover, *E. histolytica* naturally inhabits a large intestine environment low in glucose but enriched with acetate, propionate, and butyrate (approximately 63 mM, 24 mM, and 23 mM, respectively) [(32)]. Growth analysis showed neither acetate nor butyrate improved *E. histolytica* proliferation in TYI-S-33 medium lacking glucose. However, addition of propionate improved *E. histolytica* growth (Fig. 3.7). More strikingly, the EhACDkd strain did not show this improved growth upon propionate addition, indicating *E. histolytica* can utilize propionate but not acetate as a growth substrate and that EhACD is required for this.

Role of EhACK in E. histolytica

Like *E. histolytica*, *Toxoplasma gondii* also possesses a PP_i oriented glycolytic pathway. Pace *et al.*[(38)] demonstrated an increase in glycolytic activity and flux when pyrophosphatase was overexpressed, indicating a regulatory role of PP_i in glycolysis. If

EhACK supplies a significant pyrophosphate for glycolysis, EhACKkd cells would be expected to experience a decrease in glycolytic activity, leading to reduced growth or growth abnormalities. At lower glucose concentrations, this effect would worsen if ATP production and conservation was further impaired by disruption of EhACK activity. However, this was not the case as EhACKkd cells grew normally under standard conditions and in reduced glucose medium. This further argues against EhACK's role as a significant PP_i provider for glycolysis.

In vitro kinetic analysis showed PP_i-PFK and PPDK to have K_m values of 50µM and 470µM for PP_i, respectively [39]. The intracellular PP_i concentration in *E. histolytica* is estimated to be 0.41 – 0.7 mM [31, 40]. One study reported knockdown of EhACK (approximately 30-60% knockdown) only minimally decreased the overall concentration of glucose-6-phosphate, fructose-6-phosphate, and pyrophosphate [31]. Thus, EhACK may contribute to the PP_i pool but at a marginal level that may not affect the overall activity of PP_i-PFK and PPDK.

EhACD vs. glucose availability & EhACD vs. EhACK activity

Enzyme activity from cell extract was also examined to determine if EhACD and EhACK have overlapping physiological functions. If these enzymes had overlapping roles, manipulation of one enzyme may influence regulation of the other enzyme to compensate. However, no significant association was observed between the two enzymes (Fig. 3.6). This is consistent with current knowledge based on *in vitro* kinetic analysis and the biochemical reaction associated with each enzyme.

E. histolytica growth at limiting nutrient conditions

Entamoeba invadens, a close relative of *E. histolytica* that infects reptiles, also possesses an ACD. Byers *et al.* [41, 42] reported that exposures to short chain fatty acid (SCFA) inhibited encystation and ploidy level in *E. invadens.* Further investigation showed *Entamoeba* uptakes SCFA in a pH-dependent manner and causes hypoacetylation of histone H4 [43]. In yeast, AMP-acetyl-CoA synthetase (ACS) involvement in histone acetylation has also been reported. Eisenberg *et al.* [44] demonstrated cytosolic accumulation of acetate leads to ACS activation and triggering of histone acetylation in *Saccharomyces cerevisiae*. This relation between ACS and acetylation had also been reported in mice and human [45, 46]. EhACD, therefore, may be the connection between SCFA, histone acetylation and encystation. However, investigation into this link is limited by the undetectable level of histone acetylation and a lack of encystation in *in vitro* axenic growth of *E. histolytica* HM-1:IMSS.

Based on genomic sequences, an EhACD role in amino acid catabolism for ATP generation was postulated [5]. Recently, Pineda *et al.* [31] reported amino acids do not contribute to ATP production after exposing *E. histolytica* to PBS for 2 hours with and without an amino acid source. Our growth data though showed a substantial reduction in growth when tryptone was excluded , consistent with previous observation that mixture of amino acids enhanced growth and survival of *E. histolytica* [6]. No difference was observed between growth of control cells (WT and LUC) and knockdown cells (EhACKkd and EhACDkd) in tryptone excluded medium (Fig. 3.8A). Surprisingly, EhACKkd cells showed enhanced growth in medium with both glucose and tryptone

excluded (Fig. 3.8B). The molecular basis for this phenotype remains undefined but suggests EhACK may possess a novel function.

CONCLUSIONS:

Our results indicate that EhACD has a substantial role in proliferation of *E. histolytica* on glucose and other growth substrates. EhACDkd cells exhibited a growth defect in both normal and low serum TYI-S-33 media. Growth and metabolite data are consistent with EhACD playing a role to extend glycolysis for ATP generation. The substantial decreased of ATP pool in EhACDkd cells connects the growth defect to lack of ATP availability. Likewise, EhACD showed evidence to be involved in utilizing propionate for growth.

Our results also demonstrated a role for EhACK in growth. However, its role to supply pyrophosphate for glycolysis proved to be unlikely. The molecular mechanism of EhACK growth enhancement during amino acids and glucose starvation remains undefined. Further analysis is warranted to elucidate EhACK's *in vivo* function.

REFERENCES:

1. Stanley, S. L. Amoebiasis. *Lancet* **361**(2003).

2. CDC. Amebiasis. https://www.CDC.gov/dpdx/amebiasis/ (2010).

3. Haque, R., Huston, C. D., Hughes, M., Houpt, E. and Petri, W. A. Amebiasis. *New England J Med* **348**, 1565-1573 (2003).

4. Clark, C. G., *et al.* Structure and content of the *Entamoeba histolytica* genome. *Adv Parasitol* **65**, 51-190 (2007).

5. Anderson, I. J. and Loftus, B. J. *Entamoeba histolytica*: Observations on metabolism based on the genome sequence. *Exp Parasitol* **110**, 173-177 (2005).

6. Zuo, X. and Coombs, G. H. Amino acid consumption by the parasitic, amoeboid protists *Entamoeba histolytica* and *Entamoeba invadens*. *FEMS Microbiol Lett* **130**, 253-258 (1995).

7. Wolfe, A. J. The acetate switch. *Microbiol Mol Biol Rev* **69**, 12-50 (2005).

8. Kumari, S., Tishel, R., Eisenbach, M. and Wolfe, A. J. Cloning, characterization, and functional expression of acs, the gene which encodes acetyl coenzyme a synthetase in *Escherichia coli*. *J Bacteriol* **177**, 2878-2886 (1995).

9. Reeves, R. E. and Guthrie, J. D. Acetate kinase (pyrophosphate). A fourth pyrophosphate-dependent kinase from *Entamoeba histolytica*. *Biochem Biophys Res Commun* **66**, 1389-1395 (1975).

10. Ingram-Smith, C., Martin, S. R. and Smith, K. S. Acetate kinase: Not just a bacterial enzyme. *Trends Microbiol* **14**, 249-253 (2006).

11. Fowler, M. L., Ingram-Smith, C. and Smith, K. S. Novel pyrophosphate-forming acetate kinase from the protist *Entamoeba histolytica*. *Eukaryot Cell* **11**, 1249-1256 (2012).

12. Thibeaux, R., *et al.* Identification of the virulence landscape essential for *Entamoeba histolytica* invasion of the human colon. *PLoS Pathog* **9**, e1003824 (2013).

13. Hon, C. C., *et al.* Quantification of stochastic noise of splicing and polyadenylation in *Entamoeba histolytica*. *Nucleic Acids Res* **41**, 1936-1952 (2013).

14. Ehrenkaufer, G. M., Haque, R., Hackney, J. A., Eichinger, D. J. and Singh, U. Identification of developmentally regulated genes in *Entamoeba histolytica*: Insights into mechanisms of stage conversion in a protozoan parasite. *Cell Microbiol* **9**, 1426-1444 (2007).

15. Jones, C. P. and Ingram-Smith, C. Biochemical and kinetic characterization of the recombinant ADP-forming acetyl CoA synthetase from the amitochondriate protozoan *Entamoeba histolytica*. *Eukaryot Cell* **13**, 1530-1537 (2014).

16. Sanchez, L. B. and Muller, M. Purification and characterization of the acetate forming enzyme, acetyl-CoA synthetase (ADP-forming) from the amitochondriate protist, *Giardia lamblia*. *FEBS Lett* **378**, 240-244 (1996).

17. Brasen, C., Schmidt, M., Grotzinger, J. and Schonheit, P. Reaction mechanism and structural model of ADP-forming acetyl-CoA synthetase from the hyperthermophilic archaeon *Pyrococcus furiosus*: Evidence for a second active site histidine residue. *J Biol Chem* **283**, 15409-15418 (2008).

18. Mai, X. and Adams, M. W. Purification and characterization of two reversible and ADP-dependent acetyl CoA synthetases from the hyperthermophilic archaeon *Pyrococcus furiosus*. *J Bacteriol* **178**, 5897-5903 (1996).

19. Reeves, R. E., Warren, L. G., Susskind, B. and Lo, H. S. An energy-conserving pyruvate-to-acetate pathway in *Entamoeba histolytica*. Pyruvate synthase and a new acetate thiokinase. *J Biol Chem* **252**, 726-731 (1977).

20. Diamond, L. S., Harlow, D. R. and Cunnick, C. C. A new medium for the axenic cultivation of *Entamoeba histolytica* and other *Entamoeba*. *Trans R Soc Trop Med Hyg* **72**, 431-432 (1978).

21. Morf, L., Pearson, R. J., Wang, A. S. and Singh, U. Robust gene silencing mediated by antisense small RNAs in the pathogenic protist *Entamoeba histolytica*. *Nucleic Acids Res* **41**, 9424-9437 (2013).

22. Hamann, L., Nickel, R. and Tannich, E. Transfection and continuous expression of heterologous genes in the protozoan parasite *Entamoeba histolytica*. *Proc Natl Acad Sci U S A* **92**, 8975-8979 (1995).

23. Vines, R. R., *et al.* Stable episomal transfection of *Entamoeba histolytica*. *Mol Biochem Parasitol* **71**, 265-267 (1995).

24. Koushik, A. B., Welter, B. H., Rock, M. L. and Temesvari, L. A. A genomewide overexpression screen identifies genes involved in the phosphatidylinositol 3-kinase pathway in the human protozoan parasite *Entamoeba histolytica*. *Eukaryot Cell* **13**, 401-411 (2014).

25. Fowler, M. L., Ingram-Smith, C. J. and Smith, K. S. Direct detection of the acetate-forming activity of the enzyme acetate kinase. *J Vis Exp* (2011).

26. Bradford, M. M. A rapid and sensitive method for the quantitation of microgram quantities of protein utilizing the principle of protein-dye binding. *Anal Biochem* **72**, 248-254 (1976).

27. Stoscheck, C. M. Quantitation of protein. *Methods Enzymol* **182**, 50-68 (1990).

28. Strober, W. 2001. Trypan Blue Exclusion Test of Cell Viability. *Curr Prot Immunol*. 21:3B:A.3B.1–A.3B.2

29. Neubauer, S., *et al.* LC-MS/MS-based analysis of coenzyme a and short-chain acyl-coenzyme a thioesters. *Anal Bioanal Chem* **407**, 6681-6688 (2015).

30. Scorneaux, B. and Shryock, T. R. The determination of the cellular volume of avian, porcine and bovine phagocytes and bovine mammary epithelial cells and its relationship to uptake of tilmicosin. *J Vet Pharmacol Ther* **22**, 6-12 (1999).

31. Pineda, E., *et al.* Roles of acetyl-CoA synthetase (ADP-forming) and acetate kinase (PP_i-forming) in ATP and PP_i supply in *Entamoeba histolytica*. *Biochim Biophys Acta* **1860**, 1163-1172 (2016).

32. Cummings, J. H., Pomare, E. W., Branch, W. J., Naylor, C. P. and Macfarlane, G. T. Short chain fatty acids in human large intestine, portal, hepatic and venous blood. *Gut* **28**, 1221-1227 (1987).

33. Watkins, P. A., Maiguel, D., Jia, Z. and Pevsner, J. Evidence for 26 distinct acyl-CoA synthetase genes in the human genome. *J Lipid Res* **48**, 2736-2750 (2007).

34. Carman, A. J., Vylkova, S. and Lorenz, M. C. Role of acetyl CoA synthesis and breakdown in alternative carbon source utilization in *Candida albicans*. *Eukaryot Cell* **7**, 1733-1741 (2008).

35. Lyssiotis, C. A. and Cantley, L. C. Acetate fuels the cancer engine. *Cell* **159**, 1492-1494 (2014).

36. Dittrich, C. R., Bennett, G. N. and San, K. Y. Characterization of the acetate-producing pathways in *Escherichia coli*. *Biotechnol Prog* **21**, 1062-1067 (2005).

37. Gilchrist, C. A., *et al.* Impact of intestinal colonization and invasion on the *Entamoeba histolytica* transcriptome. *Mol Biochem Parasitol* **147**(2006).

38. Pace, D. A., Fang, J., Cintron, R., Docampo, M. D. and Moreno, S. N. Overexpression of a cytosolic pyrophosphatase (TgPPase) reveals a regulatory role of $PP_{(i)}$ in glycolysis for *Toxoplasma gondii*. *Biochem J* **440**, 229-240 (2011).

39. Saavedra, E., Encalada, R., Pineda, E., Jasso-Chavez, R. and Moreno-Sanchez, R. Glycolysis in *Entamoeba histolytica*. Biochemical characterization of recombinant glycolytic enzymes and flux control analysis. *FEBS J* **272**, 1767-1783 (2005).

40. Varela-Gomez, M., Moreno-Sanchez, R., Pardo, J. P. and Perez-Montfort, R. Kinetic mechanism and metabolic role of pyruvate phosphate dikinase from *Entamoeba histolytica*. *J Biol Chem* **279**, 54124-54130 (2004).

41. Byers, J. and Eichinger, D. *Entamoeba invadens*: Restriction of ploidy by colonic short chain fatty acids. *Exp Parasitol* **110**, 203-206 (2005).

42. Byers, J., Faigle, W. and Eichinger, D. Colonic short-chain fatty acids inhibit encystation of *Entamoeba invadens*. *Cell Microbiol* **7**, 269-279 (2005).

43. Byers, J. and Eichinger, D. Acetylation of the *Entamoeba histone* H4 N-terminal domain is influenced by short-chain fatty acids that enter trophozoites in a pH-dependent manner. *Int J Parasitol* **38**, 57-64 (2008).

44. Eisenberg, T., *et al.* Nucleocytosolic depletion of the energy metabolite acetyl-coenzyme a stimulates autophagy and prolongs lifespan. *Cell Metab* **19**, 431-444 (2014).

45. Wellen, K. E., *et al.* ATP-citrate lyase links cellular metabolism to histone acetylation. *Science* **324**, 1076-1080 (2009).

46. Gao, X., *et al.* Acetate functions as an epigenetic metabolite to promote lipid synthesis under hypoxia. *Nat Commun* **7**, 11960 (2016).

CHAPTER IV

CONCLUSIONS AND FUTURE PROSPECTS

Acetate metabolism has attracted increasing attention due to its involvement in tumorigenesis and metabolic disorders in humans and in pathogenesis. Typically, acetate excretion and uptake are associated with energy metabolism and utilization as an alternative carbon source. However, these pathways have also been linked to histone acetylation and protein phosphorylation and thus, play a role in regulating gene expression and activity. Therefore, it is of great interest to further explore these pathways in depth.

Entamoeba histolytica is a human protozoan parasite which infects around 90 million people each year, causing approximately 50,000-100,000 deaths. Acetate is a major metabolite produced by *E. histolytica* during growth on glucose that can be generated by ACK and ACD (Figure 4.1). The role of these two enzymes in *E. histolytica* metabolism has been the focus of this dissertation.

Physiological function of EhACK

Our results with antisense RNA mediated gene silencing revealed that ACK plays a role in growth under different conditions. However, the data are not consistent with our previously hypothesized role for ACK in providing pyrophosphate for glycolysis. An ACK knockdown strain did show enhanced growth in medium in which glucose and tryptone were omitted. This suggests ACK may possesses a novel role in *E. histolytica* contrary to initial expectations.

Currently, RNAseq is underway to characterize the molecular mechanism of the ACK knockdown phenotype during growth in the absence of glucose and tryptone. Metabolite analysis of this strain versus the WT under normal growth conditions and in the absence of glucose and tryptone will be performed to determine whether intracellular ATP or acetyl-CoA pools are affected. Determination of acetyl phosphate levels within *E. histolytica* should also be undertaken. Acetyl phosphate measurements have previously been done through either an enzyme assay or two-dimensional thin layer chromatography [1-3]. However, lability of acetyl phosphate can hinder accurate measurement. Since EhACK prefers to catalyze the acetate-forming direction of the reaction, examining the effects on intracellular acetyl phosphate concentrations remains an essential step in understanding the physiological function of this enzyme.

Another question that has yet to be answered is what provides acetyl phosphate as the substrate for ACK? At the moment, known acetyl phosphate producing enzymes have not been identified within *E. histolytica*. However, in 1954 Harting and Velick[4, 5] showed evidence that glyceraldehyde-3-phosphate dehydrogenase (GAPDH) from yeast and rabbit catalyzes the formation of acetyl phosphate from acetaldehyde and inorganic phosphate. GAPDH is a commonly associated glycolytic enzyme which converts glyceraldehyde-3-phosphate to glycerate 1, 3-bisphosphate. *E. histolytica* possesses three genes encoding GAPDH. Progress is underway to purify recombinant *E. histolytica* GAPDH to examine whether it has the ability to produce acetyl phosphate.

Anthony and Spector [6] have previously shown that *Escherichia coli* ACK can be phosphorylated by ATP or acetyl phosphate. A later study showed the *E. coli* ACK

phosphoenzyme is catalytically active, being able to transfer the phosphate to ADP or acetate [7]. Following up on Anthony and Spector's research, Fox *et al.* [8] found the ACK phosphoenzyme can also transfer the phosphate to Enzyme I of Bacterial phosphotransferase system. This evidence suggested ACK may have an alternative role as a protein kinase. This possibility has not been investigated further. This raises the intriguing question of whether EhACK role is as a protein kinase, possible in a regulatory role involving protein phosphorylation. Additional investigation into whether EhACK can be phosphorylated by PP_i or acetyl phosphate and identifying potential phosphorylation partners could lead to a better understanding of the *in vivo* role of this enzyme.

Physiological function of EhACD

ACD gene silencing resulted in a reduction in growth compared to WT cells. This was linked to a decrease of ATP pool in the ACD knockdown strain. The combination of growth and metabolite analysis supported ACD's hypothesized role to extend glycolysis to increase ATP generation, as evidence by decreased growth, decreased intracellular ATP concentration, and accumulation of acetyl-CoA.

ACD was also proposed to be able to activate acetate for utilization based on *in vitro* kinetic analysis. Unexpectedly, wild-type *E. histolytica* was found to grow on propionate but not acetate when glucose was absent from the medium. However, growth on propionate was impeded in the ACD knockdown strain. This supports that ACD is required for utilization of propionate as an alternative growth substrate in place of

glucose. This is of physiological relevance since *E. histolytica* infects and inhabits a host environment abundant in propionate.

Short chain fatty acids have been shown to influence *Entamoeba invadens* encystation and histone acetylation [9-11]. *E. invadens* is a close relative of *E. histolytica* and infects and causes similar invasive infection in reptiles. ACD is present in *E. invadens,* thus raising the question of whether ACD helped mediate these events. Regrettably, *E. histolytica* exhibited undetectable levels of histone acetylation [11] and a mechanism to induce encystation under laboratory conditions has not yet been established. Thus, investigation into a role for ACD in encystation and histone acetylation (as well as the resulting changes in gene regulation) cannot be performed in *E. histolytica* at this time and should instead be followed up on in *E. invadens.*

Since *E. histolytica* was able to grow on propionate as a growth substrate in the absence of glucose, metabolite labeling of *E. histolytica* grown on C^{13}-propionate may provide additional insights into propionate metabolism within this parasite. Additionally, Ramakrishnan *et al.* [12] have developed a tetracycline inducible overexpression system for *E. histolytica.* An ACD and ACK overexpression study will provide added perspective in learning about the physiological role of these two enzymes.

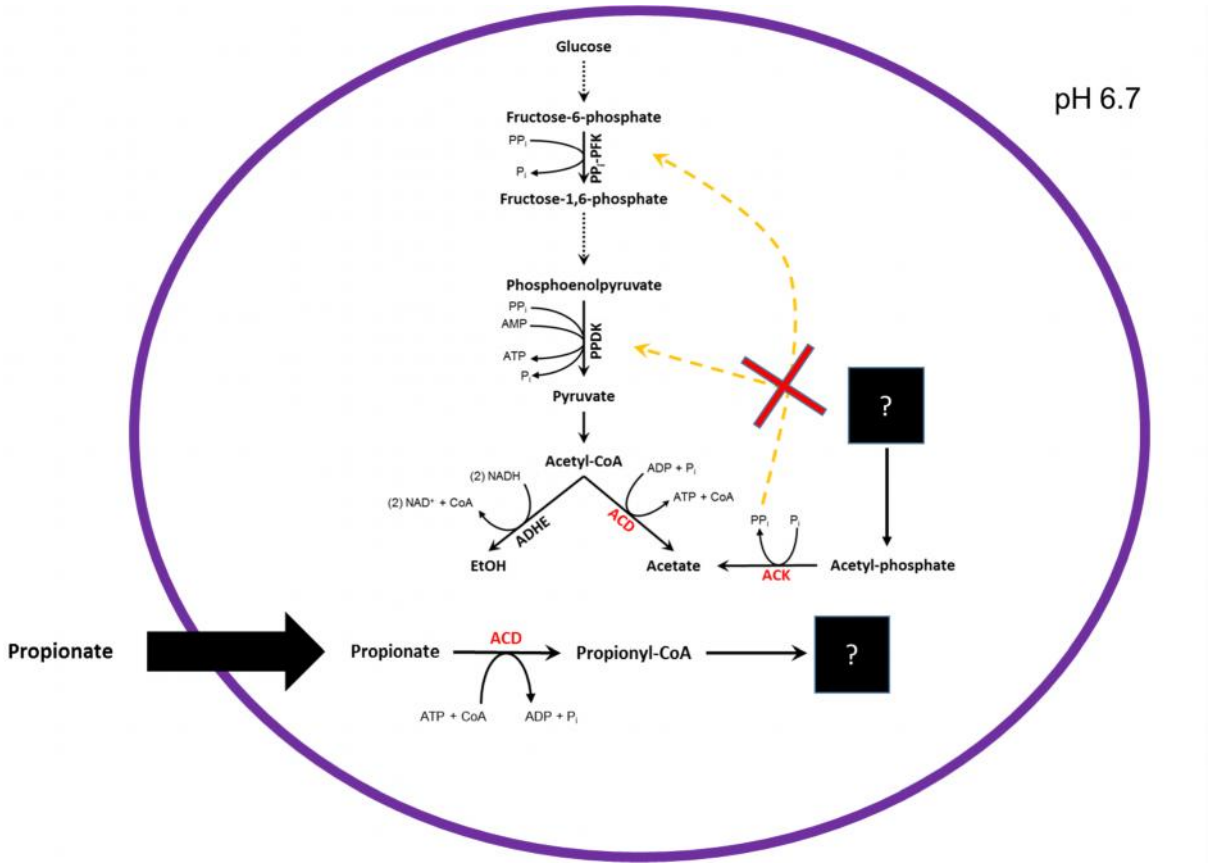

Figure 4.1: **Representation of our current understanding of the physiological roles of EhACK and EhACD in *E. histolytica*.** The pathway shown is the extended glycolytic pathway present in E. histolytica in which glucose is converted to pyruvate and then to ethanol and acetate in the extended pathway. Dashed orange arrows embody the previously hypothesized role for EhACK of providing pyrophosphate. The black boxes with a question mark represent the unknown origin of acetyl phosphate and the fate of propionyl-CoA. PP_i-PFK: pyrophosphate dependent phosphofructokinase; PPDK: pyruvate phosphate dikinase; ADHE: bifunctional aldehyde-alcohol dehydrogenase; ACD: ADP-forming acetyl CoA synthetase; ACK: acetate kinase.

Basis of EhACK phosphoryl substrate specificity

This research demonstrated *E. histolytica* ACK's phosphoryl substrate specificity is not solely dependent on substrate binding. Based on the structure, EhACK was found to lack an adenosine pocket and utilizes P_i/PP_i instead of ADP/ATP as for other ACKs. This was attributed to having several bulkier amino acids blocking the entrance to the adenosine pocket of EhACK. Even though opening the adenosine pocket did increase ATP binding to the enzyme, it did not confer activity. Similarly, closure of entrance to the *M. thermophila* ACK (MtACK) adenosine pocket did not force a phosphoryl substrate switch to PP_i.

Acetate kinase belongs to the acetate and sugar kinases/Hsc70/actin (ASKHA) enzyme superfamily. Catalysis within this superfamily is characterized by domain motion. Using tryptophan fluorescence quenching to study MtACK domain motion, Gorrell and Ferry[13] showed only nucleotide binding caused domain closure. Further analysis indicated that MtACK follows a half-site mechanism, where only half of the site are bound to the ligand at any single moment.

Alterations that opened the EhACK adenosine pocket allowed ATP and ADP to bind more effectively. However, it is unclear if this interaction stimulates domain motion as would be necessary for enzymatic activity. Progress in this aspect will advance our understanding of the nature of EhACK substrate specificity and will also improve our understanding of ACK's overall enzyme dynamics and catalytic mechanism.

Currently, EhACK is the only known ACK able to utilize pyrophosphate and inorganic phosphate as substrate. Identification of other PP_i-dependent ACKs will aid in our efforts to understand phosphoryl substrate selection and utilization by providing additional amino acid sequences necessary to further identify unique features within PP_i-dependent ACK. Blast searches using EhACK as the query sequence identified four hypothetical ACKs that share both bulkier amino acid residues within the ADENOSINE motif and an extended PHOSPHATE2 motif with sequence identity and similarity between 40-46% and 60-66%, respectively (Figure 3.7; refer to Chapter III for additional details). Interestingly, ACK sequences that contain bulkier amino acids within the ADENOSINE motif correspondingly possess an extended PHOSPHATE2 motif. Though this correlation does not indicate that these are PP_i-dependent ACK, this does warrant a closer examination.

REFERENCES:

1. Bochner, B. R. and Ames, B. N. Selective precipitation orthophosphate from mixtures containing labile phosphorylated metabolites. *Anal Biochem* **122**, 100-107 (1982).

2. Klein, A. H., Shulla, A., Reimann, S. A., Keating, D. H. and Wolfe, A. J. The intracellular concentration of acetyl phosphate in *Escherichia coli* is sufficient for direct phosphorylation of two-component response regulators. *J Bacteriol* **189**, 5574-5581 (2007).

3. Wolfe, A. J. The acetate switch. *Microbiol Mol Biol Rev* **69**, 12-50 (2005).

4. Harting, J. and Velick, S. F. Acetyl phosphate formation catalyzed by glyceraldehyde-3-phosphate dehydrogenase. *J Biol Chem* **207**, 857-865 (1954).

5. Harting, J. and Velick, S. F. Transfer reactions of acetyl phosphate catalyzed by glyceraldehyde-3-phosphate dehydrogenase. *J Biol Chem* **207**, 867-878 (1954).

6. Anthony, R. S. and Spector, L. B. A phosphoenzyme intermediary in acetate kinase action. *J Biol Chem* **245**, 6739-6741 (1970).

7. Anthony, R. S. and Spector, L. B. Phosphorylated acetate kinase. Its isolation and reactivity. *J Biol Chem* **247**, 2120-2125 (1972).

8. Fox, D. K., Meadow, N. D. and Roseman, S. Phosphate transfer between acetate kinase and Enzyme I of the bacterial phosphotransferase system. *J Biol Chem* **261**, 13498-13503 (1986).

9. Byers, J., Faigle, W. and Eichinger, D. Colonic short-chain fatty acids inhibit encystation of *Entamoeba invadens*. *Cell Microbiol* **7**, 269-279 (2005).

10. Byers, J. and Eichinger, D. *Entamoeba invadens*: Restriction of ploidy by colonic short chain fatty acids. *Exp Parasitol* **110**, 203-206 (2005).

11. Byers, J. and Eichinger, D. Acetylation of the *Entamoeba histone* H4 N-terminal domain is influenced by short-chain fatty acids that enter trophozoites in a pH-dependent manner. *Int J Parasitol* **38**, 57-64 (2008).

12. Ramakrishnan, G., Vines, R. R., Mann, B. J. and Petri, W. A., Jr. A tetracycline-inducible gene expression system in *Entamoeba histolytica*. *Mol Biochem Parasitol* **84**, 93-100 (1997).

13. Gorrell, A. and Ferry, J. G. Investigation of the *Methanosarcina thermophila* acetate kinase mechanism by fluorescence quenching. *Biochemistry* **46**, 14170-14176 (2007).

APPENDIX

SUPPLEMENTAL INFORMATION

APPENDIX A: SUPPLEMENTAL FIGURES OF CHAPTER II

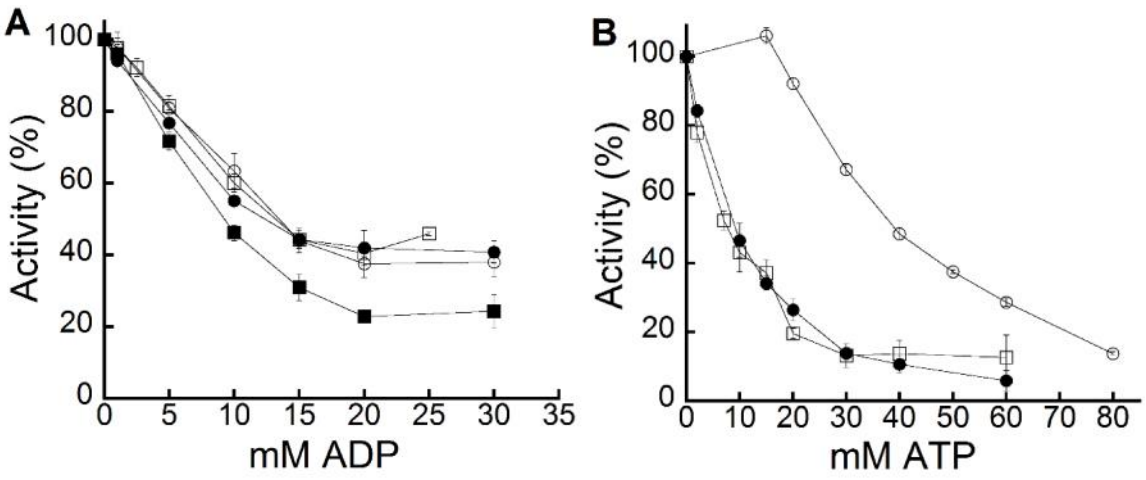

Figure A1. Inhibition curves for EhACK wild-type and variant enzymes. Enzymatic activity was determined for each enzyme in the presence of the indicated concentration of ADP, ATP, or PP_i. Activities are plotted as a percentage of the activity observed for the wild-type enzyme in the absence of inhibitor. Activities are the mean ± SD of three replicates. (A) ADP inhibition in the acetate forming direction and (B) ATP inhibition in the acetyl-phosphate-forming direction. Symbols for panels A-C: EhACK wild-type, (○); EhACK $Q^{323}G$-$M^{324}I$ variant (●); EhACK $Q^{323}A$-$M^{324}A$ variant, (□); EhACK $D^{272}A$-$R^{274}A$-$Q^{323}G$-$M^{324}I$ variant (■) (except panel C). Symbols for panels D-E: MtACK wild-type, (○); MtACK $G^{331}Q$-$I^{332}M$ variant (●);